JAERI-Tech
99-027

ITER CRYOSTAT THERMAL SHIELD DETAILED DESIGN

March 1999

Akira ITO, Masataka NAKAHIRA, Kazuya HAMADA, Hiroyuki TAKAHASHI,
Eisuke TADA, Takashi KATO and Akira NISHIKAWA*

日本原子力研究所
Japan Atomic Energy Research Institute

本レポートは、日本原子力研究所が不定期に公刊している研究報告書です。
入手の問合わせは、日本原子力研究所研究情報部研究情報課（〒319-1195　茨城県那珂郡東海村）あて、お申し越しください。なお、このほかに財団法人原子力弘済会資料センター（〒319-1195　茨城県那珂郡東海村日本原子力研究所内）で複写による実費頒布をおこなっております。

This report is issued irregularly.
Inquiries about availability of the reports should be addressed to Research Information Division, Department of Intellectual Resources, Japan Atomic Energy Research Institute, Tokai-mura, Naka-gun, Ibaraki-ken 319-1195, Japan.

編集兼発行　日本原子力研究所

ITER Cryostat Thermal Shield Detailed Design

Akira ITO, Masataka NAKAHIRA, Kazuya HAMADA, Hiroyuki TAKAHASHI,
Eisuke TADA, Takashi KATO and Akira NISHIKAWA *

Department of Fusion Engineering Research
(Tokai Site)
Naka Fusion Research Establishment
Japan Atomic Energy Research Institute
Tokai-mura, Naka-gun, Ibaraki-ken

(Received February 10, 1999)

Structural design and study on fabrication and assembly of the cryostat thermal shield for International Thermonuclear Experimental Reactor (ITER) has been conducted.

The cryostat thermal shield is attached to cover the cryostat inner wall in order to reduce the radiation heat loads applied to the superconducting coils operation at 4 K. The thermal shield consists of low-emissivity foils which are passively cooled and shield plates which are actively cooled with low temperature helium gas. The foils are multi-layered assembly and are attached on the both surfaces of the shield plates. The material of the foils are silver coated 304 stainless steel, polyimide or polyester. The silver coated stainless steel foils should be adopted to the foils at the locations where radiation dose is over 10 MGy. The route of coolant pipes for the shield plates is designed so as to keep the surface temperature of the shield plates below 100 K.

This report describes the detailed design of the cryostat thermal shield, and outlines the fabrication and assembly procedures.

Keywords : ITER, Cryostat, Thermal Shield, Thermal Insulator, Low-emissivity Foil

---

This work is conducted as an ITER design study and this report corresponds to 1996 ITER Design Task Agreement on ` Cryostat Thermal Shield Detailed Design ` (S91TD31(D314)).

* Ishikawajima Harima Heavy Industries Co.

ITERクライオスタット用熱シールドの詳細設計

日本原子力研究所那珂研究所核融合工学部
伊藤　彰・中平　昌隆・濱田　一弥・高橋　弘行
多田　栄介・加藤　崇・西川　明*

(1999年2月10日受理)

日本原子力研究所では現在までに核融合実験炉(ITER)のクライオスタット用熱シールドの構造及び製作・現地組立て手順の検討を実施してきた。

クライオスタット用熱シールドは超伝導コイルへの熱負荷を低減することを目的に、クライオスタット内壁及び真空容器外表面に取り付けられる。熱シールドは熱絶縁用低輻射フォイル及び低温ヘリウムガスによって冷却される遮蔽板から構成される。フォイルは多層に重ねられ、遮蔽板の両面に取り付けられる。フォイル用材質として、表面に銀コーティング処理を施したSUS304、ポリイミド及びポリエステルを採用する。放射線量が10MGy以上の箇所にはSUS304を使用することとした。フォイルを取り付ける遮蔽板には、その表面温度を100K以下に保つために、ヘリウム冷却用の配管が取り付けられる。

本件では、クライオスタット用熱シールドの熱構造設計及び工場製作、現地組立て手順について報告する。

本報告は、ITER工学設計の一環として実施したものであり、報告内容は1996年ITER設計タスク協定S91TD31 (D314)の「ITERクライオスタット用熱シールドの設計」に基づくものである。

那珂研究所（東海駐在）：〒３１９－１１９５　茨城県那珂郡東海村白方白根２－４
＊　石川島播磨重工業株式会社

Contents

目　次

1. Introduction

1.1 Background and Objectives

1.1.1 Background

The cryostat is a single walled vacuum chamber that is at room temperature. A thermal shield is needed to block thermal radiation from the cryostat interior wall and surfaces of structures between the cryostat and the machine, so as to reduce heat load to the super-conducting coils to approximately 2.5 kW.

The thermal shield must be capable of remote removable and replacement, and must be able to withstand the cumulative neutron and gamma dose expected over the life of machine. It must be robust enough to accommodate occasional strikes from in-chamber remote handling equipment, and must be strong enough to resist loads from gravity, seismic, and electromagnetic sources.

1.1.2 Objectives

The ultimate objective of this task is to perform the detailed design of the cryostat thermal shield including cost estimate. Pursuant to this objective, the scoping of options, exploring thermal shields in use elsewhere, selection of design concepts for the cryostat inside wall and for connections between the cryostat and the machine, and detailed design of components, will be conducted. During these activities, close coordination with the ITER cryoplant design will be continued.

1.2 Technical Outline of Task

The thermal shield is consist of actively-cooled surfaces, passive low-emissivity foils, or a combination of these. The preferred coolant, when used, is helium gas. It is desired to keep the lowest temperature of the low emissivity surfaces above 78 K so as to avoid condensation of air from leaks. The thermal shield should be designed using an expected end-of-life thermal emissivity of 0.2, with allowance for improved performance at lower emissivities. Panel sizes must be small enough to allow remote replacement. In particular, it must be possible to accommodate relative motion between the vacuum vessel port and the cryostat wall, and be able to accept infrequent fault temperatures as high as 300°C, and normal operating temperatures as high as 200°C. With a total shield area of approximately 7000 m^2 including port extensions, the average heat flux to the cold mass must be no more than about 0.35 W/m^2.

1.3 Task Description

1.3.1 Scoping

This task will establish the general configuration of the cryostat thermal shield. Preliminary work to date suggests that the cryostat wall and vacuum vessel port extensions will be covered with

metal panels cooled by helium gas in circular tubes, while other surfaces will be covered with passive insulation. The purpose of the scoping phase is to either confirm or negate this starting point and suggest alternate configurations. The assessment of thermal shields adopted for other applications should weigh significantly on the design choices. Scoping will also include thermal-hydraulic analyses including optimal coupling with cryoplant so as to minimize electricity consumption consistent with high reliability and equipment redundancy. Piping layout and manifold placement are also included in this task.

1.3.2 Concept Selection and Detailed Analysis and Design

Specific shield options will be selected in this task and analyzed in detail with emphasis on maximizing reliability and minimizing cost and electrical power and cryogen consumption. Design study drawings will be prepared to evaluate fabricability, assembly/installation and cost.

1.3.3 Detailed Design

Fabrication drawings will be prepared during this phase in sufficient detail for full fabrication and for estimating costs.

1.3.4 Cost Estimate

A detailed cost estimate is drawn up based on the fabrication drawings. The effect of site location will be included where possible.

2 Design Conditions

(1) Scope of thermal shields

Scope of the thermal shields in this task are as follows:

a. Cryostat thermal shields
   (a) Cylindrical shell thermal shields
   (b) Upper cover thermal shields
   (c) Lower cover thermal shields

b. Port thermal shields
   (a) Upper port thermal shields
   (b) Equatorial port thermal shields
   (c) Divertor port thermal shields

c. Gravity support thermal shields

Figure 2-1 shows the arrangement of these thermal shields.

(2) Limitation of heat load

Table 2-1 shows the targets of heat load limitations.

Table 2-1 Heat load limitation

Item	Target
Sum of 300K→80K heat load	≥120kW
Cryostat thermal shields	≥45kW
Port thermal shields in baking	≥75kW
Sum of 80K→4.5K heat load	≥2.5kW

(3) Cooling condition

The shield plates are forcibly cooled by gaseous helium supplied from three pairs of the valve boxes. Table 2-2 shows the coolant condition.

Table 2-2 Coolant conditions

Item	Condition
coolant	gaseous helium
inlet pressure	1.8MPa
inlet temperature	80K
overall pressure loss	≤0.1MPa
maximum temperature of shield plate	≤100K

Control valves to distribute coolant to each path of the heat transfer tube on the thermal shields are set into the valve boxes.

(4) Thermal shield structure

a. The thermal shields consist of metal plates kept at 80K by gaseous helium and are thermally isolated by multi-layer boards or multi-layer insulation set onto both of warm surface side and cold magnet side

b. The thermal shields should be removal panels and should be maintained by remote

handling tools.

c. The thermal shields can be prevented from neutron damage in their life-time.
d. The thermal shields have enough mechanical strength against the electro-magnetic force during the operation.
e. Some ports may be heated up to 300°C, so that the thermal shields can be heat-resistant up to the temperature.
f. Seismic force to be considered are 0.2G in horizontal direction and -0.2G in vertical direction.
g. The helium leak rate should be lower than 10^{-10} Pa•m^3/s.

(5) Radiation dose

Based upon the results of the dose rate analyses conducted by JAERI, the radiation dose condition were set up for each of the thermal shields as shown in Table 2-3.

Table 2-3 Radiation dose

Portion		Radiation dose (MGy)
Cryostat	Cylindrical shell	10(vicinity of the NBI ducts), 0.1(other portion)
	Upper cover	1(overhead of the NBI ducts), 0.1(other portion)
	Lower cover	0.1
Ports	Upper ports	1
	Equatorial ports	1
	Divertor ports	1
Gravity supports	----	0.1

(6) Nuclear heating rate

Based upon the results of the nuclear heating rate analyses conducted by JAERI, the nuclear heating rate were set up for each of the thermal shields as shown in Table 2-4.

Table 2-4 Nuclear heating rate

Portion		Neutron heating rate (W/cc)
Cryostat	Cylindrical shell	5×10^{-3}(vicinity of the NBI ducts) 5×10^{-4}(other portion)
	Upper cover	1×10^{-4}(vicinity of the NBI ducts) 1×10^{-5}(other portion)
	Lower cover	1×10^{-5}
Ports	Upper ports	1×10^{-4}(vicinity of the NBI ducts) 1×10^{-5}(other portion)
	Equatorial ports	1×10^{-3}(vicinity of the NBI ducts) 1×10^{-4}(other portion)
	Divertor ports	1×10^{-3}(vicinity of the NBI ducts) 1×10^{-4}(other portion)
Gravity supports	----	1×10^{-5}

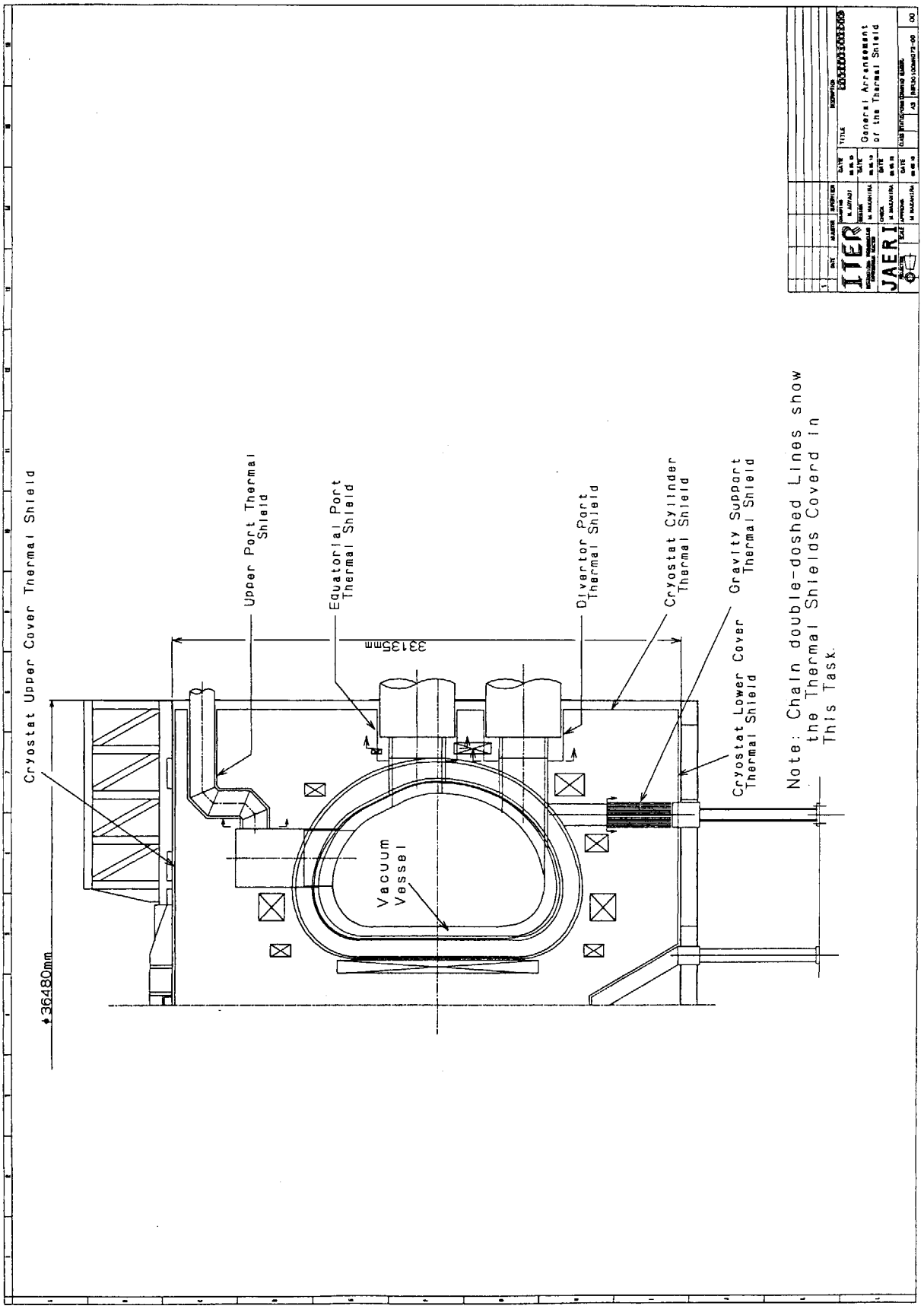

Fig. 2-1 General Arrangement of the Thermal Shield

3. Thermal shield design description

3.1 General concept

Based on the design outputs in FY'96, the thermal shield design has been performed considering the structural modification of the cryostat itself, improvement of thermal insulation, reduction of tube-bore, and so on. To keep structural integrity of the thermal shields in seismic events, the shield plates should be furnished for the warm surface directly by stiff supports. The detail is attached at the end of this section.

Figure 3-1 and Figure 3-2 show a bird's-eye view of typical thermal shield and main components of the shield, respectively.

a. Structural modification of the cryostat

From the double-wall shell structure, the cryostat cylinder was modified to a single-wall shell stiffened by T-shaped ring. According to this modification, the thermal shields of the cylindrical portion are also changed to be supported from the stiffeners. So, the spans of each thermal shield are equal to those of stiffeners.

b. Thermal insulation

As the cumulated dose reaches to 10-MGy, the thermal insulation in the vicinity of the NBI ducts should be modified to the reflecting plates made of type 304 stainless steel from the conventional MLI blanket made up of polymer films.

Table 3-1 shows the thermal insulations designed for each thermal shield.

Table 3-1 Thermal insulation for each thermal shield

Portion		Thermal insulation to be adopted	
		Cross section including NBI ducts	other cross section
Cryostat	Cylinder	1. range of 2m from edge of the NBI duct; reflecting plate 2. other portion; MLI blanket (polyimide)	MLI blanket (polyester)
	Upper cover	1. outer side of upper port; MLI blanket (polyimide) 2. inner side of upper port; MLI blanket (polyester)	MLI blanket (polyester)
	Lower cover	MLI blanket (polyester)	MLI blanket (polyester)
Ports	Upper ports	MLI blanket (polyimide)	MLI blanket (polyimide)
	Equatorial ports	----	MLI blanket (polyimide)
	Divertor ports	MLI blanket (polyimide)	MLI blanket (polyimide)
Gravity supports	Gravity supports	MLI blanket (polyester)	MLI blanket (polyester)

c. Heat transfer tube

The heat transfer tube on the shield plates was modified from a circular arrangement to a zigzag one because of EM-force reduction at the coil quench. Also, the tube-bore was reduced (smaller than 34mm in outer diameter) to eliminate bellows expansions in the crossover tube.

d. Structural Improvements

(a) Reduction of heat leak

i. Surface of the shield plate itself and both sides of each reflecting plate are silver-deposited to reduce their emissivity.

ii. The supports connected to the ring plate and warm structure are modified to be as slender as possible.

(b) Mechanical interface

i. Basically, the ring plate should be set up to the supports closely. However, to keep structural integrity of the supports subjected to thermal shrinkage of the shield plate, some loose-jointed mechanisms should be applied to the interface between the ring plate and the supports.

Study on the thermal shield suspended by rods (Appendix 3.1)

This paragraph shows a structural integrity assessment for the cryostat cylinder thermal shield suspended by rods.

(1)Structural feature

According to the JCT drawings, the thermal shield is suspended by approximately 1.5m-long rods from the cryostat inner wall with spherical joints at both ends.

(2)Natural period of the structure

The natural period of the suspended thermal shield can be calculated as

$$T = 2\pi\sqrt{\frac{L}{g}} = 2\pi\sqrt{\frac{1.5}{9.8}} = 2.458(s).$$

The peak response period of the seismically isolated tokamak pit is estimated as 2s ~ 3s. Therefore, resonance between the thermal shield and the pit will occur.

(3)Stress in the structure

By using the formula for circular rings described in the reference, the bending stress that occurs in the toroidal space frame at seismic event is evaluated as follows:

bending moment $M_A=W\bullet R/\pi=23,642\times18/\pi=135,459Nm$

where, W=23,642N and R=18m.

modulus of section $Z=15^2\times150/6=5,625mm^3$

bending stress $\sigma_b=135,454,032/5,625=24,081MPa$

allowable limit $1.5kSm=1.5\times1.2\times138=248MPa$

The stress is much larger than the allowable limit. Some damping devices are assumed to be feasible to reduce the stress. However, the conventional dampers cannot be applied because of the following problems.

i. activation of oil in the case of passive dampers
ii. uncontrollableness at loss of electric source or pressurized air in the case of active dampers

[Reference]"Formulas for Stress and Strain", Roark and Young, McGrow-Hill Book Company

(4)Conclusions

Structural integrity of the cryostat cylinder thermal shield suspended by rods in seismic events is studied. The results can be summarized as follows:

i. Natural period of the thermal shield is in resonant region with the tokamak pit.
ii. Bending stress that occurs in the thermal shield is much larger than the allowable limit.

As stated above, the concept of suspended thermal shield is not consistent with the design requirement. Therefore, the thermal shields should be fitted up with stiff supports to the warm surface.

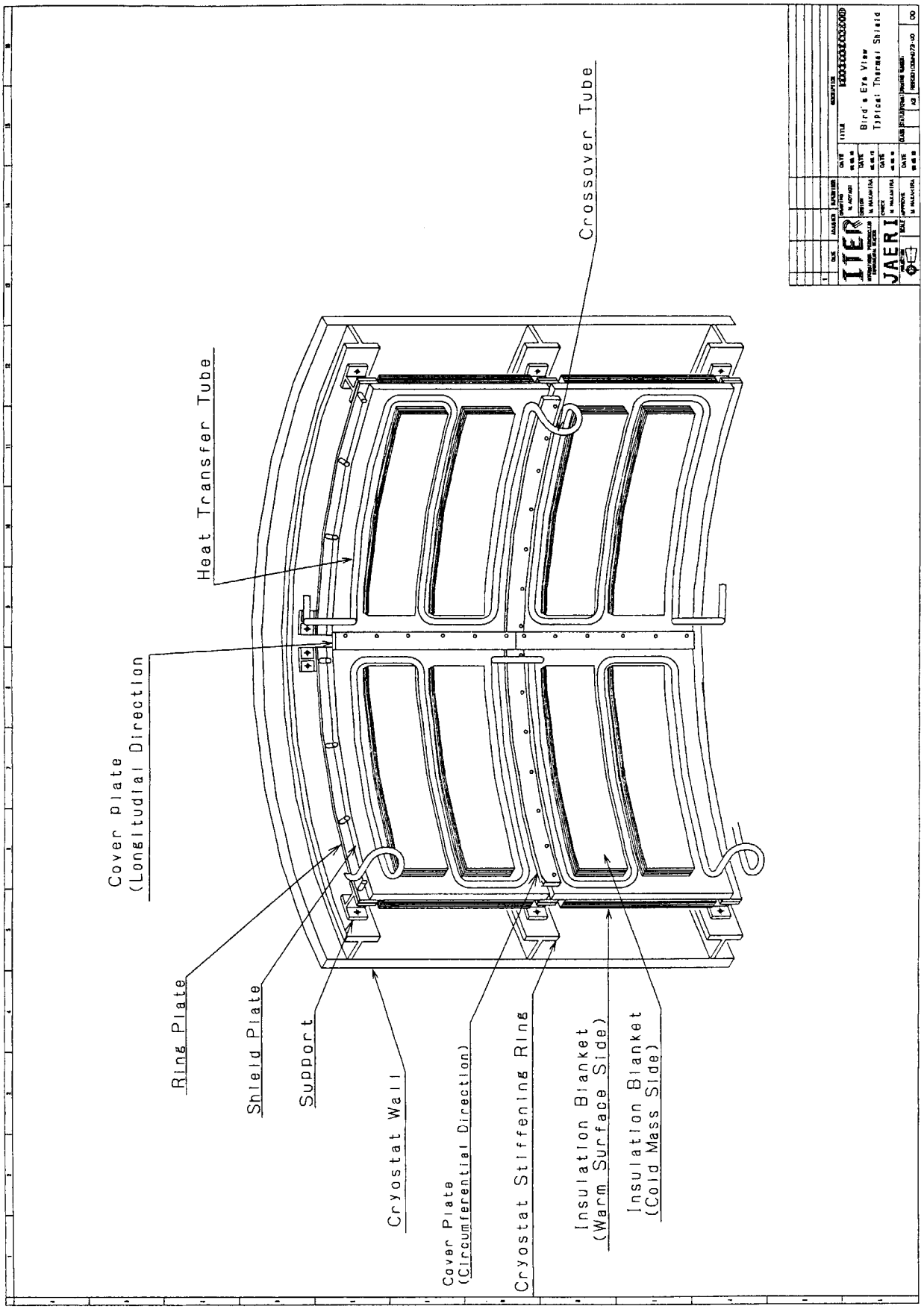

Fig. 3-1 Typical Thermal Shield (Bird's Eye View)

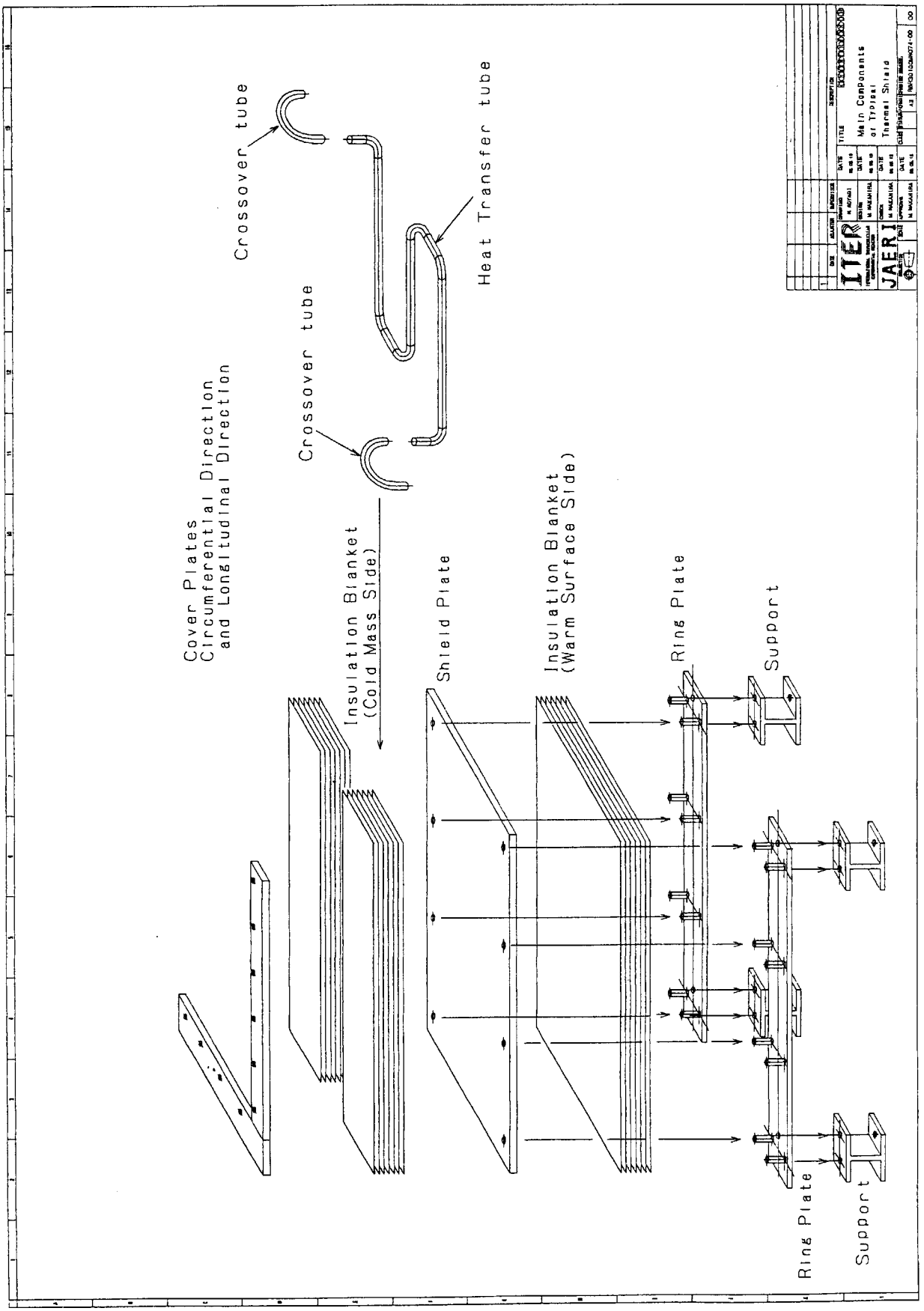

Fig 3-2 Main Components of Typical Thermal Shield

3.2 Thermal insulation

As shown in the dose rate analyses conducted by JAERI, there is a higher dose region of up to 10-MGy around the NBI ducts including the ducts themselves. The multi-layer insulation (MLI) made of polyester or polyimide cannot be used in this region any more. Therefore, multistory reflecting plates made of type 304 stainless steel should be applied to the portion. In this section, study on thermal insulation consisting of multistory reflecting plates are presented.

(1) Location

The reflecting plates are applied to the following location:

i. the NBI ducts themselves (three ducts)
ii. the cryostat cylinder at the vicinity of the ducts

(2) Material

i. reflecting plates — type 304 stainless steel with silver-coating to reduce the emissivity
ii. spacers — GFRP(S-glass)
iii. bolts and nuts GFRP (S-glass)

"GFRP" means a glass fiber reinforced plastics.

(3) Structure

a. Insulation

Considering dimension of a vacuum furnace of the deposition equipment, the size of the reflecting plates should be limited to approximately 500mm×500mm. The thickness of the plate is 0.3mm, that is the minimum thickness of the cold forming plate made of type 304 stainless steel.

As shown the figure on the right, the plates are overlapped each other.

To reduce the emissivity, the plates should be silver-deposited. The emissivity of silver-deposited surface is estimated to be 0.012 at 300K (Reference; Cryogenic Engineering Handbook). Factor of two is multiplied, so that the emissivity can be set up to 0.025. This emissivity is about one half of the aluminum-deposited surface.

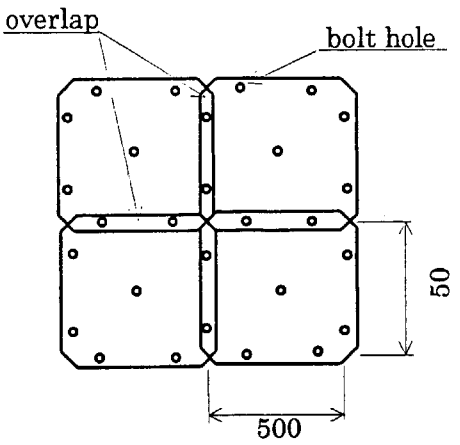

Plane view of reflecting plates

Figure 3-3 shows a concept of the insulation consisting of the reflecting plates. The thermal shield equipped with the reflecting plates should be installed at the same surface with the adjacent thermal shield equipped with the MLI blanket. As the heat leak from the thermal shield with reflecting plates seems to be larger than that with the MLI blanket, the heat transfer tube on the shield plate should be arranged more closely to equalize the heat leak as much as possible.

b. Fixtures

The fixtures consists of spacers, bolts and nuts machined from laminated plates made of GFRP. Dimension of each component is as follows:

i. spacers 7mm in inner diameter, 10mm in outer diameter and 6mm in height
ii. bolts M6 with ϕ6mm shaft
iii. nuts M6

(4) Heat flux calculation method

Radiation heating rate from warm surface at T_0(K) to cold surface at T_1(K) is

$$Q = \sigma \cdot A_p \frac{T_0^4 - T_1^4}{1/\varepsilon_c + 1/\varepsilon_h - 1} \quad (1)$$

Sum of radiation between the reflecting plates and conduction from the fixtures is,

$$Q_j = \sigma \cdot A_R \frac{T_j^4 - T_{j+1}^4}{2/\varepsilon_c - 1} + \frac{\lambda \cdot m \cdot A_c}{l}\left(T_j - T_{j+1}\right). \quad (2)$$

Where, m, A_R, A_C and l are the number of the fixture, the surface area of the reflecting plate, the sectional area of unit fixture and the length of unit spacer, respectively. ε is the emissivity and σ is the Stefen - Boltzmann constant.

Generally, emissivity of metal surface becomes smaller as temperature becomes lower. In this task, emissivity of the reflecting plates was set up to one at room temperature to make the design conservative. Heating rate through the i-th layer Q_j (for j=1-N-1) are equal to Q. Summing up the equation (2) from j=1 to j=N-1,

$$Q = \frac{1}{N-1}\left[\sigma \cdot A_R \frac{T_1^4 - T_N^4}{2/\varepsilon_c - 1} + \frac{\lambda \cdot m \cdot A_c}{l}\left(T_1 - T_N\right)\right] \quad (3)$$

From numerical calculation using the equation (1) and (3), heating rate Q and temperature T_0 can be obtained. Then, temperature at each of the reflecting plates can be obtained from the equation (2). Finally, the heat flux is defined as $q = Q/A_R$.

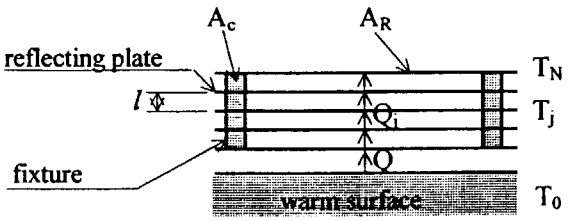

Sectional view of reflecting plates

(5) Heat flux calculation results

Figure 3-4 shows the relationship between number of the reflecting plates and heat flux. The number was set up to fifteen to keep heat flux approximately $2W/m^2$, which is almost the same as that of the MLI blanket. Figure 3-5 shows temperature at each plate in the case of fifteen layer reflecting plates.

(6) Integrity of GFRP bolt

Structural integrity of the GFRP bolt can be confirmed as follows:

i. dead weight of the reflecting plates

$$w=15\times(0.5\times0.5\times0.0003)\times7900\times9.8=87N\rightarrow100N$$

ii. number of bolts $n \geq 5$
iii. moment arm length $L=6\times(15-1)+0.3\times15=88.5mm \rightarrow 100mm$
iv. bending moment $M=(w/n)(L/2)=(100/5)\times(100/2)=1000Nmm$
v. sectional modulus $Z=\pi 6^3/32=21.2mm^3$
vi. bending stress $\sigma_b=M/Z=1000/21.2=47.2MPa$
vii. allowable limit $1.5kSm=1.5k(Su/3)=1.5\times1\times(1200/3)=600MPa$
(Criterion; ASME B&PV Code, Sec. VIII, Div.2)

(7) Supports

Number of the supports made of Ti-6Al-4V is four for the thermal shield equipped with the MLI blanket. As for the thermal shield fitted up with the reflecting plates, six supports are required to keep their integrity.

(8) Estimation of the heat leak

a. Heat leak through the insulation

heat flux; $q=2W/m^2$
surface area of insulation; $A=8.42m^2$
$\therefore Q_1=q\times A=2.0\times8.42=16.9W/shield\ plate$

b. Heat leak from the support made of Ti-6Al-4V

mean thermal conductivity; $k=5.63W/mK$[□□□]
length of the support; $L=130mm$
sectional area of the support; $A=250mm^2$
$\therefore Q_2=kA\Delta T/L=5.63\times0.00025\times(300-80)/0.13=2.4W/support$

Thermal conductivity of Ti-6Al-4V is linearly dependent on temperature such as $\lambda=0.0177T+2.2672 \quad (W/mK)$ for temperature range of 80K ≤ T ≤ 300K. Therefore, the mean thermal conductivity of the alloy is,

$$\bar{\lambda}=\frac{\int_{80}^{300}\lambda dt}{300-80}=5.63 \quad (W/mK).$$

c. Heat leak from non-insulated portion

heat flux; $q=\sigma\dfrac{T_h^4-T_c^4}{1/\varepsilon_c+1/\varepsilon_h-1}=5.678\times10^{-8}\times\dfrac{300^4-80^4}{1/0.025+1/0.5-1}=11.16W/m^2$

thermal shrinkage(300K→80K, type304SS); $\varepsilon_T=0.29\%$
total surface area of non-insulated portion; $A=3\times(0.175\times0.25)=0.132m^2$
shrinkage of insulation; $A'=[1-(1-\varepsilon_T)^2]A_0=[1-(1-0.0029)^2]\times8.12=0.047m^2$
$\therefore Q_3=q(A+A')=11.16\times(0.132+0.047)=2.0W/shield\ plate$

d. Total heat leak

As shown in Table 3-2, heat leak of the thermal shield with reflecting plates is about 1.3 times larger than that with the MLI blanket.

Table 3-2 Heat leak of insulation

heat leak / insulation	through insulation itself		from support		from non-insulated portion		total
	$q(W/m^2)$	$Q_1(W)$	$q(W)$	$Q_2(W)$	$q(W/m^2)$	$Q_3(W)$	$Q(W)$
Reflecting plates	2.0	16.9	2.4	14.4	11.16	2.0	33.3
MLI blanket	1.5	12.9	2.4	9.6	11.16	$4.0^{(*1)}$	26.5

; Thermal shrinkage of the MLI blanket is estimated ε_T=1.4%, that is an average of $\varepsilon_{T,t}$=1.6% and $\varepsilon_{T,l}$=1.2%.

(9) External heating

a. Nuclear heating

According to analytical results carried out by JAERI, heat flux at cryostat cylinder thermal shield due to neutron and γ-ray can be estimated as shown in Table 3-3. Here, heat flux is defined as the product of nuclear heating rate and thickness of the shield plate.

Table 3-3 Heat flux due to nuclear heating

insulation	nuclear heating rate (W/cc)	thickness of shield plate (mm)	heat flux (W/m^2)
Reflecting plates	5×10^{-3}	3	15.0
MLI blanket	5×10^{-4}	3	1.5

b. Joule heating

Heat flux of Joule heating due to the coil quench can be estimated as $0.5W/m^2$ referring to the EM-force analyses conducted in FY'96. Because the heat flux is absolutely small, the effect of Joule heating on necessary mass-flow-rate of coolant seems to be negligible.

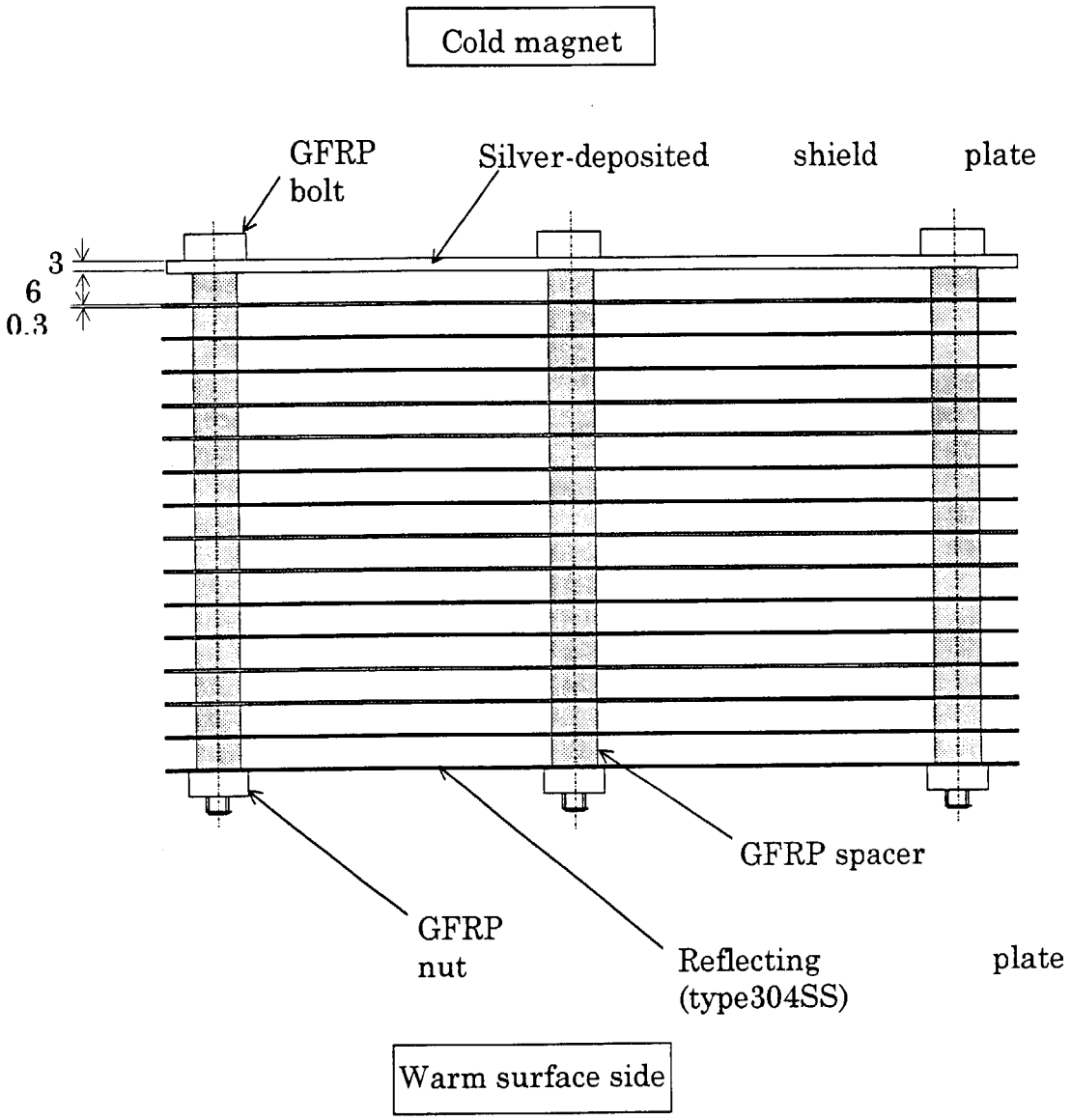

Fig. 3-3 Schematic figure of the reflecting plates

3.3 Arrangement of heat transfer tube

To keep the shield plate temperature lower than 100K, suitable arrangement of the heat transfer tube on the plate was studied using finite element analyses (FEA). The cryostat cylinder thermal shield is selected as a typical one. Both of the thermal shield equipped with the MLI blanket and that with the reflecting plates are analyzed.

(1) Analytical conditions

Table 3-4 shows the analytical conditions with brief summary of the results. The parameters of FEA are as follows:

i. Arrangement of heat transfer tube on the shield plate
ii. Type of the thermal insulation (MLI blanket or reflecting plates)

Table 3-4 Analysis conditions with judgment

No.	arrangement of heat transfer tube on the shield plate	type of thermal insulation	overall heat transfer coefficient (W/m^2K)	thickness of the shield plate (mm)	judgment
1	two-turn	MLI blanket	457	3	good
2	three-turn				good
3	two-turn	Reflecting plates			NG
4	three-turn				NG
5	four-turn				good

(2) FEA model

Specifications of the FEA model are as follows:

i. two dimensional model of unit thermal shield plate
ii. schematic figure of the model; refer to Figure 3-6
iii. boundary condition; adiabatic condition at each edge of the plate
iv. tube size; ODϕ34.0mm, t3.0mm
v. FEA program; ANSYS

(3) Temperature distribution analysis method

a. Type of analyses

i. steady state temperature distribution analysis

b. Heat inputs

Followings are heat inputs considered in the analyses. Table 3-5 shows each heat flux. In Figure 3-6, the points to set the following ii and iii are also indicated.

i. heat leak through insulation (uniformly distributed heat flux)
ii. heat leak from support (concentrated heat flux)
iii. heat leak from non-insulated portion (locally distributed heat flux)
iv. nuclear heating (uniformly distributed heat flux)
v. Joule heating (uniformly distributed heat flux)

Table 3-5 Summary of Heat Flux

type of thermal insulation / heat input	MLI blanket	Reflecting plats
i. heat leak through insulation (W/m^2)	1.5	2.0
ii. heat leak from support (W/point)	1.2	1.2
iii. heat leak from non-insulated portion (W/m^2)	11.2	11.2
iv. nuclear heating (W/m^2)	1.5	38.0
v. Joule heating (W/m^2)	0.5	0.5
uniformly distributed heat flux [i +iv +v] (W/m^2)	3.5	40.5
locally distributed heat flux [iii] (W/m^2)	11.2	11.2
concentrated heat flux [ii] (W/point)	1.2	1.2

As the heat flux will be distributed to the adjacent plate, half of heat flux described in 3.2-(8)-b was set up to the analyses.

c. Coolant condition
   i. bulk temperature of the coolant; T=80K
   ii. overall heat transfer coefficient; $U=457 W/m^2K$ (refer to 3.5.1 -e -(d))

d. Thermophysical properties

Table 3-6 shows thermophysical properties of type 304 stainless steel.

Table 3-6 Thermophysical properties of type304SS

temperature(K)	item	property
80~100	thermal conductivity (W/m K)	9.5
	specific heat (J/g K)	0.2
	density (kg/m^3)	7920

(4) Results of temperature distribution analyses

Temperature distribution obtained by the analyses are shown in the following figure. Here, "HTT" means the heat transfer tube arranged onto the shield plate.

i. MLI blanket, two-turn HTT Figure 3-7
ii. MLI blanket, three-turn HTT Figure 3-8
iii. Reflecting plates, two-turn HTT Figure 3-9
iv. Reflecting plates, three-turn HTT Figure 3-10
v. Reflecting plates, four-turn HTT Figure 3-11

From these results, followings can be confirmed.

i. Hot spot temperature on the shield plate equipped with the MLI blanket is 86.7K for two-turn HTT arrangement and 84.0K for three-turn arrangement. Two-turn

for two-turn HTT arrangement and 84.0K for three-turn arrangement. Two-turn HTT arrangement is applicable to keep the shield plate lower than 100K.

ii. As for the reflecting plates, the hot spot temperature is 115.3K for two-turn arrangement, 101.5K for three-turn arrangement and 96.1K for four-turn arrangement. Therefore, four-turn HTT arrangement is required to keep the shield plate lower than 100K.

iii. Hot spots appear at the edges in the long side direction where HTT is not arranged. So, HTT should be arranged as closely as possible to the edges of the shield plate.

(5) Stress analyses

Stress analyses due to the temperature distribution were carried out under following conditions. The FEA program applied is ANSYS.

Case-1 MLI blanket, two-turn HTT arrangement

Case-2 Reflecting plates, four-turn HTT arrangement

a. Boundary condition

Following boundary conditions are defined at the mechanical interfaces to the support.

long side direction (X); elastic support

short side direction (Y); free

vertical direction (Z); constraint

The spring constant defined to the long side direction is estimated by following manner:

$$K = \frac{3EI}{L^3} = \frac{3 \times 118000 \times \left(50 \times 5^3 / 12\right)}{130^3} = 84 N / mm$$

b. Mechanical properties

Table 3-7 shows mechanical properties of type 304 stainless steel.

Table 3-7 Mechanical properties of type304SS

temperature (K)	item	property
80~100	modulus of longitudinal elasticity (GPa)	200
	Poisson's ratio (---)	0.3
	linear expansion coefficient (1/K)	13.3×10^{-6}

c. Analysis results

Figure 3-12 and Figure 3-13 show stress intensity distribution of the shield plate under each of the cases. Unit of the stress intensity is N/m^2. From the results, maximum stress intensity including supposed error as indicated "SMXB" in these figures are as follows:

Case-1 11.7MPa

Case-2 19.3MPa

As the stress intensity is classified into the secondary stress, the allowable stress limit is 3Sm=414MPa. The stresses appear in the shield plate are sufficiently lower than the allowable stress limit. The short side direction of the shield plate, e.g. the stiff axis of the

support, should be free to prevent higher stresses. Therefore, a loose-jointed mechanism is required at the interface between the ring plate and the supports in the short side direction.

Maximum in-plane deflection of the shield plate as indicated "DMX" in Figure 3-12 and 3-13 are as follows:

Case-1	9.4mm
Case-2	9.3mm

(6) Conclusions

Suitable arrangement of the heat transfer tube (HTT) on the shield plate is studied using FEA. The conclusions obtained are as follows:

i. For the thermal shield equipped with the MLI blanket, two-turn HTT arrangement can be applied.
ii. For the thermal shield equipped with reflecting plates, four-turn HTT arrangement should be required.
iii. To mitigate hot spot temperature, HTT should be arranged as closely as possible to edges of the shield plate especially in the long side direction.
iv. The stress intensity due to the temperature distribution is sufficiently lower than the allowable stress limit. However, the short side direction of the shield plate should be loose to prevent higher stresses.

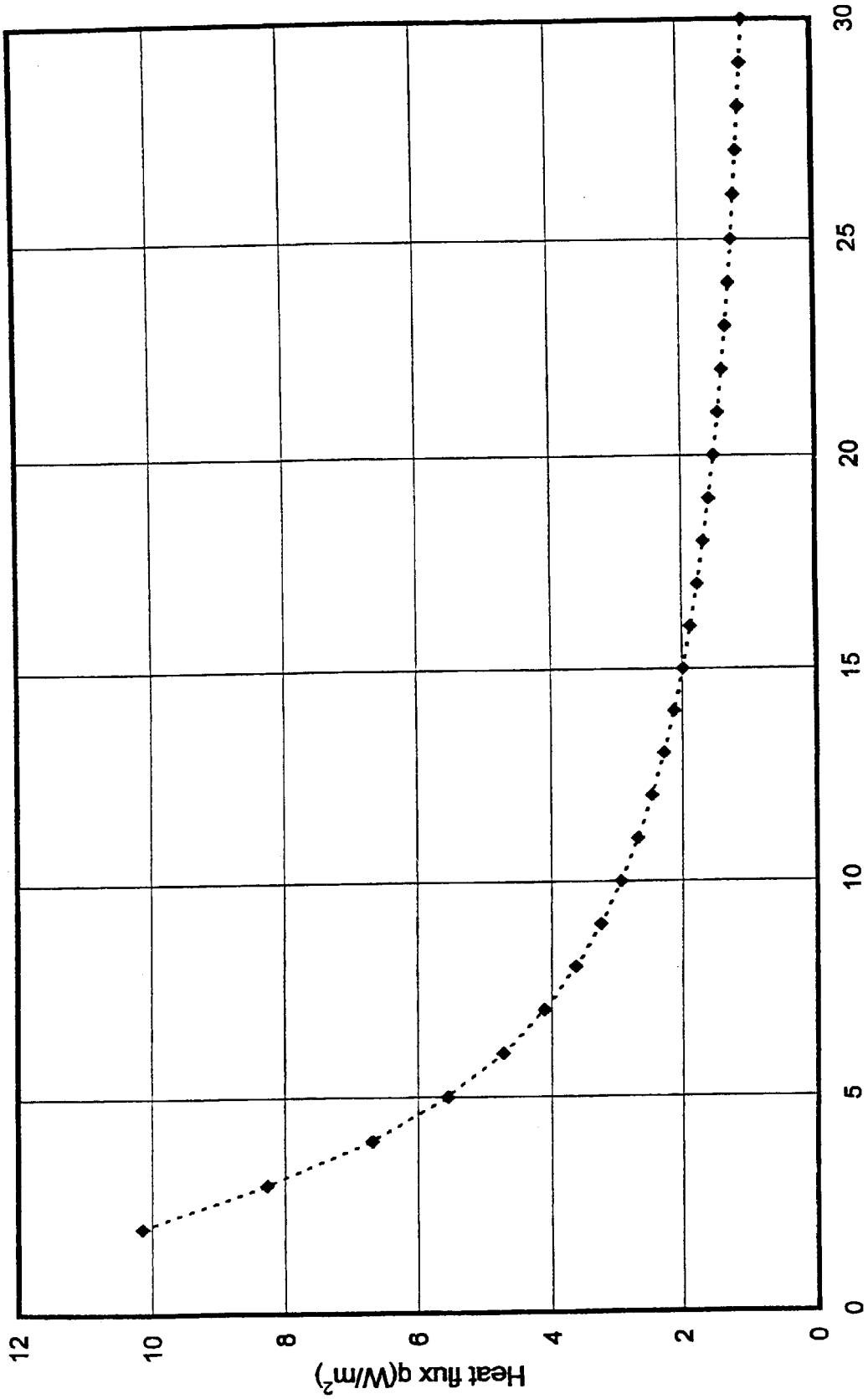

Fig. 3-4 Heat flux as a function of number of the reflection plates

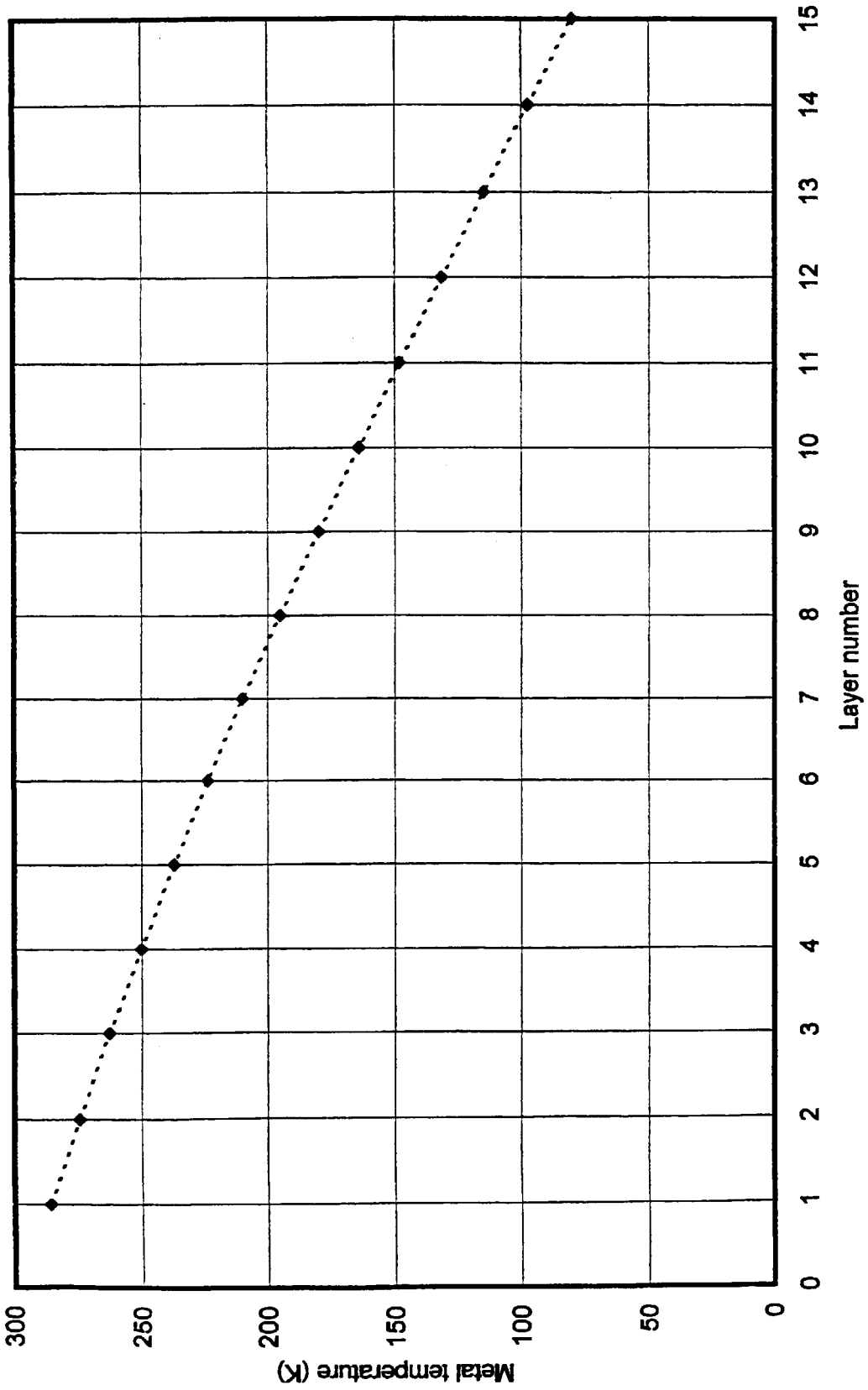

Fig. 3-5 Temperature of the reflection plates as a function of layer number

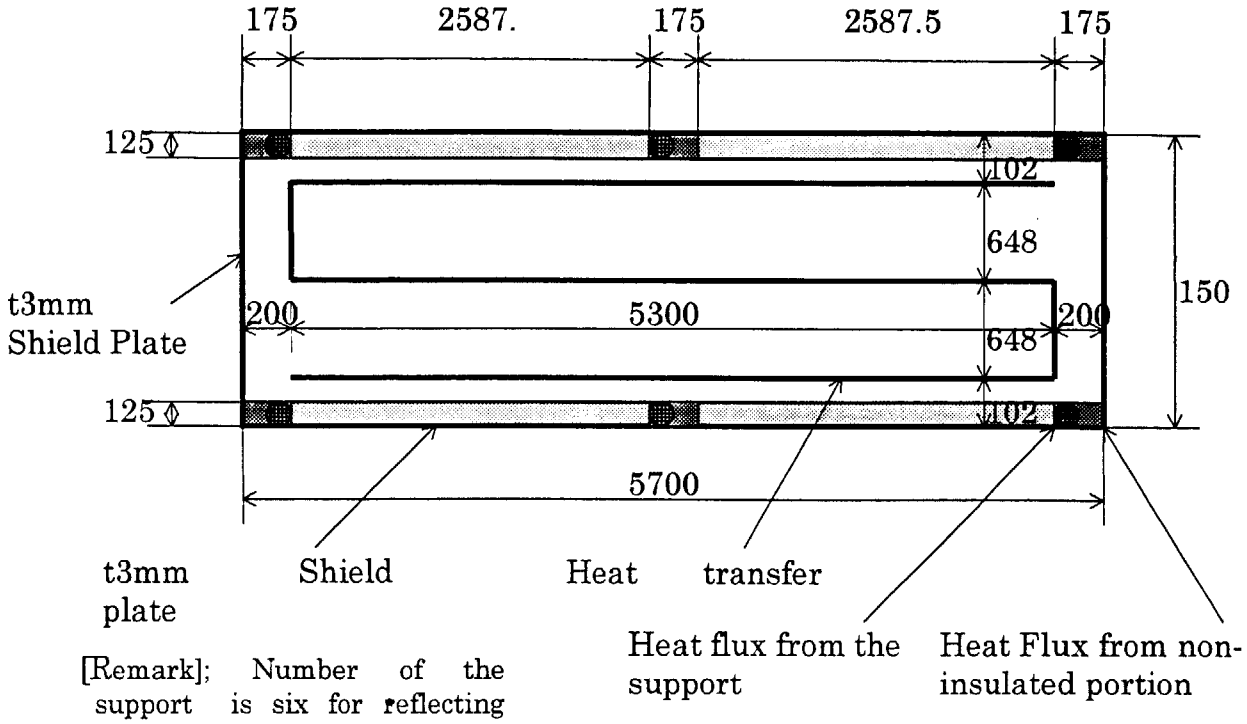

[Remark]; Number of the support is six for reflecting plates and four for the MLI blanket.

(1) Two-turn HTT

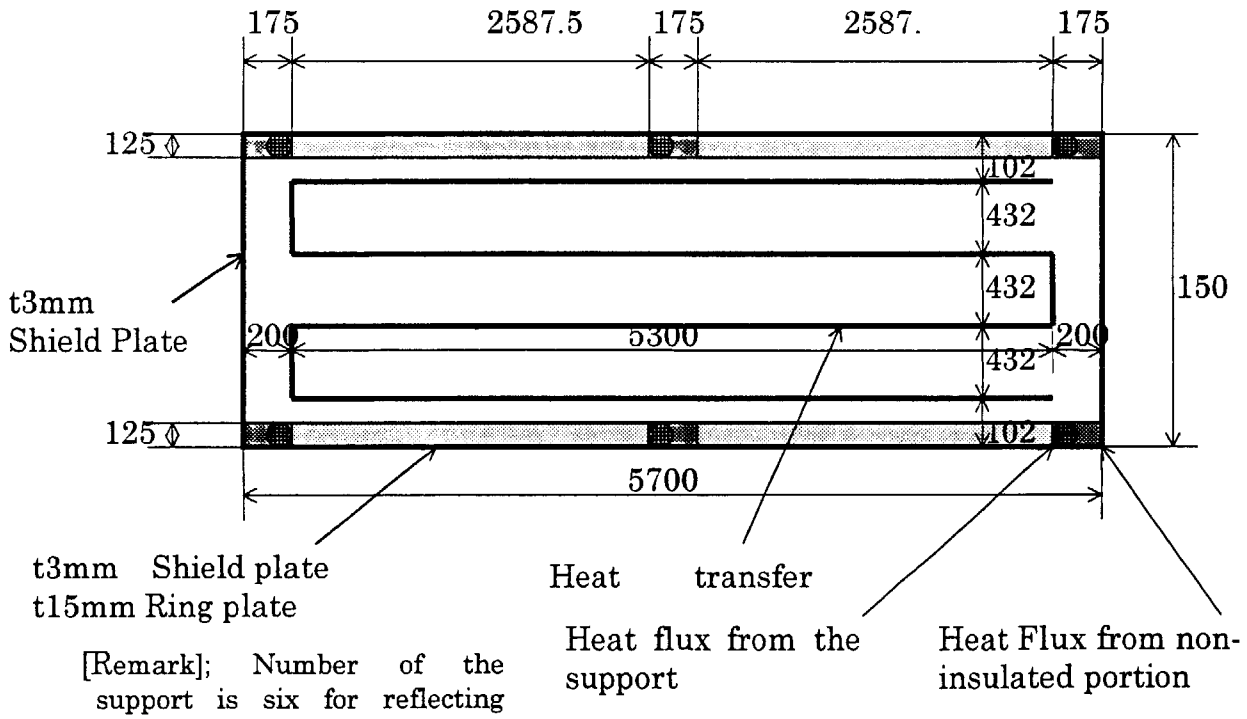

[Remark]; Number of the support is six for reflecting plates and four for the MLI blanket.

(2) Three-turn HTT

Fig. 3-6(1/2) FEA model of the thermal shield

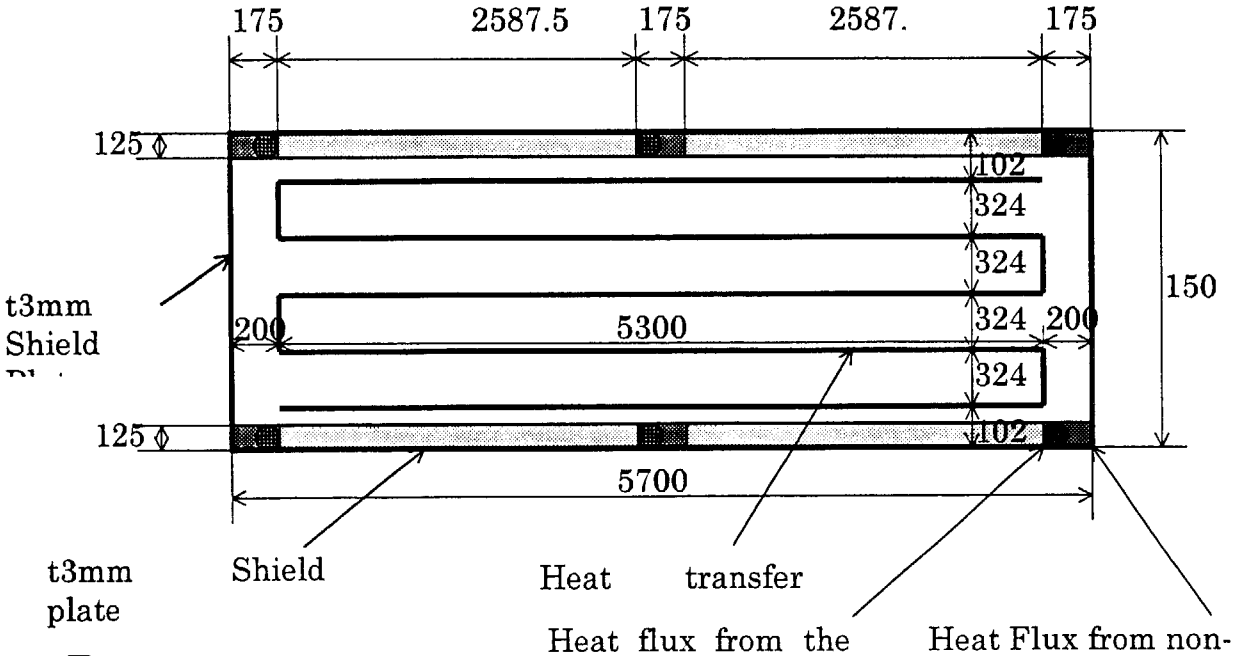

[Remark]; Number of the support is six for reflecting plates and four for the MLI blanket.

(3) Four-turn HTT

Fig. 3-6(2/2) FEA model of the thermal shield

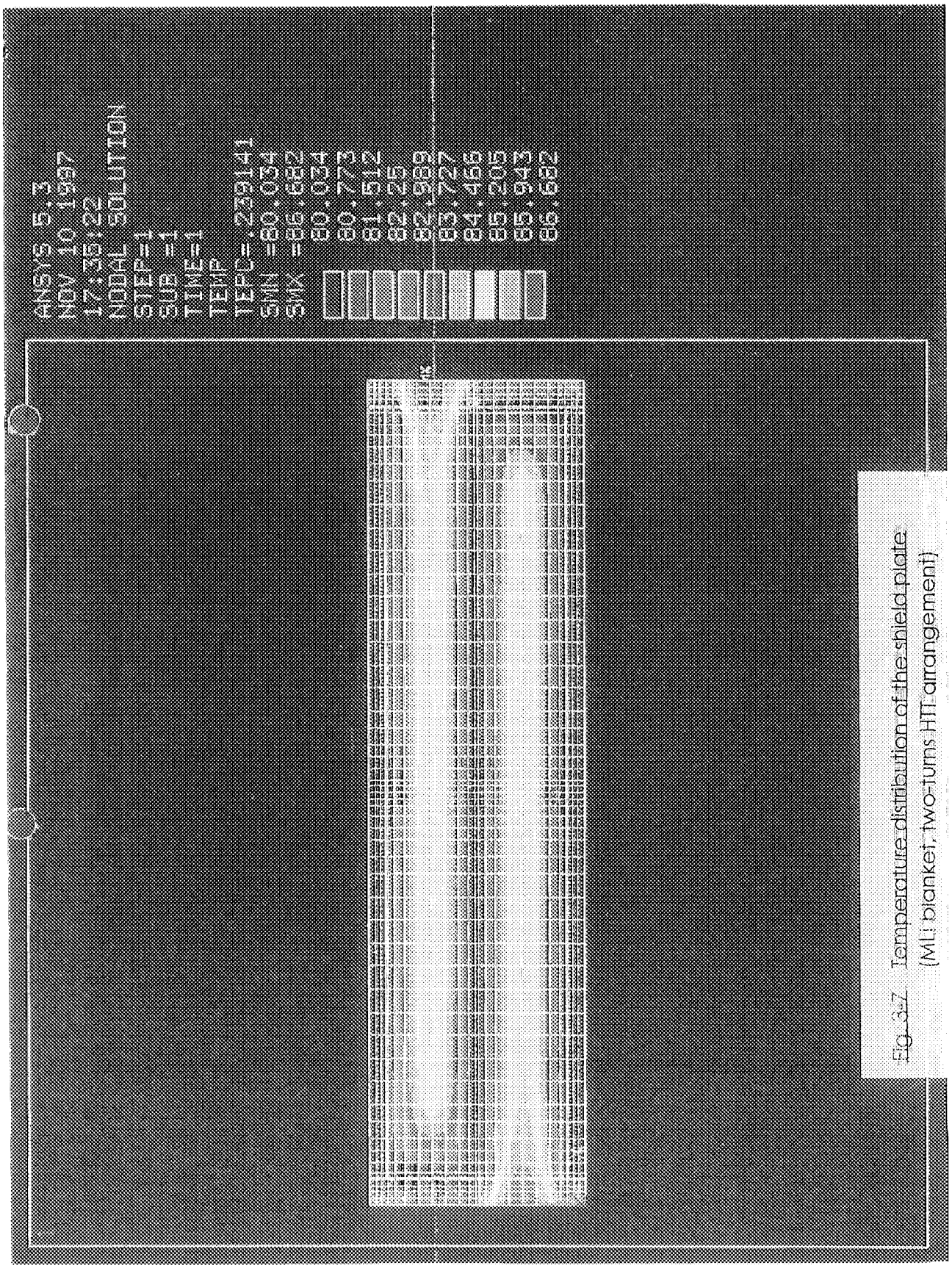

Fig. 3.7 Temperature distribution of the shield plate (ML: blanket, two-turns HTS arrangement)

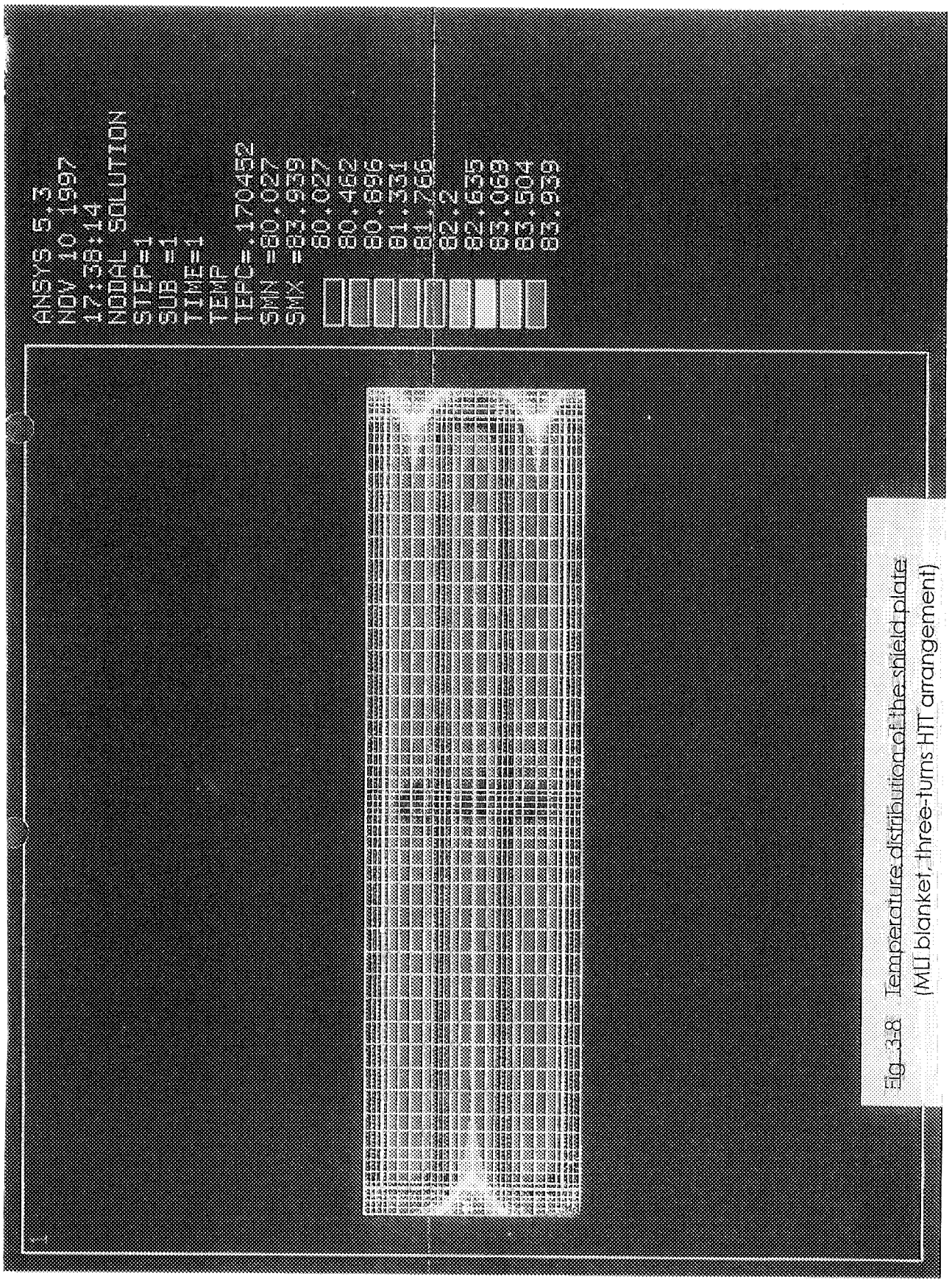

Fig. 3-8 Temperature distribution of the shield plate (MLI blanket, three-turns HTT arrangement)

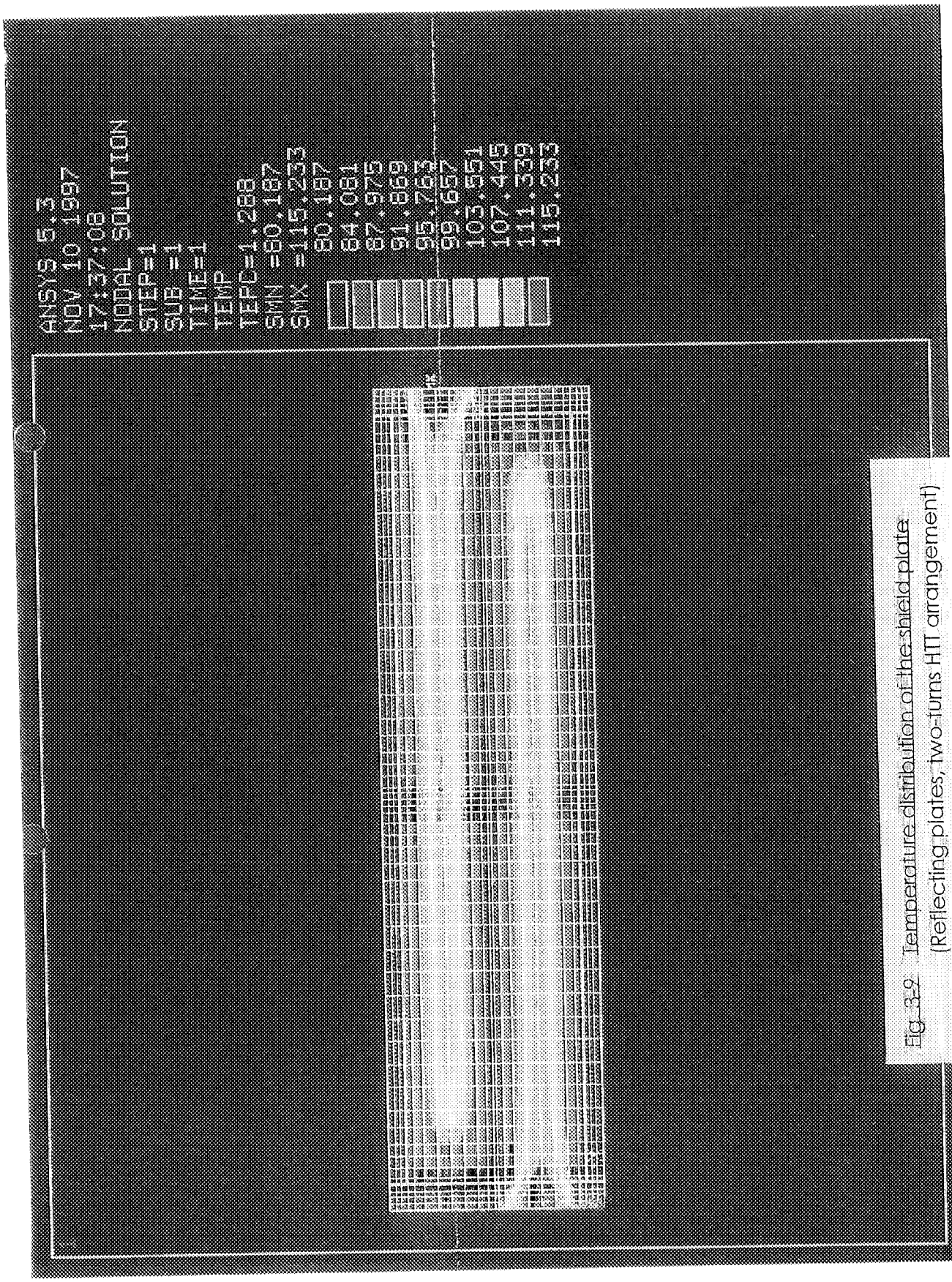

Fig. 3-9 Temperature distribution of the shield plate (Reflecting plates, two-turns HTI arrangement)

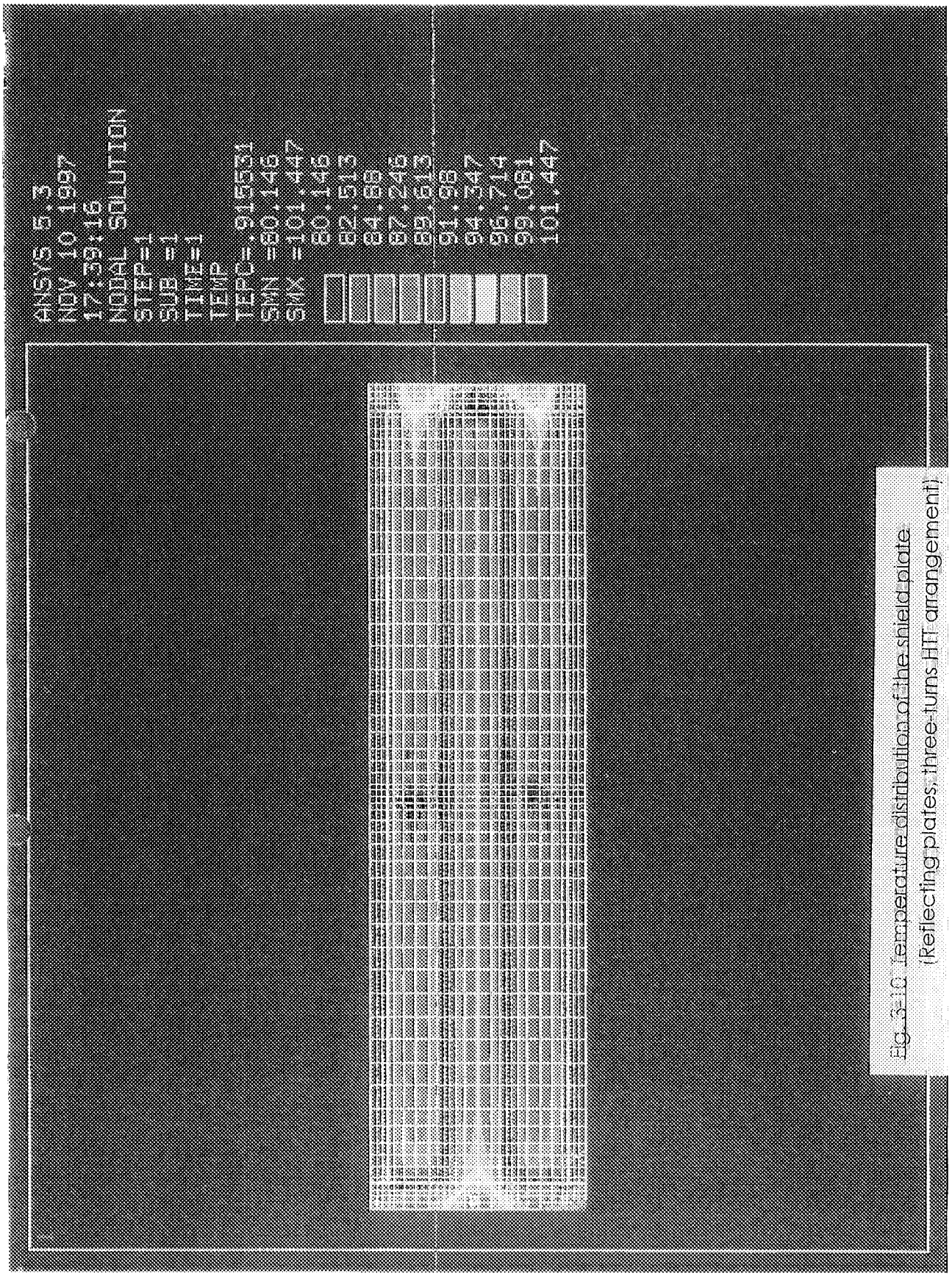

Fig. 3-10 Temperature distribution of the shield plate (Reflecting plates, three-turns HTT arrangement)

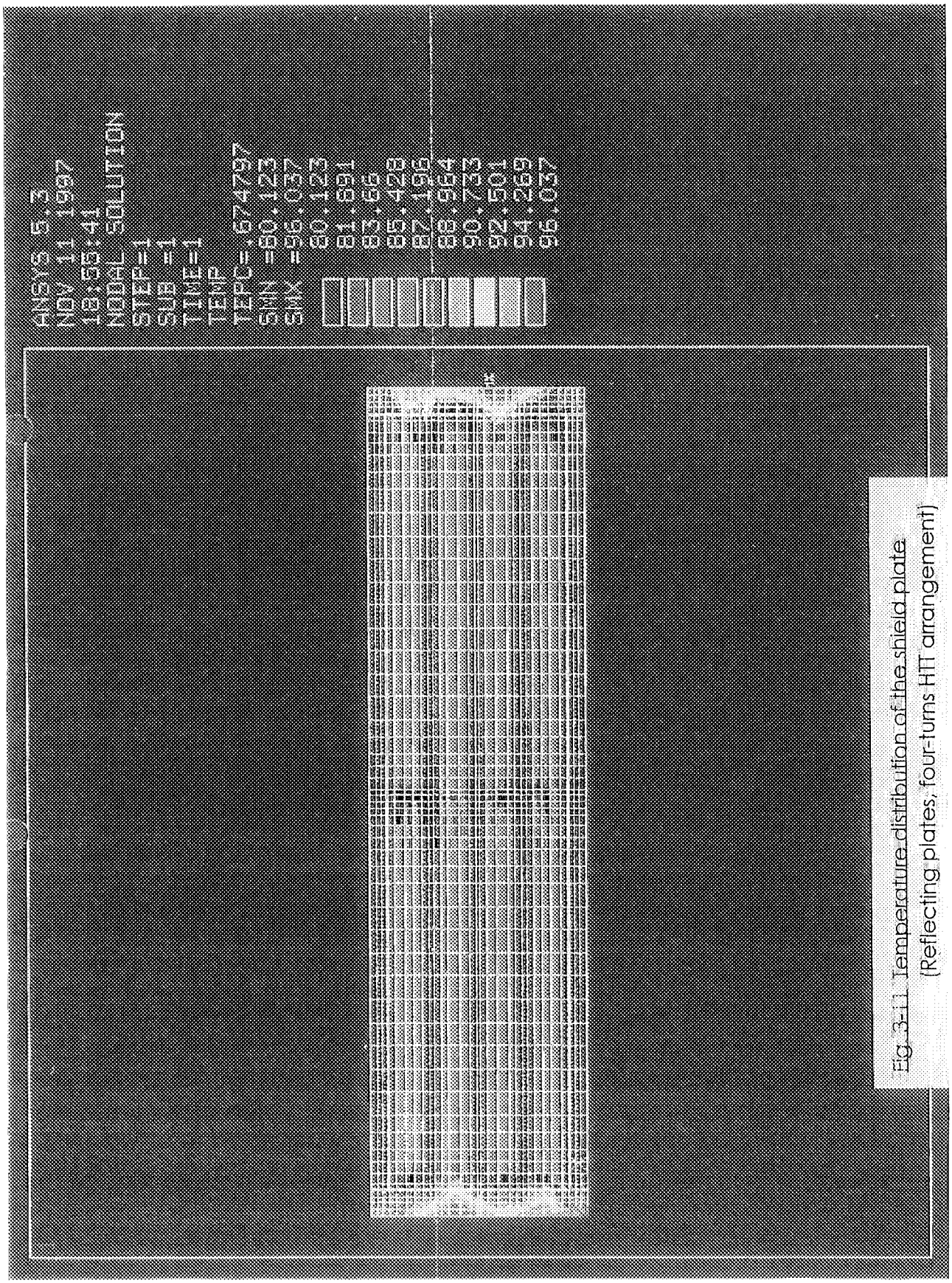

Fig. 3-11 Temperature distribution of the shield plate
(Reflecting plates, four-turns HTT arrangement)

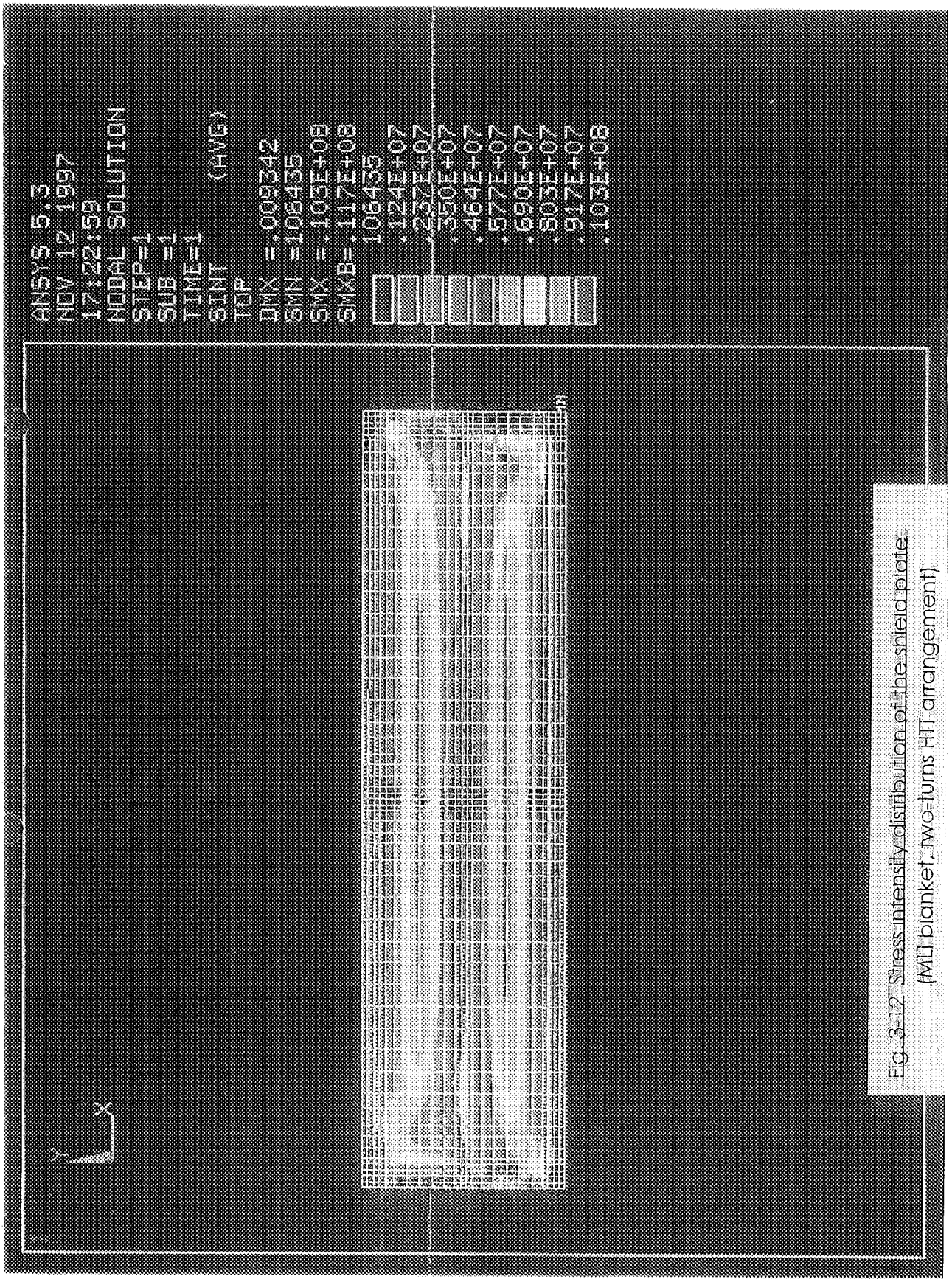

Fig.3.12 Stress intensity distribution of the shield plate (MLI blanket, two-turns HTI arrangement)

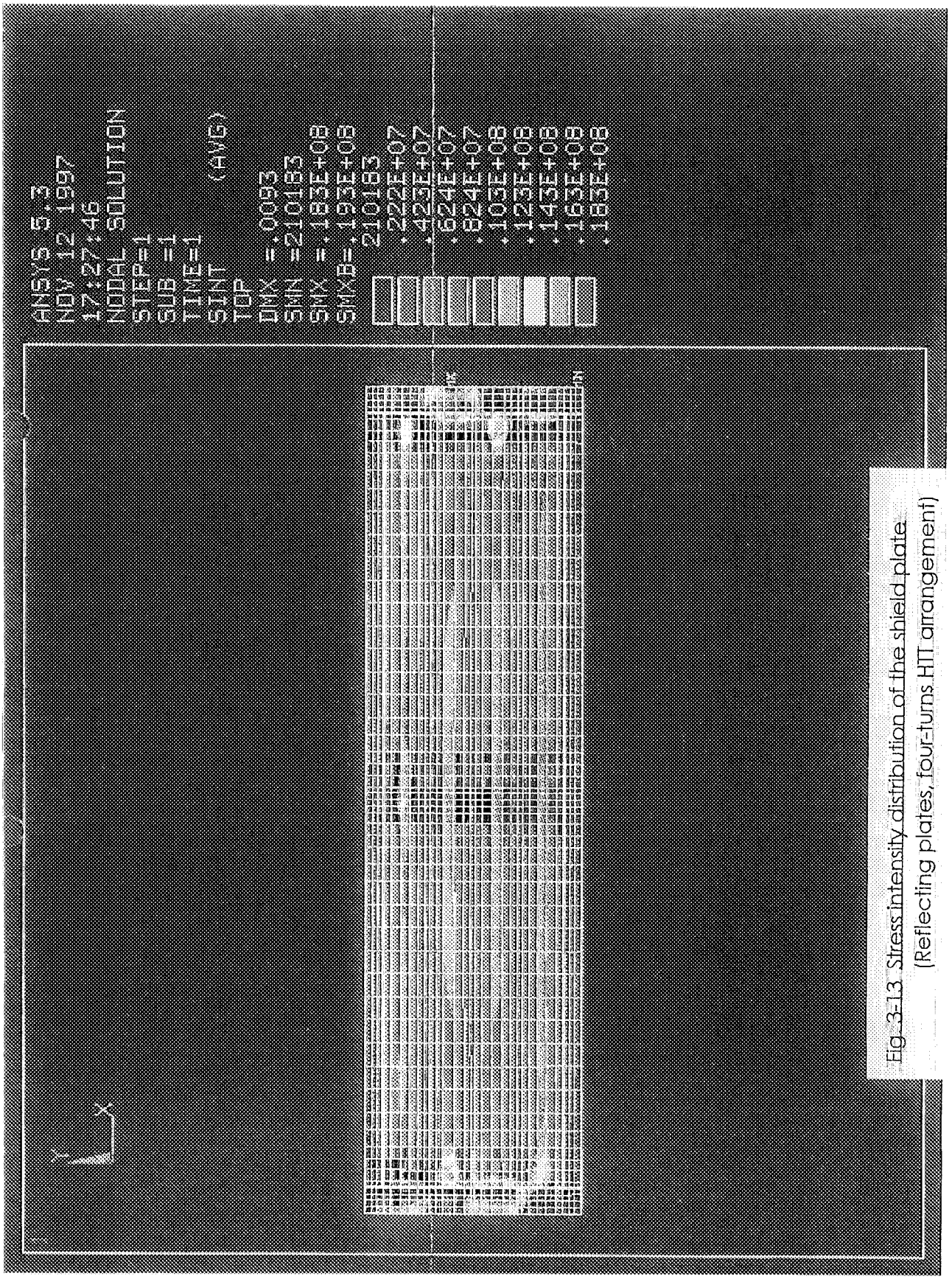

Fig. 3-13 Stress intensity distribution of the shield plate (Reflecting plates, four-turns HTT arrangement)

3.4 Crossover tube between adjacent thermal shield

The crossover tube between adjacent thermal shield is subjected to forced displacement by thermal shrinkage of the shield plate. Stresses appear in the tube was analyzed and the integrity was assessed.

(1) Configuration of the crossover tube

The crossover tube consists of two 90° bending pipe and a 180° bending pipe. The radius of curvature of the bending pipe is three times as long as the outer diameter.

Due to following design requirements, piping elbows standardized by JIS were not applied to the crossover tube.

i. reduction of pressure loss ($\Delta P \propto R$)
ii. reduction of stress index ($C_2 \propto R$)
iii. elimination of welding joints

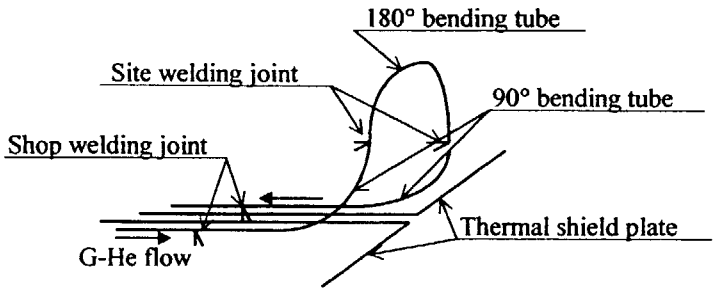

(2) FEA model

i. three dimensional beam model
ii. tube size; OD34mm, t3mm
iii. radius of curvature; 102mm
iv. material; type 304 stainless steel
v. FEA model; refer to Figure 3-14
vi. FEA program; SAP

(3) FEA conditions

Forced displacement of 4.4mm at #5-point is subjected in X-direction under constraint at #1-point for all degree of freedom. Mechanical properties of type 304 stainless steel are tabulated in Table 3-7.

Thermal shrinkage of typical shield plate in the short side direction is estimated as $\delta=1500\times0.0029=4.35$mm.

(4) Stress evaluation method

Using stress index, C_2 prescribed in ASME B&PV Code, Section III, Class-1 piping, stress intensity were evaluated. As the stresses are classified into the secondary stress, the allowable stress is equal to the shakedown limit, 3Sm. For type 304 stainless steel, the limit can be estimated as $3\times138=414$MPa.

; The stress index, C_2, of a pipe bend is estimated as $C_2=1.95/h^{2/3}$. Here, h is the flexibility characteristic and can be obtained as $h= t_n R/r^2$. The symbols, t_n, R, r, are the nominal thickness, the bend radius and the mean radius of the pipe, respectively.

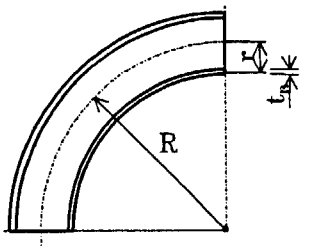

(5) Results

Evaluated stresses are tabulated in Table 3-8. In the middle plane of 180°-bending tube, e.g. #3-point, the stress intensity is multiplied by the stress index, C_2 =1.66.

The maximum stress intensity, 280MPa, is lower than the corresponding allowable stress limit. Therefore, structural integrity of the crossover tube without any bellows expansions can be confirmed.

Table 3-8 Stress intensity evaluation results

point	evaluated stress intensity $C_2 \times \sigma_{nom}$ (MPa)	allowable stress limit 3Sm (MPa)
#1	211.4	414
#2	30.6	
#3	280.0	
#4	30.4	
#5	211.4	

(6) Conclusions

Structural integrity of crossover tube not equipped with bellows expansions was confirmed by FEA.

The outside diameter of the crossover tube considered in this stress analysis is ϕ34mm. For a smaller crossover tube, stresses that appear in the tube will be lower than above mentioned results. This can be easily understood by considering a simple model. Stress at the fixed end of a cantilever-pipe subjected to forced displacement at the tip of the pipe is $\sigma = \frac{3ED\delta}{2L^2}$. Here, σ, E, D, δ and L are the stress, modulus of longitudinal elasticity, outside diameter, forced displacement and pipe length, respectively. From the equation above, stress is directly proportional to the outer diameter and inversely proportional to a square of the pipe length. Therefore, smaller tube is more advantageous to keep integrity of the crossover tube.

3.5 Detailed design description of thermal shield

In this chapter, detailed design outputs of each thermal shield based on structural integrity, heat leak and cooling performance are presented. As for the electromagnetic force and the Joule heating that occur in the shield plates at the coil quench, the results analyzed in FY'96 were used, because the subdivision and the thickness of the shield plates are almost the same as previous analyses.

3.5.1 Cryostat cylinder thermal shield

a. Design concept

i. The thermal shields should be furnished for each stiffening ring of the cryostat cylindrical shell with the supports and the ring plates.
ii. To the interfaces between the ring plate and the supports, a loose-jointed mechanism should be applied not to prevent thermal shrinkage of the shield plate, especially in the stiff axis of the support.
iii. The heat transfer tube should be directly welded to the shield plate at the cold magnet side.
iv. The heat transfer tube made of type 304 stainless steel is 34mm in outer diameter and 3mm in thickness.
v. Basically, the insulation fitted up to the shield plate is the MLI blanket. However, the multistoried reflecting plates should be applied to the vicinity of the NBI duct. Each reflecting plate and the shield plate should be coated with silver to reduce their emissivity.
vi. The thermal shields equipped with reflecting plates should be installed at the same surface with the adjacent shields equipped with the MLI blankets.
vii. Zigzag arrangement in vertical direction should be applied to the heat transfer tube on the shield plates.
viii. Passive insulation without heat transfer tube should be applied to the rids of each RM-port.

b. Configuration

Figure 3-15 shows the configuration of the thermal shield and arrangement of the heat transfer tube.

The shield plate passed through by a pipe or a duct should be divided into two pieces at the penetration point as shown in the figure on the right. Cover plates should be also set up along the split line on the shield plate.

This is a common concept in the current thermal shield design.

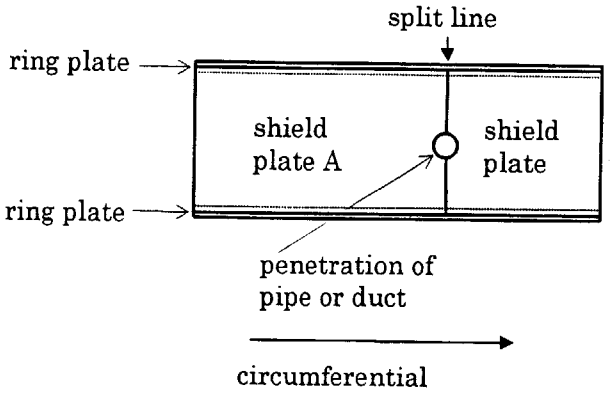

subdivision of a penetrated shield

c. Heat leak

Heat leak of the thermal shield is estimated for the typical one with dimension of 1.5 by 5.7 meters.

(a) Heat leak from the support

$$q = A \cdot \bar{\lambda} \frac{\Delta T}{L} = (0.05 \times 0.005) \times 5.63 \times \frac{300 - 80}{0.13} = 2.4W$$

i.	MLI blanket	4-pieces/plate	9.6W/plate
ii.	reflecting plates	6-pieces/plate	14.4W/plate

(b) Heat leak through the insulation

i.	MLI blanket	$q=1.5W/m^2$	12.9W/plate
ii.	reflecting plates	$q=2.0W/m^2$	16.9W/plate

(c) Heat leak from the non-insulated portion (radiation between silver deposited surface to stainless steel surface)

$$q = \sigma \frac{T_h^4 - T_c^4}{1/\varepsilon_c + 1/\varepsilon_h - 1} = 5.678 \times 10^{-8} \times \frac{300^4 - 80^4}{1/0.025 + 1/0.5 - 1} = 11.2W/m^2$$

i.	MLI blanket	4.0W/plate
ii.	reflecting plates	2.0W/plate

(d) Summation of heat leak

i.	MLI blanket	9.6+12.9+4.0=	26.5W/plate
ii.	reflecting plates	14.4+16.9+2.0=	33.3W/plate

d. Structural integrity

Based upon the criteria prescribed in ASME Boiler & Pressure Vessel Code, Section-VIII, Division-2, structural integrity of the major parts is evaluated.

(a) Integrity of the support made of Ti-6Al-4V

Dead weight of unit thermal shield

Shield plate (1.5m×5.7m×t3mm)	2000N
Ring plate (0.25m×5.7m×t15mm+stiffner)	2000N
MLI blanket (1.5m×5.7m×t12μm×40-layer)	60N
Heat transfer tube (OD34mm×t3mm×25m) 570N	
Total	4630N→×1.2→5600N

safety factor

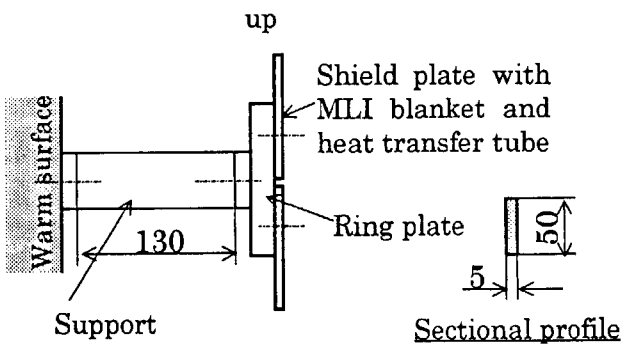

i. Stress due to dead weight

Applied force V=5600/2=2800N

Bending moment M=VL=2800×130=364000Nmm

Modulus of section $Z_V=5\times50^2/6=2083mm^3$

Bending stress $\sigma_b=M/Z=364000/2083=175MPa$
Allowable limit $1.5kSm=1.5\times1\times298=447MPa$

ii. Stress due to seismic force [Horizontal/0.2G, Vertical/-1.2G]

Applied force $H=0.2\times5600/2=560N$ [Horizontal]
$V=(1+0.2)\times5600/2=3360N$ [Vertical]
Bending moment $M_H=HL=560\times130=72800Nmm$ [Horizontal]
$M_V=3360\times130=436800Nmm$ [Vertical]
Modulus of section $Z_H=50\times5^2/6=208mm^3$ [Horizontal]
$Z_V=5\times50^2/6=2083mm^3$ [Vertical]
Bending stress $\sigma_{b,H}=M_H/Z_H=72800/208=350MPa$ [Horizontal]
$\sigma_{b,V}=M_V/Z_V=436800/2083=210MPa$ [Vertical]
Allowable limit $1.5kSm=1.5\times1.2\times298=536MPa$

iii. Stress due to thermal shrinkage [300K→80K, type304SS]

Thermal shrinkage $\delta_1=(5700/2)\times0.0029=8.3mm$ [long side direction]
Thermal shrinkage $\delta_2=(1500/2)\times0.0029=2.2mm$ [short side direction]
[thermal strain under 300K→80K cooling is -0.0029]
Constraint disp. $\Delta\delta=\delta_1=8.3mm$
Bending stress $\sigma_b=3Eh\Delta\delta/(2L^2)$
$=3\times118000\times5\times8.3/(2\times130^2)=435MPa$
Allowable limit $3Sm=3\times298=894MPa$

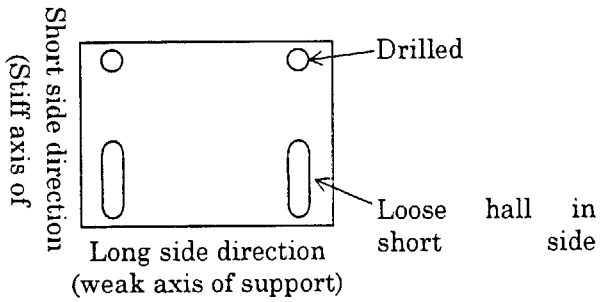

iv. Stress due to combined loading

Load combination thermal shrinkage +(dead weight + seismic force)
Evaluated stress $435+350=785MPa$
Allowable stress $3Sm=3\times298=894MPa$

(b) Natural period of the thermal shield

i. Natural period of in-plane mode

Mass $M=F/g=5600/9.8=572kg$
Stiffness $K=2\times(3EI/L^3)$
$=2\times[3\times(1.18\times10^{11})\times(0.005^3\times0.05/12)]/0.13^3$
$=167843N/m$
Natural period $T=2\pi(M/K)^{1/2}=2\pi(572/167843)^{1/2}=0.37s$

ii. Natural period of out-of-plane mode

Natural period of a square plate supported two opposite sides can be estimated as

$T = \frac{2\pi}{k}\sqrt{\frac{\rho h a^4}{D}}$. (Reference; Harvey, J. Fretscher, J. of Applied Mechanics, 26, Series E, 1959.)

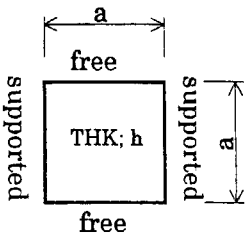

Density $\rho=7900\times(2000+60+570)/2000$
$=10389 kg/m^3$
(The density above is corrected by the added masses excluding the ring plate)

Flexural rigidity $D=Eh^3/12(1-\nu^2)$
$=2\times10^{11}\times0.003^3/12/(1-0.3^2)$
$=495 N/m$
where E, h and ν is the modulus of longitudinal elasticity, the thickness and the Poisson's ratio, respectively.

Factor $k=9.631$

Equivalent side length

$$\bar{a} = \sqrt{a \times b} = \sqrt{1.5 \times 5.7} = 2.93m$$

Natural period $$T = \frac{2\pi}{k}\sqrt{\frac{\rho h \bar{a}^4}{D}} = \frac{2\pi}{9.631} \times \sqrt{\frac{10389 \times 0.003 \times 2.93^4}{495}} = 1.41s$$

(c) Integrity and deflection of the ring plate

i. Stress and deflection due to dead weight

Bending moment $M=FL/12=5600\times5700/12=2660000 Nmm$

Modulus of section $Z_V=(b_1h_1^2+b_2h_2^2)/6h_2$
$=(50\times15^3+15\times250^3)/(6\times250)=156362 mm^3$

Bending stress $\sigma_b=M/Z_V=2660000/156250=17.1 MPa$

Allowable limit $1.5kSm=1.5\times1\times138=207 MPa$

Deflection $\delta=FL^3/(384EI_V)$
$=5600\times5700^3/[384\times200000\times19545312]=0.7 mm$

ii. Stress and deflection due to seismic force

(i) Horizontal direction, 0.2G

Bending stress $\sigma_b=(0.2FL/12)/Z_H$
$=(0.2\times5600\times5700/12)/132005=4.1 MPa$

Allowable limit $1.5kSm=1.5\times1.2\times138=248 MPa$

Deflection $\delta=0.2FL^3/(384EI_H)$
$=0.2\times5600\times5700^3/(384\times200000\times6415468)=0.5 mm$

(ii) Vertical direction, 1.2G

Bending stress $\sigma_b=(1.2FL/12)/Z_V$
$=(1.2\times5600\times5700/12)/156362=20.5 MPa$

Allowable limit $1.5kSm=1.5\times1.2\times138=248 MPa$

Deflection $\delta=1.2FL^3/(384EI_V)$
$=1.2\times5600\times5700^3/(384\times200000\times19545312)=0.9 mm$

(d) Integrity and deflection of the shield plate

Stress and in-plane deflection due to the seismic force in horizontal direction are evaluated as follows:

Applied force $F=5600-2000=3600 N$ (except for the ring plate)

Uniform pressure	$q=F/(ab)=0.2\times3600/(5700\times1500)=0.00084$MPa
Bending stress	$\sigma_b=\beta qb^2/h^2=0.73\times0.000084\times1500^2/3^2=15.4$MPa
Allowable limit	$1.5kSm=1.5\times1.2\times138=248$MPa
In-plane deflection	$\delta=\alpha qb^4/(Eh^3)$
	$=0.14\times0.000084\times1500^4/(200000\times3^3)=11.0$mm

e. Heat transfer and pressure loss

Performance of heat transfer and pressure loss is evaluated. The heat transfer tube made of type 304 stainless steel is 34mm in outer diameter and 3mm in thickness.

Number of the tube-path is twenty and each path should be arranged at every 18° in circumferential direction. A heat transfer path cools down eighteen shield plates in all. Considering a section including the NBI duct, five plates equipped with the reflecting plates and thirteen plates equipped with the MLI blanket are cooled down by the same tube-path.

(a) Heat removal of unit tube-path

i. Heat leak

MLI blanket	$13\times(9.6+12.9+4.0)=13\times26.5=$	345W/path
Reflecting plates	$5\times(14.4+16.9+2.0)=5\times33.3=$	167W/path
Rid of RM-port (passive)	$2\pi\times0.003\times16\times(300-80)\times1=$	67W/path
Summation		579W/path

Total heat leak from the thermal shield of the cryostat cylinder is $20\times579=11.6$kW.

ii. External heating

MLI blanket	$12\times(5.7\times1.5)\times(1.5+0.5)=$	206W/path
reflecting plates	$5\times(5.7\times1.5)\times(15.0+0.5)=$	663W/path
Summation		869W/path

iii. Total removal heating 1448W/path→ 1500W/path

(b) Necessary flow rate of coolant

The necessary flow rate of gaseous helium to keep the shield plates lower than 100K is estimated under the condition that the bulk-temperature rises by 10K and the pressure drops by 0.05MPa through the path. The assumptions above correspond to half of the limitation shown in Table 2-2.

Enthalpy drop	$\Delta h=h_{90K,\ 1.75MPa}-h_{80K,\ 1.8MPa}=487.4-435.2=52.2$J/g
Mass flow rate	$G=Q/\Delta h=1500/52.2=28.7$g/s
Mean velocity in tube	$u=(G/\rho)/A$
	$=(28.7\times10^{-3}/9.105)/(0.028^2\pi/4)=5.12$m/s
Reynolds number	$Re = ud\rho/\eta$
	$=5.12\times0.028\times9.105/(9.372\times10^{-6})=1.393\times10^5$

The thermophysical properties of gaseous helium used above are under the condition of 90K and 1.75MPa.

(c) Pressure loss

i. Pressure loss due to friction in unit tube length, ΔP_1

Friction factor $\lambda=0.3164/Re^{0.25}=0.3164/(1.393\times10^5)^{0.25}=0.0164$

Pressure loss $\Delta P_1=\lambda/d\times(\rho u^2/2)$

$=0.0164/0.028\times(9.105\times5.12^2/2)=7.20\times10^{-5}$MPa/m

ii. Pressure loss at a 180° bending tube, ΔP_2

Pressure loss $\Delta P_2=K_{180°}\times(\rho u^2/2)$

$=1.015\times(9.105\times5.12^2/2)=1.21\times10^{-4}$MPa

iii. Pressure loss at a 90° bending tube, ΔP_3

Pressure loss $\Delta P_3=K_{90°}\times(\rho u^2/2)$

$=1.301\times(9.105\times5.12^2/2)=6.97\times10^{-4}$MPa

iv. Evaluation

(i) Shield plate equipped with the MLI blanket (13 shield plates)

$\Delta P_{MLI}=N(L\times\Delta P_1+N_2\times\Delta P_2+N_3\times\Delta P_3)$

$=13\times[20\times(7.20\times10^{-5})+1\times(1.21\times10^{-4})+6\times(1.55\times10^{-4})]$

$=0.033$MPa/path

(ii) Shield plate equipped with the reflecting plates (5 shield plates)

$\Delta P_{MRP}=N(L\times\Delta P_1+N_2\times\Delta P_2+N_3\times\Delta P_3)$

$=5\times[30\times(7.20\times10^{-5})+1\times(1.21\times10^{-4})+10\times(1.55\times10^{-4})]$

$=0.020$MPa/path

(iii) Total pressure loss

$\Delta P=\Delta P_{MLI}+\Delta P_{MRP}=0.033+0.020=0.053$MPa/path

As shown above, the total pressure loss of the unit heat transfer path at the cylindrical portion is lower than the target, 0.1MPa.

(d) Heat transfer performance

Nusselt number $N_u=0.023R_e^{0.8}P_r^{0.4}=0.023\times(1.393\times10^5)^{0.8}\times0.6939^{0.4}=259.1$

Heat transfer coefficient

$h=N_uk/d=259.1\times0.0705/0.028=652.4$W/m^{2}K

Heat resistance of tube thickness

$R=t/k_{T304SS}=0.003/9.3=1/3100$m^{2}K/W

Fouling factor $h_f=3000$W/m^{2}K

Overall heat transfer coefficient

$U=1/[1/h+1/h_f+R]$

$=1/[1/652.4+1/3000+1/3100]=457$W/m^{2}K

Using the overall heat transfer coefficient, temperature distribution analyses of the shield plates are conducted as described in section 3.3. In consequence, the highest temperature, e.g. the hot spot temperature, is evaluated as follows:

(i) the shield plate with the MLI blanket and two-turn HTT

86.7K [temperature rise=6.7K]

(ii) the shield plate with the reflecting plates and four-turn HTT

96.1K [temperature rise=16.1K]

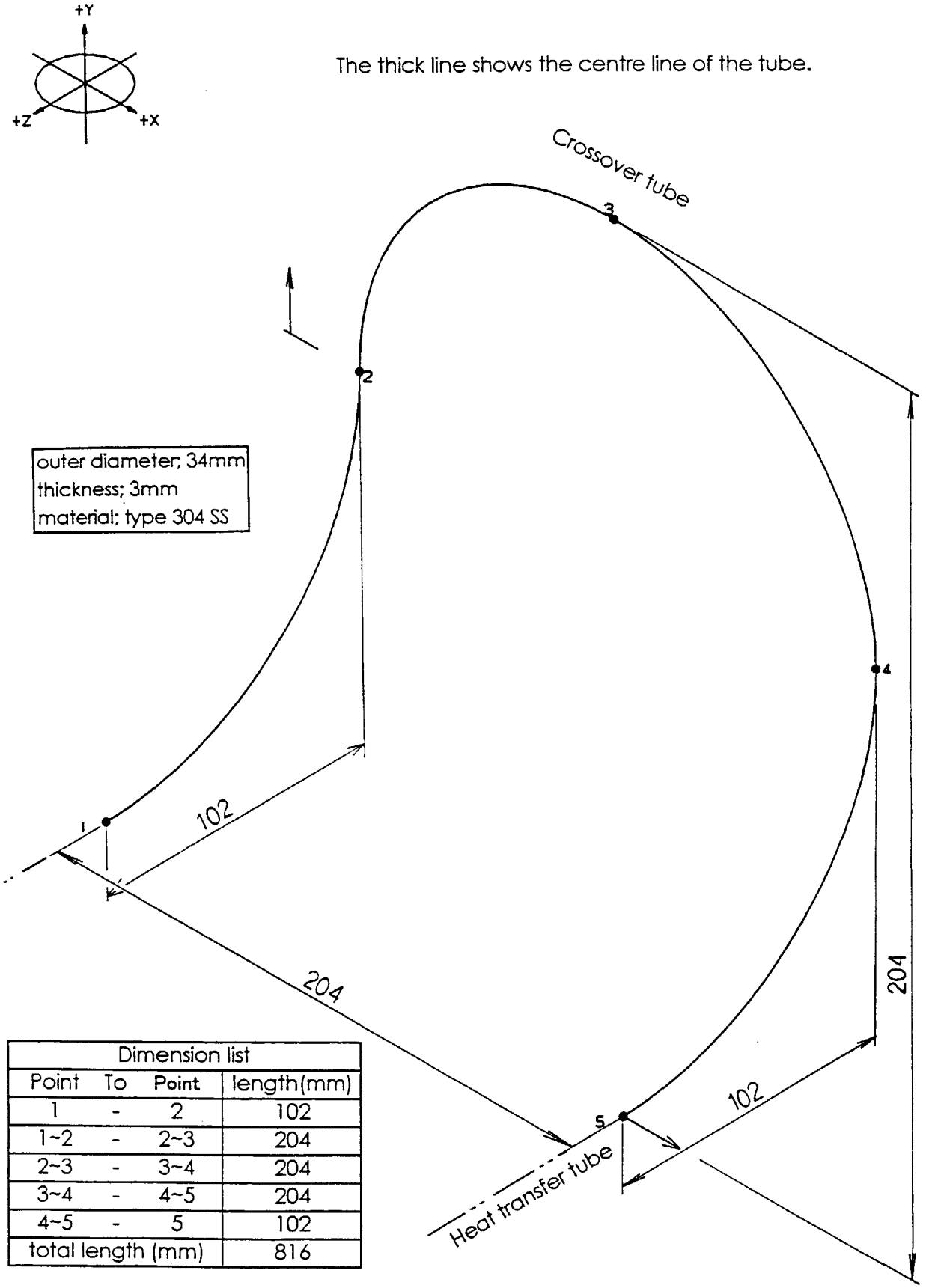

Dimension list			
Point	To	Point	length(mm)
1	-	2	102
1~2	-	2~3	204
2~3	-	3~4	204
3~4	-	4~5	204
4~5	-	5	102
total length (mm)			816

Fig. 3-14 FEA model of the crossover tube

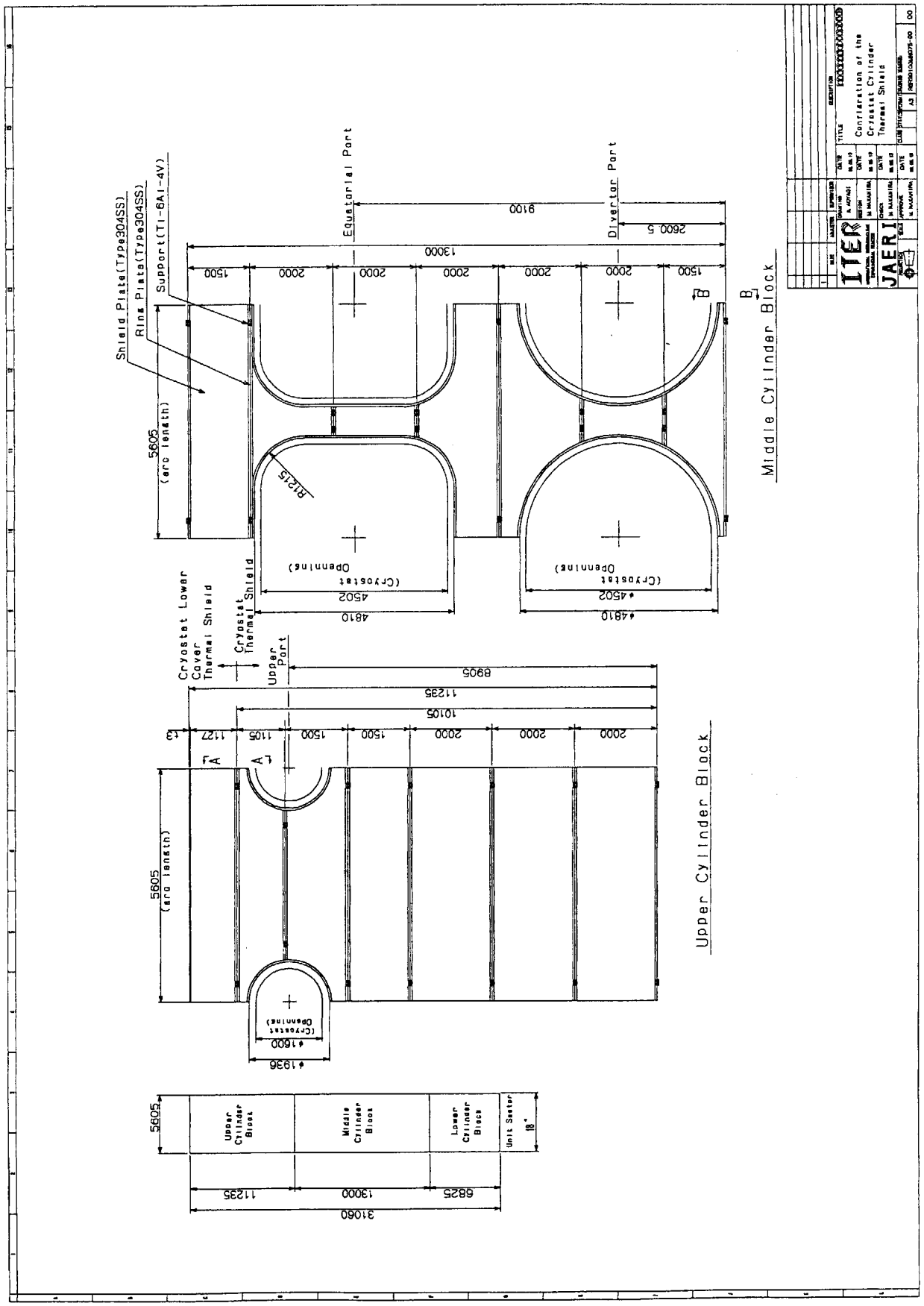

Fig. 3-15(1/3) Configuration of the Cryostat Cylinder Thermal Shield

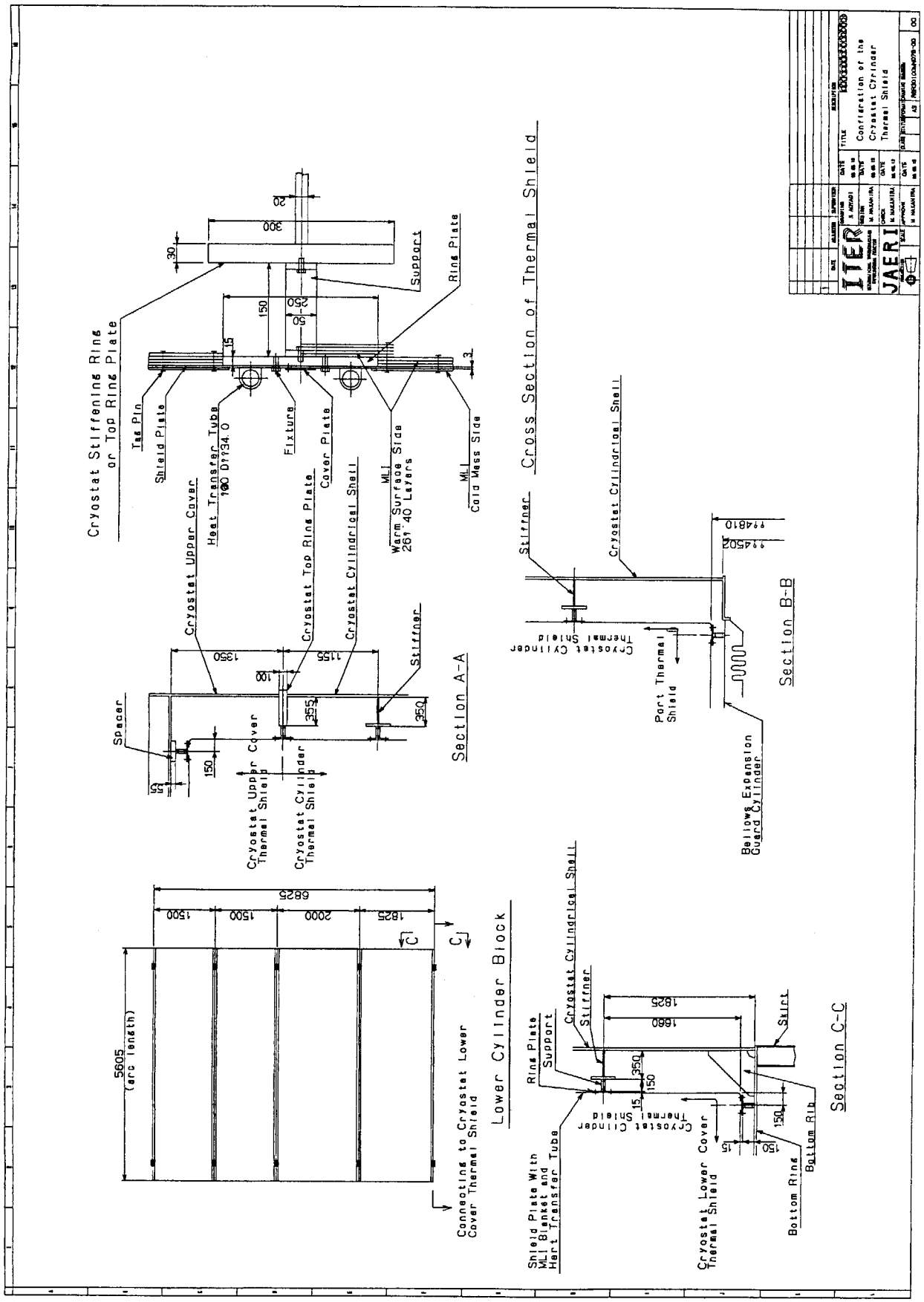

Fig.3-15(2/3) Configuration of the Cryostat Cylinder Thermal Shield

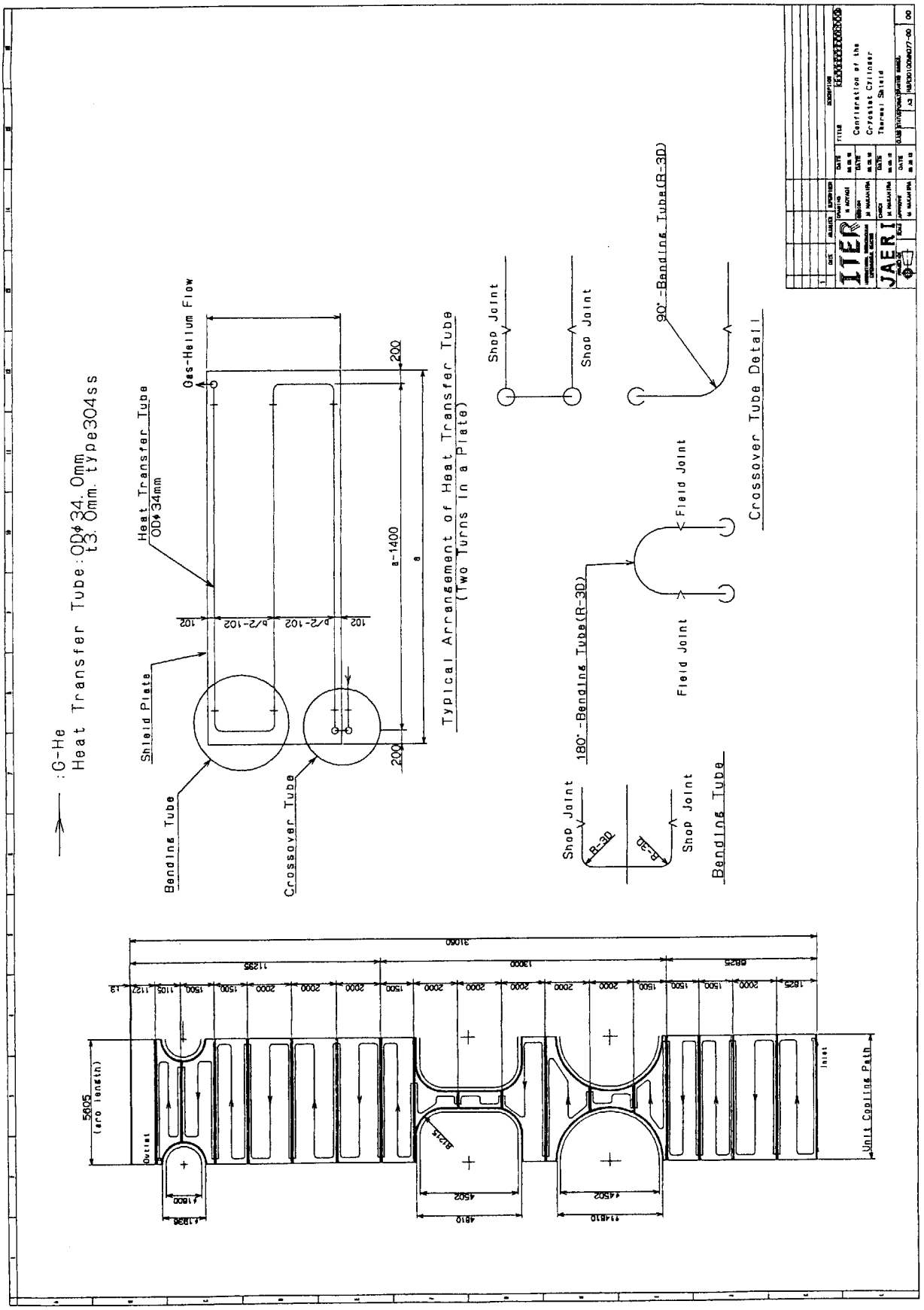

Fig.3-15(3/3) Configuration of the Cryostat Cylinder Thermal Shield

3.5.2 Cryostat upper cover thermal shield

a. Design concept

i. Basically, the concept is the same as the cryostat cylinder thermal shield.
ii. The heat transfer tube to be applied is 27.2mm in outer diameter and 2.5mm in thickness.
iii. Only the MLI blanket should be applied for the insulation.
iv. Zigzag arrangement in radial direction should be applied to the heat transfer tube on the shield plates.
v. Passive insulation without heat transfer tube should be applied to the rids of twenty RH-ports (R900mm) and the center opening for the CS coil removal (R1000mm).
vi. Spacers made of GFRP should be set up to the gap between the cover itself and the shield's support to make the surface flat.
vii. The tube-path on the inner block of the cover should be independent with that on the outer block for easy removal.

b. Configuration

Figure 3-16 shows the configuration of the thermal shield and arrangement of the heat transfer tube.

The thermal shield are divided equally into forty segments for the outer block and ten segments for the inner block. The number of the tube-path for each of the blocks is set up to roughly equalize the cooling area to that of the cylindrical portion.

Cooling area $A=(2\times18\pi\times30)/20=170m^2$ (as the reference-area)

Necessary tube-path

Outer block	$N_1=(18^2-7^2)\pi/A=5.1$	→ 10 paths	(every 36°)
Inner block	$N_2=(7^2-1^2)\pi/A=1.3$	→ 2 paths	(every 180°)

c. Heat leak

(a) Heat leak from the support

$$q = A\cdot\bar{\lambda}\frac{\Delta T}{L} = (0.05\times0.005)\times5.63\times\frac{300-80}{0.13} = 2.4W/support$$

(b) Heat leak through the insulation

$q=1.5W/m^2$

(c) Heat leak from the non-insulated portion

$$q = \sigma\frac{T_h^4 - T_c^4}{1/\varepsilon_c + 1/\varepsilon_h - 1} = 5.678\times10^{-8}\times\frac{300^4 - 80^4}{1/0.025 + 1/0.5 - 1} = 11.2W/m^2$$

d. Structural integrity

(a) Integrity of the support made of Ti-6Al-4V

Dead weight of unit thermal shield

Shield plate (1.5m×2.85m×t6mm)	2000N
Ring plate (0.25×2.85m×t15mm+stiffner)	1000N
MLI blanket (1.5m×2.85m×t12μm×40-layer)	30N
Heat transfer tube (OD27.2mm×t2.5mm×12m)	280N
Total	3310N→×1.2→4000N

i. Stress due to dead weight

Applied force V=4000/2=2000N
Sectional area A=5×50=250mm^2
Tensile stress σ_a=V/A=2000/250=8.0MPa
Allowable limit kSm=1×298=298MPa

ii. Stress due to seismic force [Horizontal/0.2G, Vertical/-1.2G]
Applied force H=0.2×4000/2=400N [Horizontal]
V=(1+0.2)×4000/2=2400N [Vertical]
Bending moment M_H=HL=400×130=52000Nmm
Modulus of section Z_H=50×5^2/6=208mm^3
Bending stress $\sigma_{b,H}$= M_H/Z_H=52000/208=250MPa [Horizontal]
Allowable limit 1.5kSm=1.5×1.2×298=536MPa
Tensile stress $\sigma_{t,V}$= V/A=2400/250=10MPa [Vertical]
Allowable limit kSm=1.2×298=357MPa

iii. Stress due to thermal shrinkage [300K→80K, type304SS]
Thermal shrinkage δ_1=(2850/2)×0.0029=4.2mm [long side direction]
Thermal shrinkage δ_2=(1500/2)×0.0029=2.2mm [short side direction]
Constraint disp. $\Delta\delta=\delta_1$=4.2mm
Bending stress $\sigma_b=3Eh\Delta\delta/(2L^2)$
=3×118000×5×4.2/(2×130^2)=220MPa
Allowable limit 3Sm=3×298=894MPa

iv. Stress due to combined loading
Load combination thermal shrinkage +(dead weight + seismic force)
Evaluated stress 220+250=470MPa
Allowable stress 3Sm=3×298=894MPa

(b) Natural period of the thermal shield

i. Natural period of in-plane mode
Mass M=F/g=4000/9.8=409kg
Stiffness $K=2\times(3EI/L^3)$
$=2\times[3\times(1.18\times10^{11})\times(0.005^3\times0.05/12)]/0.13^3$
=167843N/m
Natural period $T=2\pi(M/K)^{1/2}=2\pi(409/167843)^{1/2}$=0.31s

ii. Natural period of out-of-plane mode
Corrected density ρ=7900×(2000+30+280)/2000=9125kg/m^3
Flexural rigidity $D=Eh^3/12(1-\nu^2)=2\times10^{11}\times0.003^3/12/(1-0.3^2)$=495N/m
Factor k=9.631
Equivalent side length

$$\bar{a}=\sqrt{a\times b}=\sqrt{1.5\times2.85}=2.07m$$

Natural period

$$T=\frac{2\pi}{k}\sqrt{\frac{\rho h\bar{a}^4}{D}}=\frac{2\pi}{9.631}\times\sqrt{\frac{9125\times0.006\times2.07^4}{3956}}=0.33s$$

(c) Integrity and deflection of the ring plate

i. Stress and deflection due to dead weight
Bending moment M=FL/12=4000×2850/12=950000Nmm
Modulus of section Z_V=132005mm^3
Bending stress $\sigma_b=M/Z_V$=950000/132005=7.2MPa
Allowable limit 1.5kSm=1.5×1×138=207MPa
Deflection $\delta=FL^3/(384EI_V)$

$=4000\times2850^3/[384\times200000\times6445468]=0.2$mm

ii. Stress and deflection due to seismic force

(i) Horizontal direction, 0.2G

Bending stress $\sigma_b=(0.2FL/12)/Z_H$
$=(0.2\times4000\times2850/12)/156362=1.3$MPa

Allowable limit $1.5kSm=1.5\times1.2\times138=248$MPa

Deflection $\delta=0.2FL^3/(384EI_H)$
$=0.2\times4000\times2850^3/(384\times200000\times19545312)=0.1$mm

(ii) Vertical direction, 1.2G

Bending stress $\sigma_b=(1.2FL/12)/Z_V$
$=(1.2\times4000\times2850/12)/132005=8.7$MPa

Allowable limit $1.5kSm=1.5\times1.2\times138=248$MPa

Deflection $\delta=1.2FL^3/(384EI_V)$
$=1.2\times4000\times2850^3/(384\times200000\times6415468)=0.3$mm

(d) Integrity and deflection of the shield plate

Applied force $F=4000-1000=3000$N (except for the ring plate)

Uniform pressure $q=F/(ab)=1.2\times3000/(2850\times1500)=0.000842$MPa

Bending stress $\sigma_b=\beta qb^2/h^2=0.73\times0.000842\times1500^2/6^2=38.5$MPa

Allowable limit $1.5kSm=1.5\times1.2\times138=248$MPa

In-plane deflection $\delta=\alpha qb^4/(Eh^3)$
$=0.14\times0.000842\times1500^4/(200000\times6^3)=13.8$mm

e. Heat transfer and pressure loss

The performance of heat transfer and pressure loss is evaluated. The heat transfer tube made of type 304 stainless steel is 27.2mm in outer diameter and 2.5mm in thickness. The number of the tube-path is ten for outer block ($7043\leq R\leq18150$) and two for the inner block ($1060\leq R\leq6873$).

(a) Heat removal of unit tube-path

Outer block

i. Heat leak

through the MLI blanket	$q\bullet A=1.5\times\pi(18.15^2-7.043^2)/10=$	132W/path
from the support	$q\bullet N=2.4\times720/10=$	173W/path
from non-insulated portion	$q\bullet A=11.2\times(320/10\times0.3)=$	108W/path
from the rid of RH-port	$Q\bullet N=(2\pi\times0.006\times16\times220)\times2=$	266W/path
Summation		679W/path

ii. External heating

Nuclear heating	$q\bullet V=100\times\pi(18.15^2-7.043^2)\times0.006/10=$	53W/path
Joule heating	$37/10=$	4W/path
Summation		57W/path

iii. Total removal heating 736W/path → 800W/path

Inner block

i. Heat leak

through the MLI blanket	$q\bullet A=1.5\times\pi6.783^2/2=$	109W/path
from the support	$q\bullet N=2.4\times100/2=$	120W/path
from non-insulated portion	$q\bullet A=11.2\times(40/2\times0.4)=$	90W/path
from the central opening	$Q\bullet N=(2\pi\times0.006\times16\times220)/2=$	133W/path

Summation 699W/path

ii. External heating

Nuclear heating $q \bullet V=100\times\pi(6.783^2-1.06^2)\times0.006/2=$ 43W/path

Joule heating 425/2= 213W/path

Summation 256W/path

iii. Total removal heating 575W/path→ 700W/path

The total heat leak from the thermal shield of the cryostat upper cover is $10\times697+2\times319=7.7$kW.

(b) Necessary flow rate of coolant

Outer block

i. Mass flow rate of coolant

Mass flow rate $G=Q/\Delta h=800/52.2=15.4$g/s

Mean velocity in tube

$u=(G/\rho)/A$

$=(15.4\times10^{-3}/9.105)/(0.0222^2\pi/4)=4.37$m/s

Reynolds number $Re = ud\rho/\eta$

$=4.37\times0.0222\times9.105/(9.372\times10^{-6})=9.425\times10^4$

ii. Pressure loss due to friction in unit tube length, ΔP_1

Friction factor $\lambda=0.3164/Re^{0.25}=0.3164/(9.425\times10^4)^{0.25}=0.0181$

Pressure loss $\Delta P_1=\lambda/d\times(\rho u^2/2)$

$=0.0181/0.0222\times(9.105\times4.37^2/2)=7.09\times10^{-5}$MPa/m

iii. Pressure loss at a 180° bending tube, ΔP_2

Pressure loss $\Delta P_2=K_{180°}\times(\rho u^2/2)$

$=1.015\times(9.105\times4.37^2/2)=8.38\times10^{-5}$MPa

vi. Pressure loss at a 90° bending tube, ΔP_3

Pressure loss $\Delta P_3=K_{90°}\times(\rho u^2/2)$

$=1.301\times(9.105\times4.37^2/2)=1.14\times10^{-4}$MPa

v. Evaluation

Total pressure loss $\Delta P=L\times\Delta P_1+N_2\times\Delta P_2+N_3\times\Delta P_3$

$=250\times(7.09\times10^{-5})+32\times(8.83\times10^{-5})+200\times(1.14\times10^{-4})$

$=0.044$MPa/path

Inner block

i. Mass flow rate of coolant

Mass flow rate $G=Q/\Delta h=700/52.2=13.4$g/s

Mean velocity in tube

$u=(G/\rho)/A$

$=(13.4\times10^{-3}/9.105)/(0.0222^2\pi/4)=3.81$m/s

Reynolds number $Re = ud\rho/\eta$

$=3.81\times0.0222\times9.105/(9.372\times10^{-6})=8.218\times10^4$

ii. Pressure loss due to friction in unit tube length, ΔP_1

Friction factor $\lambda=0.3164/Re^{0.25}=0.3164/(8.218\times10^4)^{0.25}=0.0187$

Pressure loss $\Delta P_1=\lambda/d\times(\rho u^2/2)$

$=0.0187/0.0222\times(9.105\times3.81^2/2)=5.57\times10^{-5}$MPa/m

iii. Pressure loss at a 180° bending tube, ΔP_2

Pressure loss $\Delta P_2=K_{180°}\times(\rho u^2/2)$

$=1.015\times(9.105\times3.81^2/2)=6.71\times10^{-5}$MPa

vi. Pressure loss at a 90° bending tube, ΔP_3

Pressure loss $\Delta P_3=K_{90°}\times(\rho u^2/2)$

$=1.301\times(9.105\times3.81^2/2)=8.60\times10^{-5}$MPa

v. Evaluation

Total pressure loss $\Delta P=L\times\Delta P_1+N_2\times\Delta P_2+N_3\times\Delta P_3$

$=220\times(5.57\times10^{-5})+20\times(6.71\times10^{-5})+120\times(8.60\times10^{-5})$

$=0.024$MPa/path

As shown above, the total pressure loss of the unit heat transfer path at the upper cover is lower than the target, 0.1MPa.

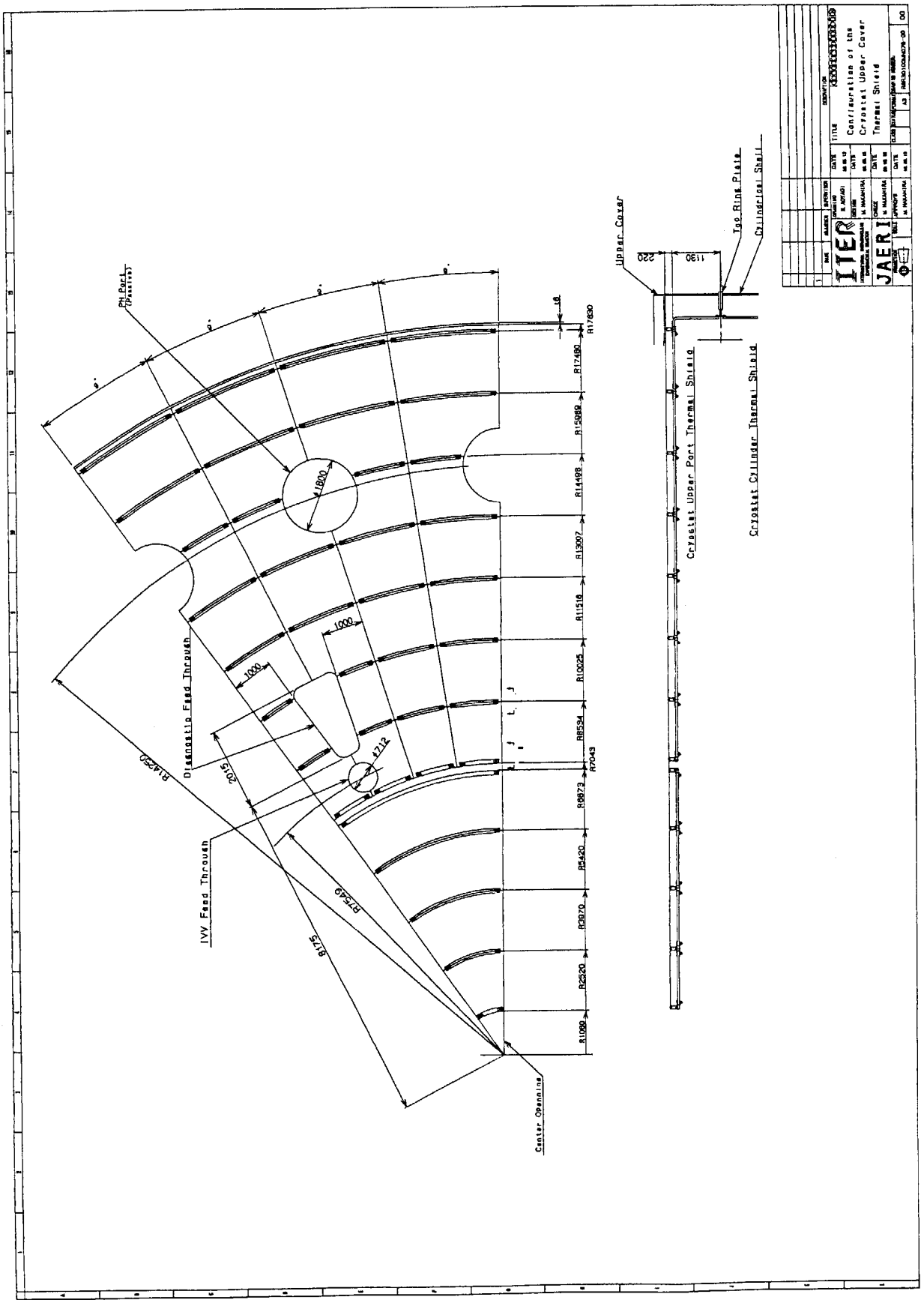

Fig. 3-16(1/3) Configuration of the Cryostat Upper Cover Thermal Shield

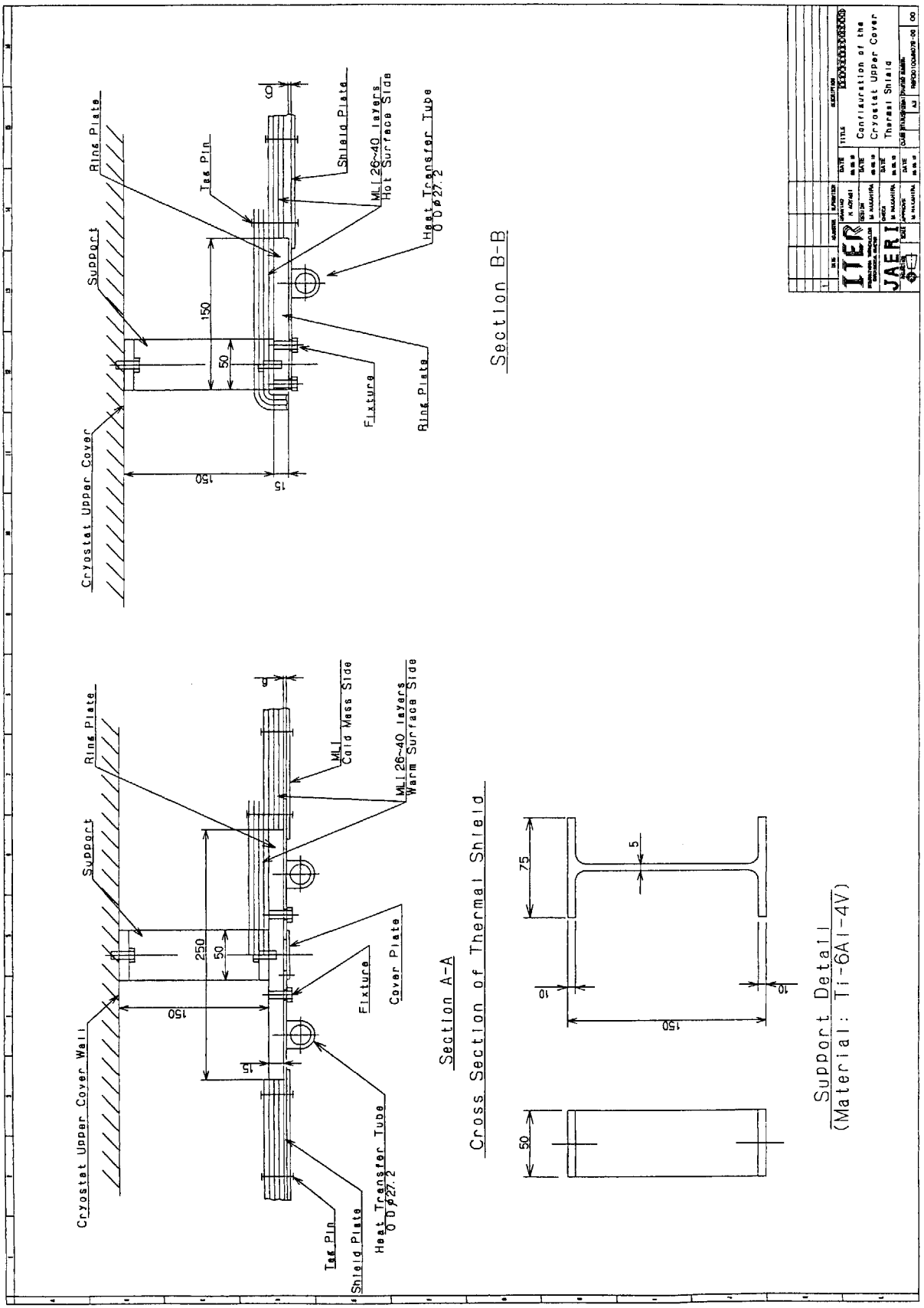

Fig. 3-16(2/3) Configuration of the Cryostat Upper Cover Thermal Shield

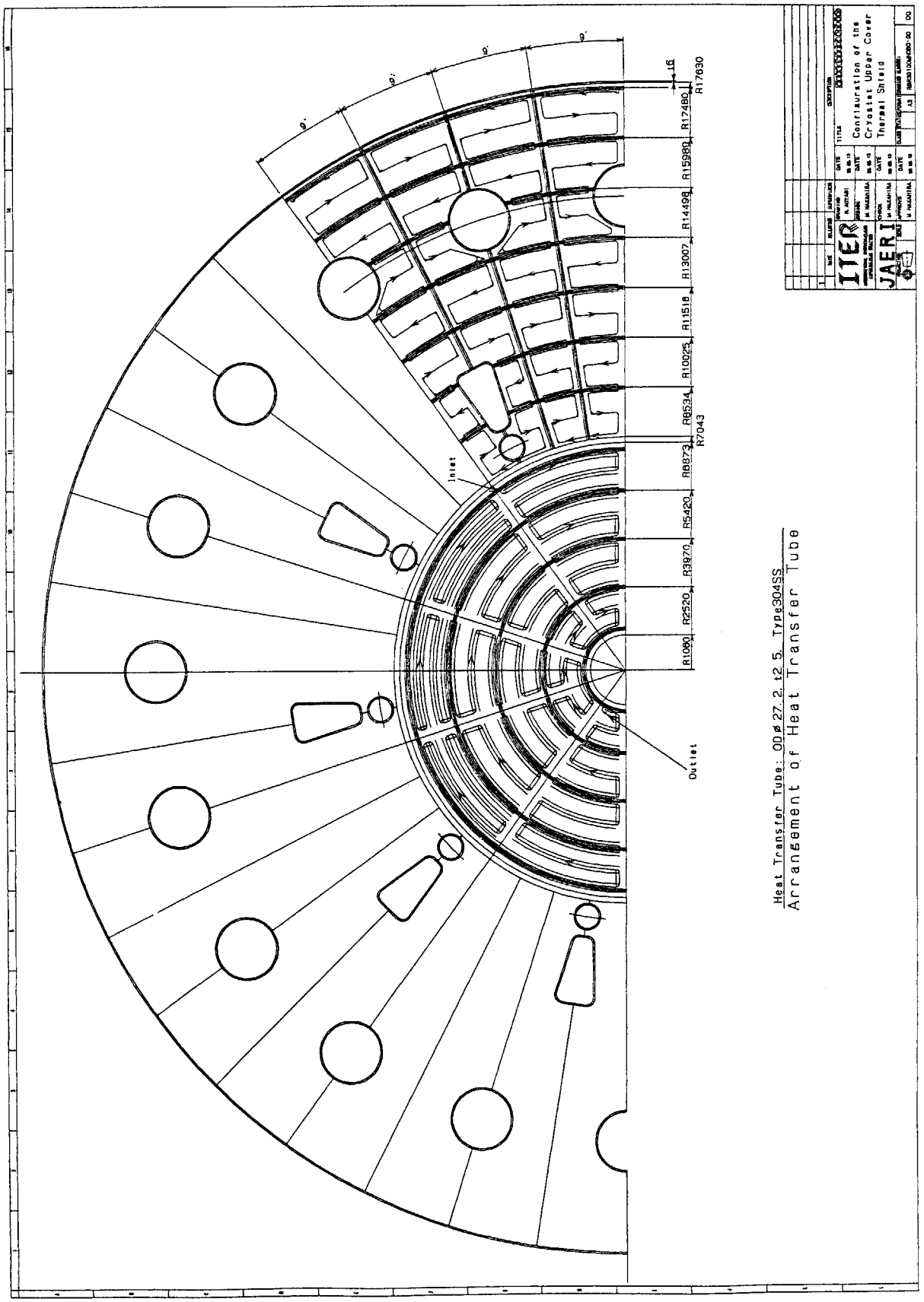

Fig. 3-16(3/3) Configuration of the Cryostat Upper Cover Thermal Shield

3.5.3 Lower cover thermal shield

a. Design concept

i. Basically, the concept is the same as the cryostat cylinder thermal shield.
ii. The heat transfer tube to be applied is 34mm in outer diameter and 3mm in thickness.
iii. Only the MLI blanket should be applied for the insulation.
iv. Zigzag arrangement in radial direction should be applied to the heat transfer tube on the shield plates.
v. Passive insulation without heat transfer tube should be applied to the rids of four RH-ports (R800mm).
vi. Spacers made of GFRP should be set up to the gap between the cover itself and the shield's support to make the surface flat.
vii. The tube-path on the middle block of the cover with the CS support assembly should be independent of that on the outer block for easy removal.

b. Configuration

Figure 3-17 shows the configuration of the thermal shield and arrangement of the heat transfer tube.

The thermal shield are divided equally into forty segments for the outer block, twenty segments for the middle block and four segments for the central solenoid support assembly. The ring pedestal block is covered by the gravity support thermal shields, so this portion is out of the scope for the lower cover's thermal shield.

The number of the tube-path for each of the blocks is set up to roughly equalize the cooling area to that of the cylindrical portion.

Cooling area $A=(2\times18\pi\times30)/20=170m^2$ (as the reference-area)

Necessary tube-path

Outer block $N_1=\pi(18^2-12.2^2)/A=3.3$ → 4 paths (every 90°)

Middle block with CS support assembly

$N_2=[\pi(10.6^2-3.0^2)+64]/A=2.3$ → 4 paths (every 90°)

c. Heat leak

(a) Heat leak from the support

$$q = A \cdot \bar{\lambda} \frac{\Delta T}{L} = (0.05 \times 0.005) \times 5.63 \times \frac{300-80}{0.13} = 2.4W/support$$

(b) Heat leak through the insulation

$q=1.5W/m^2$

(c) Heat leak from the non-insulated portion

$$q = \sigma \frac{T_h^4 - T_c^4}{1/\varepsilon_c + 1/\varepsilon_h - 1} = 5.678 \times 10^{-8} \times \frac{300^4 - 80^4}{1/0.025 + 1/0.5 - 1} = 11.2W/m^2$$

d. Structural integrity

The stresses that appear in each part of the lower cover's thermal shield will be lower than those in the upper cover's. Therefore, the stress-evaluation for this thermal shield is omitted.

e. Heat transfer and pressure loss

The performance of heat transfer and pressure loss is evaluated. The heat transfer tube

made of type 304 stainless steel is 34mm in outer diameter and 3mm in thickness.

(a) Heat removal of unit tube-path

Outer block

i. Heat leak

through the MLI blanket	$q \bullet A=1.5\times\pi(17.563^2-12.219^2)=$	750W/path
from the support	$q \bullet N=2.4\times400/4=$	240W/path
from non-insulated portion	$q \bullet N=2.4\times400/4=$	240W/path
Summation		1125W/path

ii. External heating

Nuclear heating	$q \bullet V=10\times\pi(17.563^2-12.219^2)\times0.006=$	30W/path
Joule heating	28/4=	7W/path
Summation		37W/path

iii. Total removal heating 1162W/path → 1300W/path

Inner block with CS support assembly

i. Heat leak

through the MLI blanket	$q \bullet A=1.5\times[\pi(10.595^2-3.002^2)+64]=$	583W/path
from the support	$q \bullet N=2.4\times(240+32)/4=$	164W/path
from non-insulated portion	$q \bullet A=11.2\times[(100+16)/4\times0.4]=$	130W/path
from rid of RH-ports	$Q \bullet N=(2\pi\times0.006\times16\times220)\times1=$	133W/path
Summation		1010W/path

ii. External heating

Nuclear heating	$q \bullet V=10\times\pi(10.595^2-3.002^2)\times0.006=$	20W/path
Joule heating	668/4=	167W/path
Summation		187W/path

iii. Total removal heating 1197W/path→ 1300W/path

The total heat leak from the thermal shield of the cryostat lower cover is $4\times1125+4\times1010=8.6$kW.

(b) Necessary flow rate of coolant

Outer block

i. Mass flow rate of coolant

Mass flow rate $G=Q/\Delta h=1300/52.2=24.9$g/s

Mean velocity in tube

$$u=(G/\rho)/A$$
$$=(24.9\times10^{-3}/9.105)/(0.0222^2\pi/4)=4.44\text{m/s}$$

Reynolds number $Re = ud\rho/\eta$

$$=4.44\times0.0222\times9.105/(9.372\times10^{-6})=1.208\times10^5$$

ii. Pressure loss due to friction in unit tube length, ΔP_1

Friction factor $\lambda=0.3164/Re^{0.25}=0.3164/(1.208\times10^5)^{0.25}=0.0170$

Pressure loss $\Delta P_1=\lambda/d\times(\rho u^2/2)$

$$=0.0170/0.028\times(9.105\times4.44^2/2)=5.45\times10^{-5}\text{MPa/m}$$

iii. Pressure loss at a 180° bending tube, ΔP_2

Pressure loss $\Delta P_2=K_{180°}\times(\rho u^2/2)$

$$=1.015\times(9.105\times4.44^2/2)=9.11\times10^{-5}\text{MPa}$$

vi. Pressure loss at a 90° bending tube, ΔP_3

Pressure loss $\Delta P_3=K_{90°}\times(\rho u^2/2)$
$=1.301\times(9.105\times4.44^2/2)=1.17\times10^{-4}$MPa

v. Evaluation

Total pressure loss $\Delta P=L\times\Delta P_1+N_2\times\Delta P_2+N_3\times\Delta P_3$
$=350\times(5.45\times10^{-5})+40\times(9.11\times10^{-5})+240\times(1.17\times10^{-5})$
$=0.051$MPa/path

Inner block with CS support assembly

i. Mass flow rate of coolant

Mass flow rate $G=Q/\Delta h=1300/52.2=24.9$g/s

Mean velocity in tube
$u=(G/\rho)/A$
$=(24.9\times10^{-3}/9.105)/(0.028^2\pi/4)=4.44$m/s

Reynolds number $Re = ud\rho/\eta$
$=4.44\times0.028\times9.105/(9.372\times10^{-6})=1.208\times10^5$

ii. Pressure loss due to friction in unit tube length, ΔP_1

Friction factor $\lambda=0.3164/Re^{0.25}=0.3164/(1.208\times10^5)^{0.25}=0.0170$

Pressure loss $\Delta P_1=\lambda/d\times(\rho u^2/2)$
$=0.0170/0.028\times(9.105\times4.44^2/2)=5.45\times10^{-5}$MPa/m

iii. Pressure loss at a 180° bending tube, ΔP_2

Pressure loss $\Delta P_2=K_{180°}\times(\rho u^2/2)$
$=1.015\times(9.105\times4.44^2/2)=9.11\times10^{-5}$MPa

vi. Pressure loss at a 90° bending tube, ΔP_3

Pressure loss $\Delta P_3=K_{90°}\times(\rho u^2/2)$
$=1.301\times(9.105\times4.44^2/2)=1.17\times10^{-4}$MPa

v. Evaluation

Total pressure loss $\Delta P=L\times\Delta P_1+N_2\times\Delta P_2+N_3\times\Delta P_3$
$=250\times(5.45\times10^{-5})+29\times(9.11\times10^{-5})+174\times(1.17\times10^{-4})$
$=0.037$MPa/path

As shown above, the total pressure loss of the unit heat transfer path at the lower cover is lower than the target, 0.1MPa.

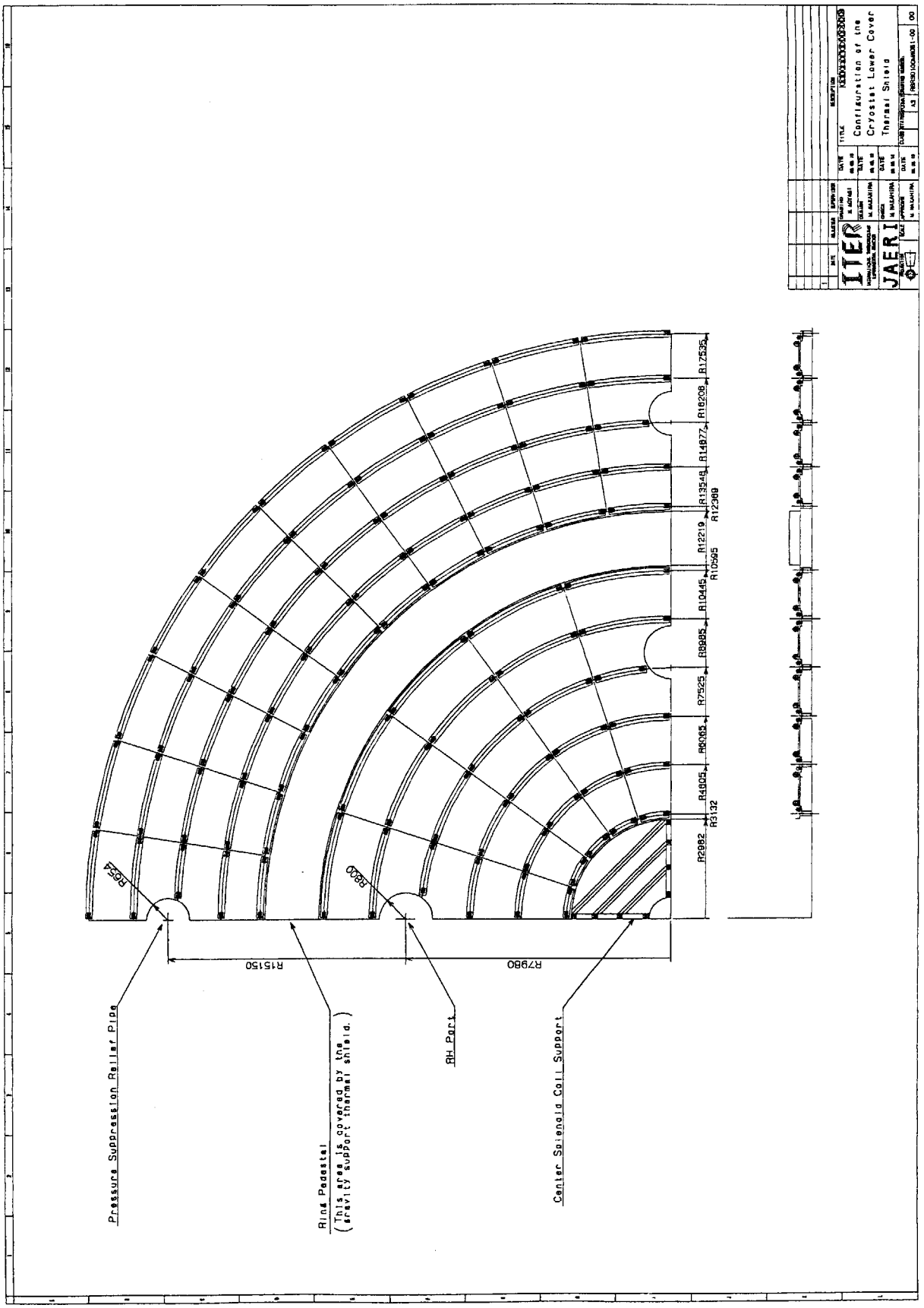

Fig. 3-17(1/3) Configuration of the Cryostat Lower Cover Thermal Shield

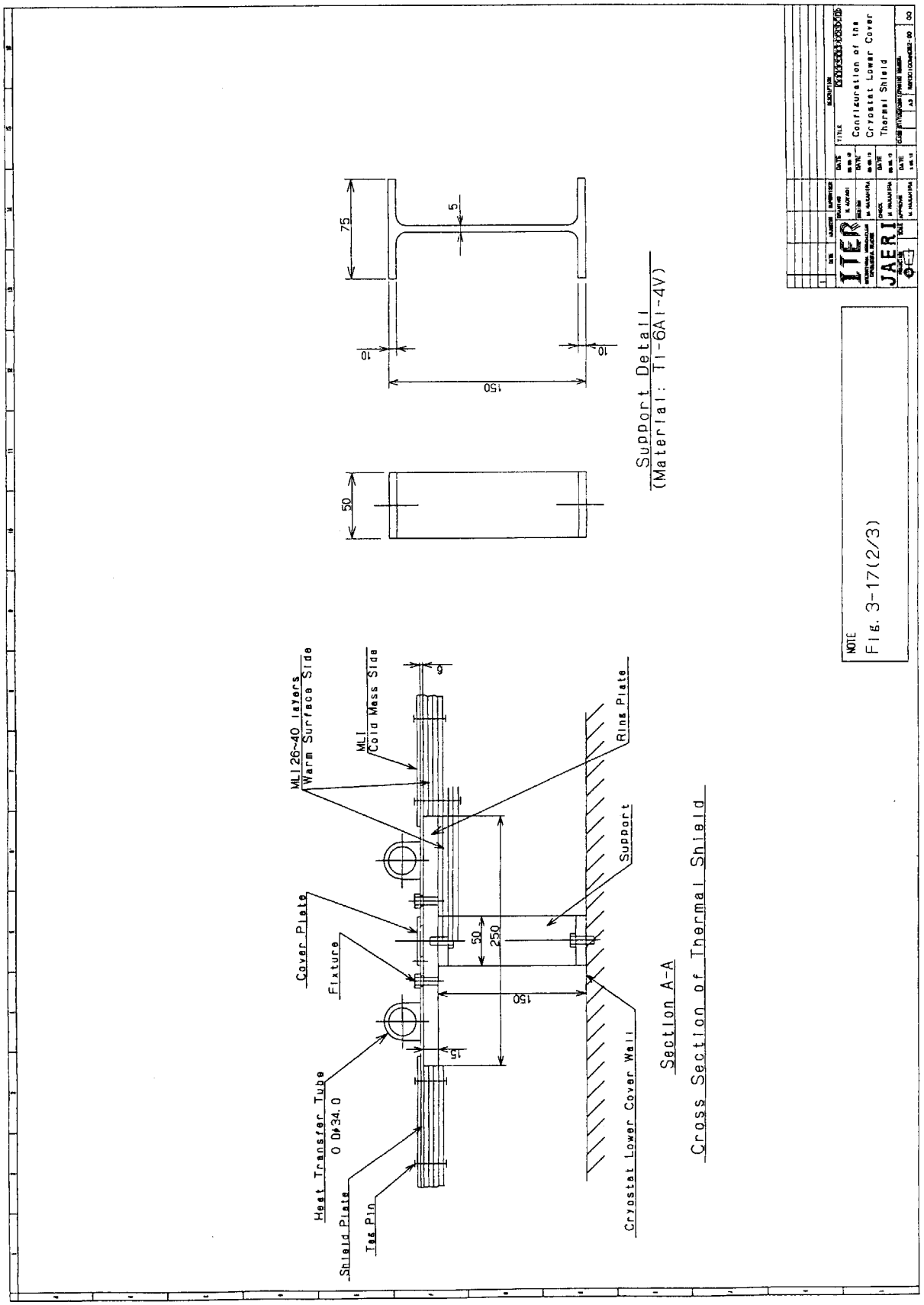

Fig. 3-17(2/3) Configuration of the Cryostat Lower Cover Thermal Shield

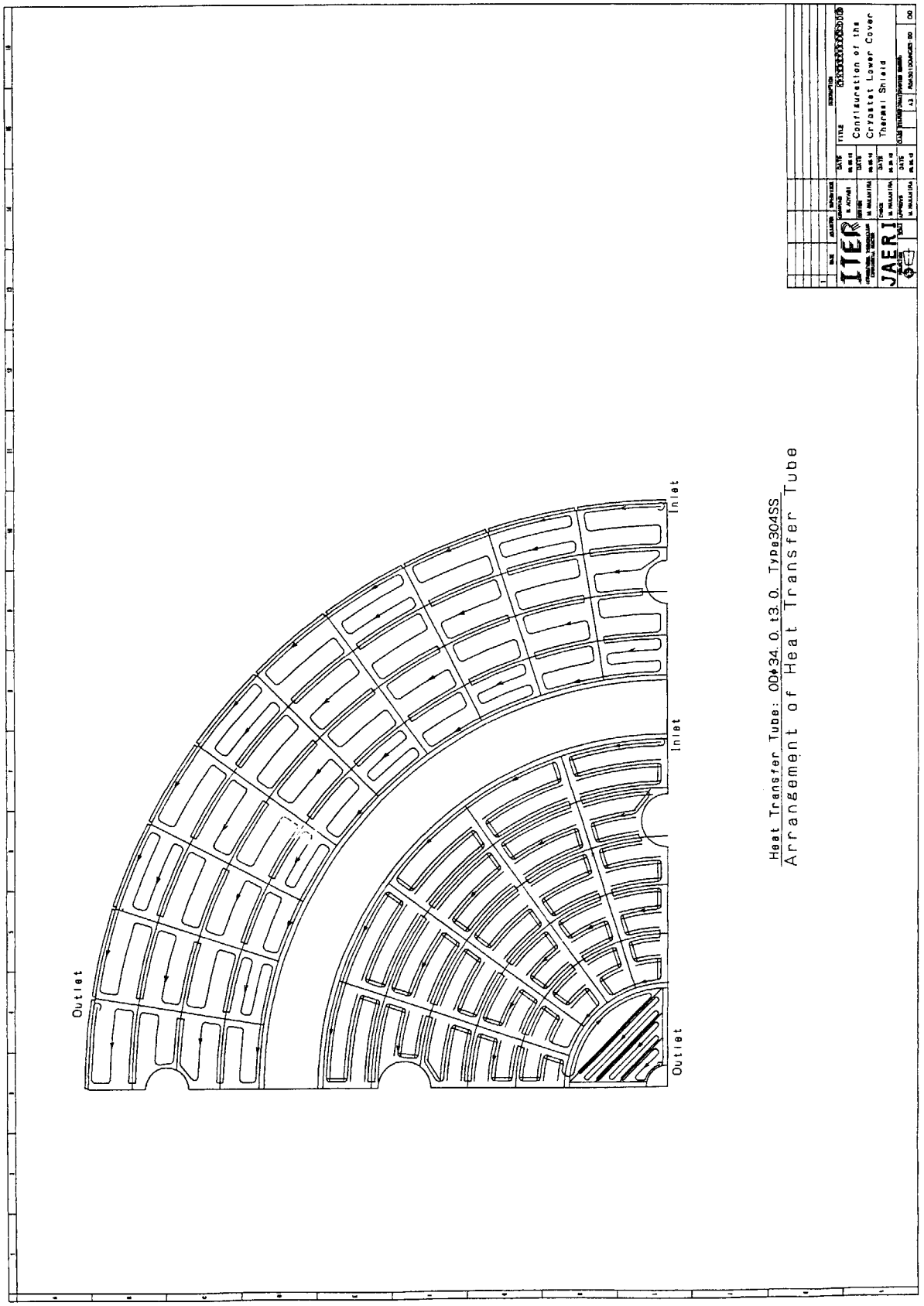

Fig. 3-17(3/3) Configuration of the Cryostat Lower Cover Thermal Shield

3.5.4 Upper port thermal shield

a. Design concept

i. Basically, the concept is the same as the cryostat cylinder thermal shield.
ii. The heat transfer tube to be applied is 34mm in outer diameter and 3mm in thickness.
iii. The MLI blanket should be applied for the insulation. As the ports will be heated up to 473K at baking of the vacuum vessel, the MLI blanket applied to the ports should be heat-proof of up to 573K (300°C).
iv. Both sides of the shield plate should be required silver-coating by deposition or plating to reduce their emissivity.
v. Zigzag arrangement should be applied to the heat transfer tube on the shield plates.

The ports will be heated up to 473K at baking of the vacuum vessel. In this design, the insulation applied to the ports is assumed to be a combination of two kind of blanket. The inner blanket consists of multistory embossed-films made of polyimide which are widely used for baking of vacuum components. The outer blanket is the so-called MLI blanket consisting of crinkled polyimide films, dimpled polyimide films or plane polyimide films with silk-net spacers. All of the polyimide films are aluminum-deposited on both sides.

Polyimide is a highly heat-proof polymer. The heat resisting temperature of this material is about 670K. Some of the ports are assumed to be heated up to 573K during the operation. The insulation made of polyimide is applicable to the ports because of above mentioned characteristics.

b. Configuration

Figure 3-18 shows the configuration of the thermal shield and arrangement of the heat transfer tube.

c. Heat leak

Heat leak of the thermal shield is estimated for the typical one with dimension of 1.59 by 1.96 meters, which is corresponding to the shield plate at the bellows cover assembly. As shown in Figure 3-18, the number of the shield plate and the support made of titanium alloy is 28 and 64, respectively for a port.

(a) Heat leak from the support

$$q = A \cdot \bar{\lambda} \frac{\Delta T}{L} = (0.05 \times 0.005) \times 7.16 \times \frac{473 - 80}{0.13} = 5.5W$$

5.5×64= 352W/port

(b) Heat leak through the insulation

$$q = q_0 \frac{T^4 - T_c^4}{T_h^4 - T_c^4} = 1.5 \times \frac{473^4 - 80^4}{273^4 - 80^4} = 9.3W / m^2$$

$A=1.59\times1.96=3.2m^2$

9.3×28×3.2= 834W/port

(c) Heat leak from the non-insulated portion

$$q = \sigma \frac{T_h^4 - T_c^4}{1/\varepsilon_c + 1/\varepsilon_h - 1} = 5.678 \times 10^{-8} \times \frac{473^4 - 80^4}{1/0.025 + 1/0.5 - 1} = 69.3 W/m^2$$

$A=64\times(0.175\times0.25)+28\times[1-(1-0.014^2)]\times3.2=5.308m^2$

$69.3\times5.308=$ 368W/port

(d) Summation of heat leak

352+834+368=1554W/port

The total heat leak from the thermal shield of the upper ports is $20\times1554=31.2kW$.

d. Structural integrity

(a) Integrity of the support made of Ti-6Al-4V ($1.59m\times1.96m=3.2m^2$)

Dead weight of typical thermal shield

Shield plate ($3.2m^2\times t3mm$)	750N
Ring plate ($0.25\times2.12m\times t15mm$+stiffner)	740N
MLI blanket ($4.2m^2\times t12\mu m\times50$-layer)	30N
Heat transfer tube (OD34mm×t3mm×7m)	160N
Total	1680N→×1.2→2100N

i. Stress due to dead weight

Applied force V=2100/2=1050N

Bending moment $M=VL=1050\times130=136500Nmm$

Modulus of section $Z_V=5\times50^2/6=2083mm^3$

Bending stress $\sigma_b=M/Z=136500/2083=66MPa$

Allowable limit $1.5kSm=1.5\times1\times298=447MPa$

ii. Stress due to seismic force [Horizontal/0.2G, Vertical/-1.2G]

Applied force $H=0.2\times2100/2=210N$ [Horizontal]

$V=(1+0.2)\times2100/2=1260N$ [Vertical]

Bending moment $M_H=HL=210\times130=27300Nmm$ [Horizontal]

$M_V=VL=1260\times130=163800Nmm$ [Vertical]

Modulus of section $Z_H=50\times5^2/6=208mm^3$ [Horizontal]

$Z_V=5\times50^2/6=2083mm^3$ [Vertical]

Bending stress $\sigma_{b,H}=M_H/Z_H=27300/208=132MPa$ [Horizontal]

$\sigma_{b,V}=M_V/Z_V=163800/2083=79MPa$ [Vertical]

Allowable limit $1.5kSm=1.5\times1.2\times298=536MPa$

iii. Stress due to thermal shrinkage [473K→80K, type304SS]

Thermal shrinkage $\delta_1=(1590/2)\times0.0062=5.0mm$ [long side direction]

Thermal shrinkage $\delta_2=(1960/2)\times0.0062=6.1mm$ [short side direction]

[thermal strain under 473K→80K cooling is -0.0062]

Constraint disp. $\Delta\delta=\delta_1=5.0mm$

Bending stress $\sigma_b=3Eh\Delta\delta/(2L^2)$

$=3\times118000\times5\times5.0/(2\times130^2)=262MPa$

Allowable limit $3Sm=3\times298=894MPa$

iv. Stress due to combined loading

Load combination thermal shrinkage +(dead weight + seismic force)

Evaluated stress 262+132=394MPa

Allowable stress $3Sm=3\times298=894MPa$

(b) Natural period of the thermal shield

i. Natural period of in-plane mode

Mass $M=F/g=2100/9.8=215kg$

Stiffness $K=2\times(3EI/L^3)$
$=2\times[3\times(1.18\times10^{11})\times(0.005^3\times0.05/12)]/0.13^3$
$=167843N/m$

Natural period $T=2\pi(M/K)^{1/2}=2\pi(215/167843)^{1/2}=0.23s$

ii. Natural period of out-of-plane mode

Corrected density $\rho=7900\times(750+30+160)/750=9910kg/m^3$

Flexural rigidity $D=Eh^3/12(1-\nu^2)$
$=2\times10^{11}\times0.003^3/12/(1-0.3^2)$
$=495N/m$

Factor $k=9.631$

Equivalent side length

$$\bar{a}=\sqrt{a\times b}=\sqrt{1.59\times1.96}=1.77m$$

Natural period

$$T=\frac{2\pi}{k}\sqrt{\frac{\rho h\bar{a}^4}{D}}=\frac{2\pi}{9.631}\times\sqrt{\frac{9910\times0.003\times1.77^4}{495}}=0.50s$$

(c) Integrity and deflection of the ring plate

i. Stress and deflection due to dead weight

Bending moment $M=FL/12=2100\times1590/12=278250Nmm$

Modulus of section $Z_V=132005mm^3$

Bending stress $\sigma_b=M/Z_V=278250/132005=2.2MPa$

Allowable limit $1.5kSm=1.5\times1\times138=207MPa$

Deflection $\delta=FL^3/(384EI_V)$
$=2100\times1590^3/[384\times200000\times6445468]=0.1mm$

ii. Stress and deflection due to seismic force

(i) Horizontal direction, 0.2G

Bending stress $\sigma_b=(0.2FL/12)/Z_H$
$=(0.2\times2100\times1590/12)/156362=0.4MPa$

Allowable limit $1.5kSm=1.5\times1.2\times138=248MPa$

Deflection $\delta=0.2FL^3/(384EI_{MIN})$ $I_{MIN}=MIN(I_X, I_Y)$
$=0.2\times2100\times1590^3/(384\times200000\times6415468)=0.1mm$

(ii) Vertical direction, 1.2G

Bending stress $\sigma_b=(1.2FL/12)/Z_V$
$=(1.2\times2100\times1590/12)/132005=2.6MPa$

Allowable limit $1.5kSm=1.5\times1.2\times138=248MPa$

Deflection $\delta=1.2FL^3/(384EI_V)$
$=1.2\times2100\times1590^3/(384\times200000\times6415468)=0.1mm$

e. Heat transfer and pressure loss

Performance of heat transfer and pressure loss is evaluated. The heat transfer tube made of type 304 stainless steel is 34mm in outer diameter and 3mm in thickness.

(a) Heat removal of unit tube-path

i. Heat leak

through the MLI blanket		834W/path
from the support		352W/path
from non-insulated portion		368W/path
Summation		1554W/path

ii. External heating

Nuclear heating	$q \bullet V=21\times[(24000\times0.3)\times1\times10^{-4}]=$	16W/path
Joule heating	6W/path	
Summation		19W/path

iii. Total removal heating 1573W/path→ 1700W/path

(b) Necessary flow rate of coolant

i. Mass flow rate of coolant

Mass flow rate $G=Q/\Delta h=1700/52.2=32.6g/s$

Mean velocity in tube

$$u=(G/\rho)/A$$
$$=(32.6\times10^{-3}/9.105)/(0.028^2\pi/4)=5.82m/s$$

Reynolds number $Re = ud\rho/\eta$

$$=5.82\times0.028\times9.105/(9.372\times10^{-6})=1.582\times10^5$$

ii. Pressure loss due to friction in unit tube length, ΔP_1

Friction factor $\lambda=0.3164/Re^{0.25}=0.3164/(1.582\times10^5)^{0.25}=0.0159$

Pressure loss $\Delta P_1=\lambda/d\times(\rho u^2/2)$

$$=0.0159/0.028\times(9.105\times5.82^2/2)=8.76\times10^{-5}MPa/m$$

iii. Pressure loss at a 180° bending tube, ΔP_2

Pressure loss $\Delta P_2=K_{180°}\times(\rho u^2/2)$

$$=1.015\times(9.105\times5.82^2/2)=1.57\times10^{-4}MPa$$

vi. Pressure loss at a 90° bending tube, ΔP_3

Pressure loss $\Delta P_3=K_{90°}\times(\rho u^2/2)$

$$=1.301\times(9.105\times5.82^2/2)=2.01\times10^{-4}MPa$$

v. Evaluation

Total pressure loss $\Delta P=L\times\Delta P_1+N_2\times\Delta P_2+N_3\times\Delta P_3$

$$=200\times(8.76\times10^{-5})+28\times(1.57\times10^{-4})+168\times(2.01\times10^{-4})$$
$$=0.056MPa/path$$

As shown above, the total pressure loss of the unit heat transfer path at the upper port is lower than the target, 0.1MPa.

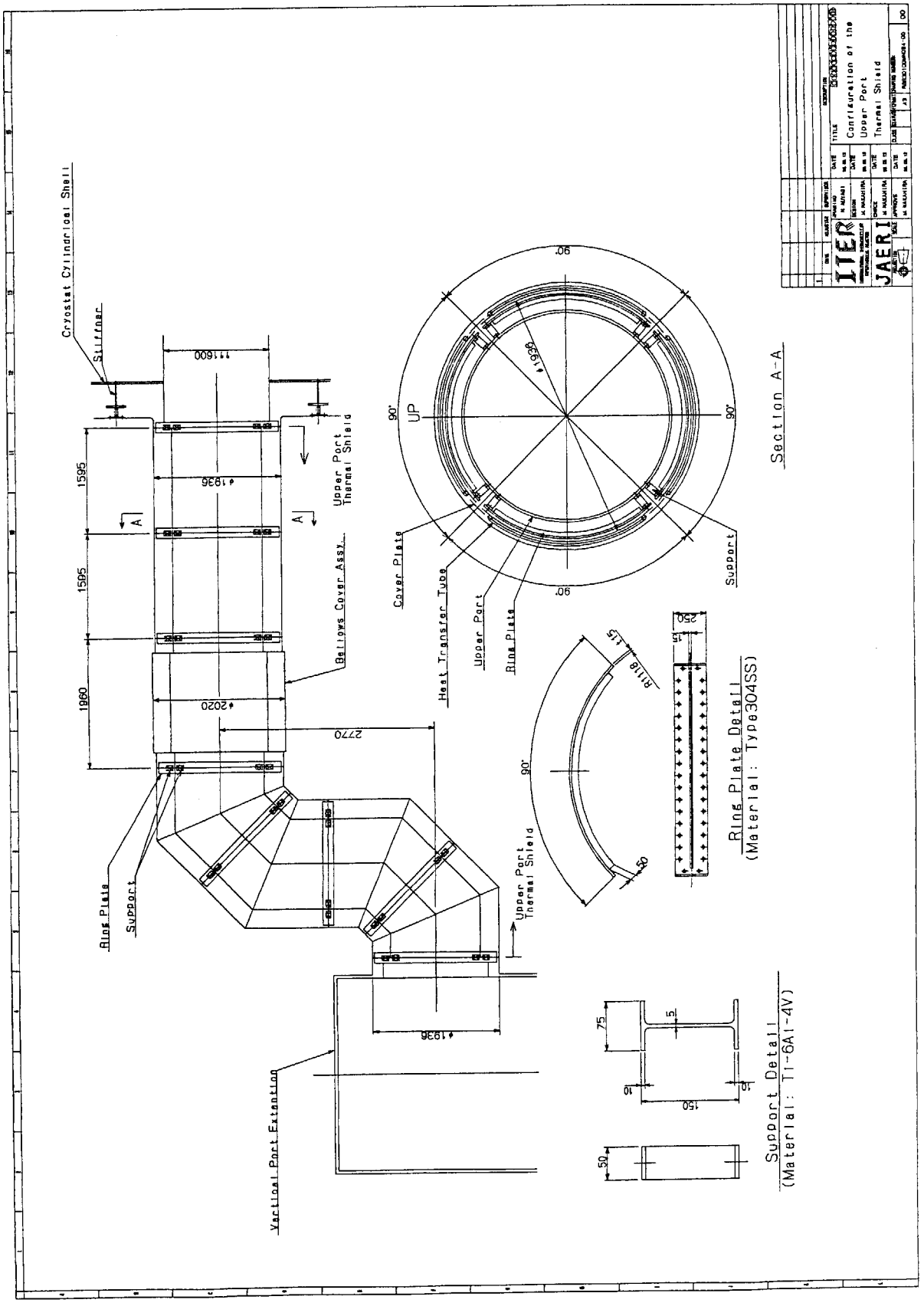

Fig. 3-18(1/2) Configuration of the Upper Port Thermal Shield

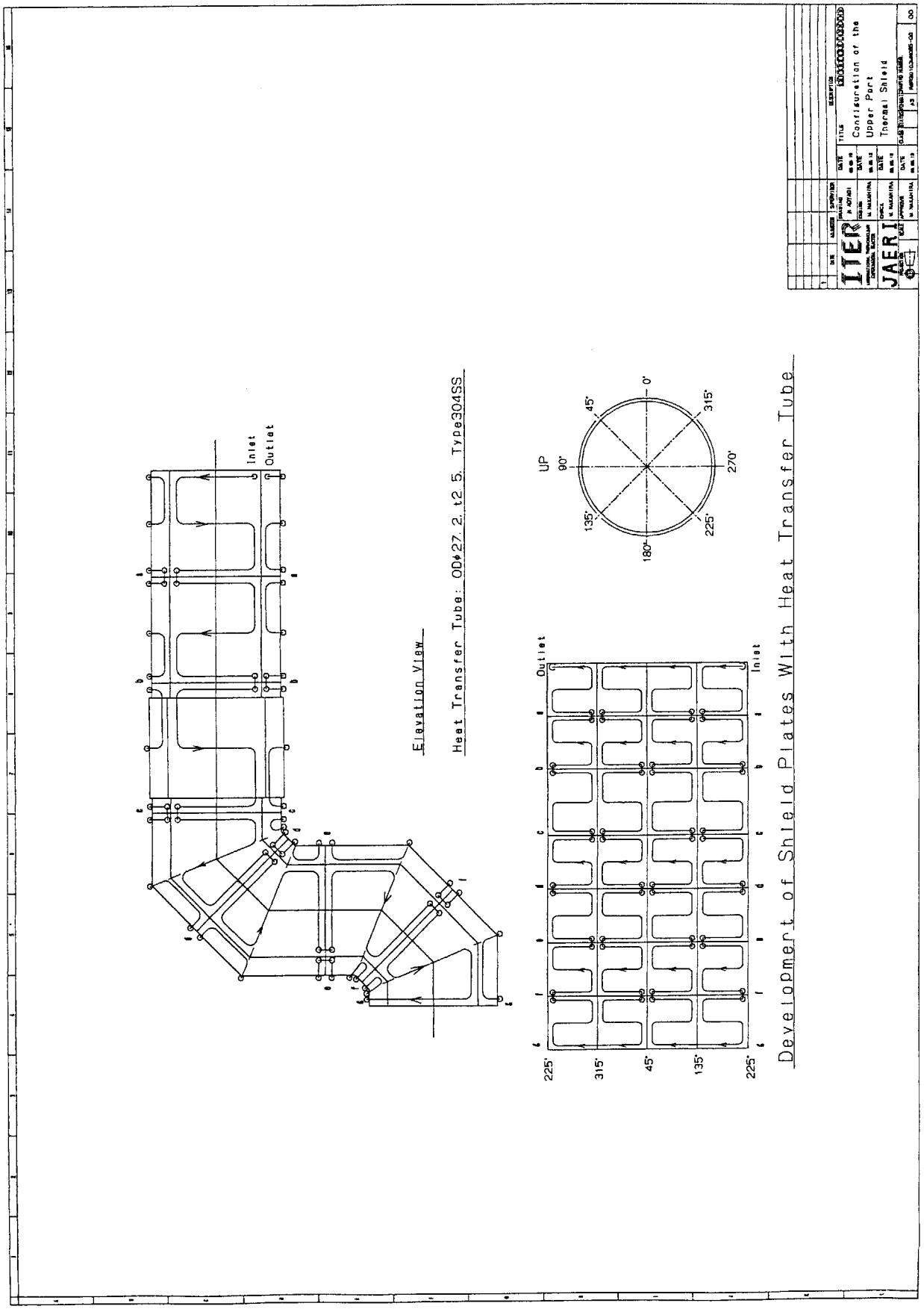

Fig. 3-18(2/2) Configuration of the Upper Port Thermal Shield

3.5.5 Equatorial port thermal shield

a. Design concept

i. Basically, the concept is the same as the upper port thermal shield.

ii. The heat transfer tube to be applied is 27.2mm in outer diameter and 2.5mm in thickness.

b. Configuration

Figure 3-19 shows the configuration of the thermal shield and arrangement of the heat transfer tube.

c. Heat leak

Heat leak of the thermal shield is estimated for the typical one with dimension of 2.53 by 2.27 meters, which is corresponding to the shield plate at the bellows cover assembly. As shown in Figure 3-19, the number of the shield plate and the support made of titanium alloy is 12 and 36, respectively.

(a) Heat leak from the support

$$q = A \cdot \bar{\lambda} \frac{\Delta T}{L} = (0.05 \times 0.005) \times 7.16 \times \frac{473 - 80}{0.13} = 5.5W$$

5.5×36= 198W/port

(b) Heat leak through the insulation

$$q = q_0 \frac{T^4 - T_c^4}{T_h^4 - T_c^4} = 1.5 \times \frac{473^4 - 80^4}{273^4 - 80^4} = 9.3W/m^2$$

A=2.53×2.27=3.4m^2

9.3×12×3.4= 380W/port

(c) Heat leak from the non-insulated portion

$$q = \sigma \frac{T_h^4 - T_c^4}{1/\varepsilon_c + 1/\varepsilon_h - 1} = 5.678 \times 10^{-8} \times \frac{473^4 - 80^4}{1/0.025 + 1/0.5 - 1} = 69.3W/m^2$$

A=36×(0.175×0.25)+12×[1-(1-0.014)^2]×3.4=2.710m^2

69.3×2.710= 188W/port

(d) Summation of heat leak

198+380+188= 766W/port

The total heat leak from the thermal shield of the equatorial ports is 20×766=15.4kW.

d. Structural integrity

(a) Integrity of the support made of Ti-6Al-4V

Dead weight of typical thermal shield (2.53m×2.27m=5.8m^2)

Shield plate (5.8m^2×t3mm)	1350N
Ring plate (0.25×2.53m×t15mm+stiffner)	890N
MLI blanket (4.2m^2×t12μm×50-layer)	50N
Heat transfer tube (OD27.2mm×t2.5mm×12m)	280N
Total	2570N→×1.2→3090N

i. Stress due to dead weight

Applied force V=3090/2=1545N

Bending moment $M=VL=1545\times130=200850Nmm$
Modulus of section $Z_V=5\times50^2/6=2083mm^3$
Bending stress $\sigma_b=M/Z=200850/2083=97MPa$
Allowable limit $1.5kSm=1.5\times1\times298=447MPa$

ii. Stress due to seismic force [Horizontal/0.2G, Vertical/-1.2G]

Applied force $H=0.2\times3090/2=310N$ [Horizontal]
$V=(1+0.2)\times3090/2=1854N$ [Vertical]
Bending moment $M_H=HL=310\times130=40300Nmm$ [Horizontal]
$M_V=VL=1854\times130=241020Nmm$ [Vertical]
Modulus of section $Z_H=50\times5^2/6=208mm^3$ [Horizontal]
$Z_V=5\times50^2/6=2083mm^3$ [Vertical]
Bending stress $\sigma_{b,H}=M_H/Z_H=40300/208=194MPa$ [Horizontal]
$\sigma_{b,V}=M_V/Z_V=241020/2083=116MPa$ [Vertical]
Allowable limit $1.5kSm=1.5\times1.2\times298=536MPa$

iii. Stress due to thermal shrinkage [473K→80K, type304SS]

Thermal shrinkage $\delta_1=(2530/2)\times0.0062=7.9mm$ [long side direction]
Thermal shrinkage $\delta_2=(2270/2)\times0.0062=7.1mm$ [short side direction]
Constraint disp. $\Delta\delta=\delta_1=7.9mm$
Bending stress $\sigma_b=3Eh\Delta\delta/(2L^2)$
$=3\times118000\times5\times7.9/(2\times130^2)=414MPa$
Allowable limit $3Sm=3\times298=894MPa$

iv. Stress due to combined loading

Load combination thermal shrinkage +(dead weight + seismic force)
Evaluated stress $414+194=608MPa$
Allowable stress $3Sm=3\times298=894MPa$

(b) Natural period of the thermal shield

i. Natural period of in-plane mode

Mass $M=F/g=3090/9.8=316kg$
Stiffness $K=2\times(3EI/L^3)$
$=2\times[3\times(1.18\times10^{11})\times(0.005^3\times0.05/12)]/0.13^3$
$=167843N/m$
Natural period $T=2\pi(M/K)^{1/2}=2\pi(316/167843)^{1/2}=0.28s$

ii. Natural period of out-of-plane mode

Corrected density $\rho=7900\times(1260+50+280)/1260=9970kg/m^3$
Flexural rigidity $D=Eh^3/12(1-\nu^2)$
$=2\times10^{11}\times0.003^3/12/(1-0.3^2)$
$=495N/m$
Factor $k=9.631$
Equivalent side length

$$\bar{a}=\sqrt{a\times b}=\sqrt{2.53\times2.27}=2.40m$$

Natural period

$$T=\frac{2\pi}{k}\sqrt{\frac{\rho h\bar{a}^4}{D}}=\frac{2\pi}{9.631}\times\sqrt{\frac{9970\times0.003\times2.40^4}{495}}=0.93s$$

(c) Integrity and deflection of the ring plate

i. Stress and deflection due to dead weight

Bending moment $M=FL/12=3090\times2530/12=651475Nmm$
Modulus of section $Z_V=132005mm^3$

Bending stress $\sigma_b=M/Z_V=651475/132005=5.0MPa$
Allowable limit $1.5kSm=1.5\times1\times138=207MPa$
Deflection $\delta=FL^3/(384EI_V)$
$=3090\times2530^3/[384\times200000\times6445468]=0.2mm$

ii. Stress and deflection due to seismic force

(i) Horizontal direction, 0.2G

Bending stress $\sigma_b=(0.2FL/12)/Z_H$
$=(0.2\times3090\times2530/12)/156362=0.9MPa$
Allowable limit $1.5kSm=1.5\times1.2\times138=248MPa$
Deflection $\delta=0.2FL^3/(384EI_{MIN})$ $I_{MIN}=MIN(I_X, I_Y)$
$=0.2\times3090\times2530^3/(384\times200000\times6415468)=0.1mm$

(ii) Vertical direction, 1.2G

Bending stress $\sigma_b=(1.2FL/12)/Z_V$
$=(1.2\times3090\times2530/12)/132005=6.0MPa$
Allowable limit $1.5kSm=1.5\times1.2\times138=248MPa$
Deflection $\delta=1.2FL^3/(384EI_V)$
$=1.2\times3090\times2530^3/(384\times200000\times6415468)=0.2mm$

e. Heat transfer and pressure loss

The performance of heat transfer and pressure loss is evaluated. The heat transfer tube made of type 304 stainless steel is 27.2mm in outer diameter and 2.5mm in thickness.

(a) Heat removal of unit tube-path

i. Heat leak

through the MLI blanket		380W/path
from the support		198W/path
from non-insulated portion		188W/path
Summation		766W/path

ii. External heating

Nuclear heating	$q\bullet V=6\times[(58000\times0.3)\times1\times10^{-3}]=$	123W/path
Joule heating	86W/path	
Summation		209W/path

iii. Total removal heating 975W/path→ 1100W/path

□□□; Factor of two is multiplied by the analytical result conducted in FY'96 because of volumetric correction for the shield plate.

(b) Necessary flow rate of coolant

i. Mass flow rate of coolant

Mass flow rate $G=Q/\Delta h=1100/52.2=21.1g/s$
Mean velocity in tube
$u=(G/\rho)/A$
$=(21.1\times10^{-3}/9.105)/(0.0222^2\pi/4)=5.99m/s$
Reynolds number $Re = ud\rho/\eta$
$=5.99\times0.0222\times9.105/(9.372\times10^{-6})=1.292\times10^5$

ii. Pressure loss due to friction in unit tube length, ΔP_1

Friction factor $\lambda=0.3164/Re^{0.25}=0.3164/(1.292\times10^5)^{0.25}=0.0167$

Pressure loss $\Delta P_1=\lambda/d\times(\rho u^2/2)$

$=0.0167/0.0222\times(9.105\times5.99^2/2)=1.29\times10^{-4}$MPa/m

iii. Pressure loss at a 180° bending tube, ΔP_2

Pressure loss $\Delta P_2=K_{180°}\times(\rho u^2/2)$

$=1.015\times(9.105\times5.99^2/2)=1.67\times10^{-4}$MPaa

vi. Pressure loss at a 90° bending tube, ΔP_3

Pressure loss $\Delta P_3=K_{90°}\times(\rho u^2/2)$

$1.301\times(9.105\times5.99^2/2)=2.13\times10^{-4}$MPa

v. Evaluation

Total pressure loss $\Delta P=L\times\Delta P_1+N_2\times\Delta P_2+N_3\times\Delta P_3$

$=120\times(1.29\times10^{-4})+12\times(1.67\times10^{-4})+84\times(2.13\times10^{-4})$

$=0.036$MPa/path

As shown above, the total pressure loss of the unit heat transfer path at the equatorial port is lower than the target, 0.1MPa.

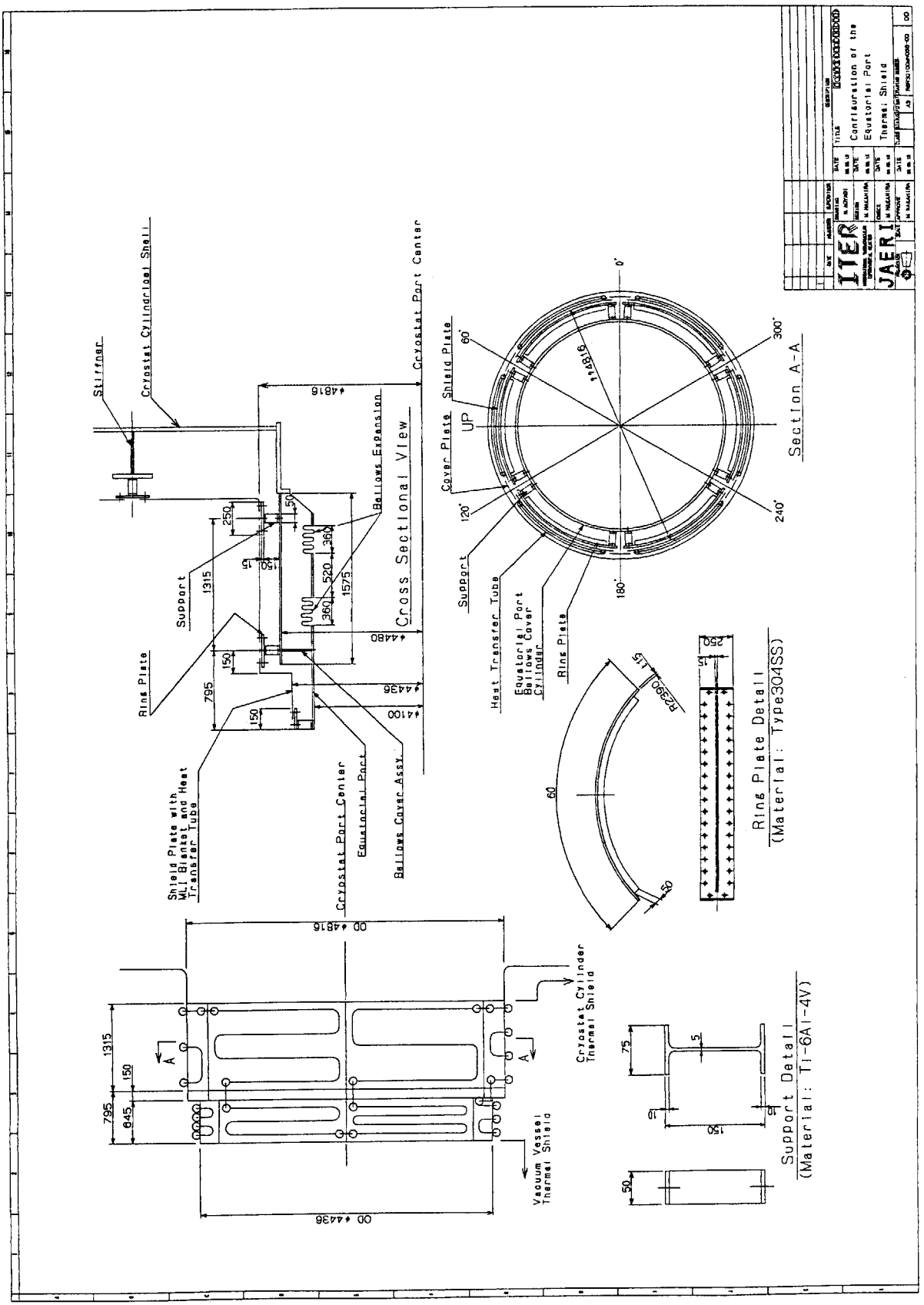

Fig. 3-19(1/2) Configuration of the Equatorial Port Thermal Shield

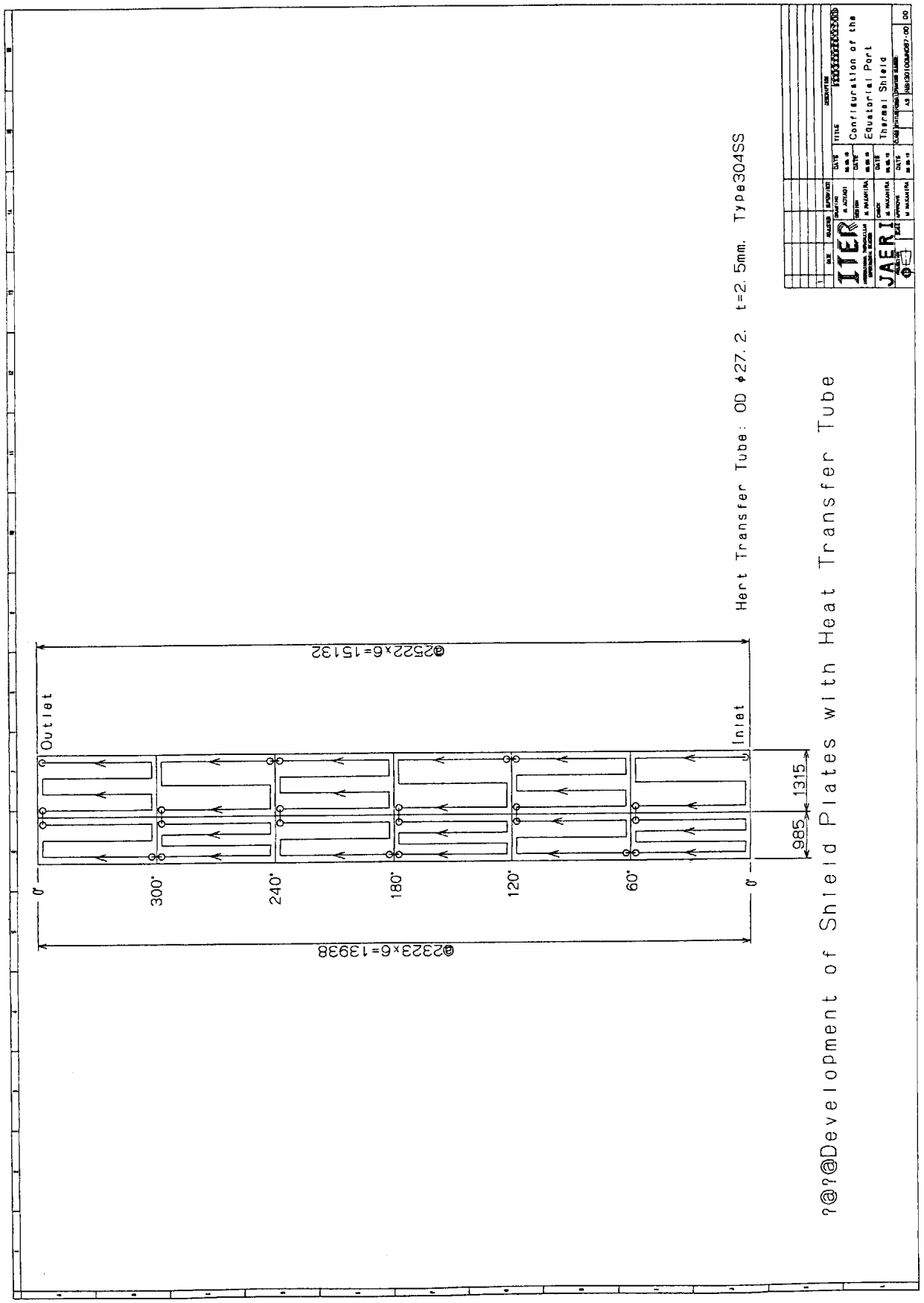

Fig. 3-19(2/2) Configuration of the Equatorial Port Thermal Shield

3.5.6 Divertor port thermal shield

a. Design concept

i. Basically, the concept is the same as the upper port thermal shield.
ii. The heat transfer tube to be applied is 27.2mm in outer diameter and 2.5mm in thickness.
iii. As pressure loss per unit port is relatively small, two ports can be cooled down by a unit tube-path.

b. Configuration

Figure 3-20 shows the configuration of the thermal shield and arrangement of the heat transfer tube.

c. Heat leak

Heat leak of the thermal shield is estimated for the typical one that dimension is 2.53 by 1.15 meters which is corresponding to the shield plate at the bellows cover assembly. As shown in Figure 3-20, number of the shield plate and the support made of titanium alloy is 6 and 24, respectively.

(a) Heat leak from the support

$$q = A \cdot \bar{\lambda} \frac{\Delta T}{L} = (0.05 \times 0.005) \times 7.16 \times \frac{473 - 80}{0.13} = 5.5W$$

5.5×24= 132W/port

(b) Heat leak through the insulation

$$q = q_0 \frac{T^4 - T_c^4}{T_h^4 - T_c^4} = 1.5 \times \frac{473^4 - 80^4}{273^4 - 80^4} = 9.3W/m^2$$

$A=2.53\times1.15=3.0m^2$

9.3×6×3.0= 168W/port

(c) Heat leak from the non-insulated portion

$$q = \sigma \frac{T_h^4 - T_c^4}{1/\varepsilon_c + 1/\varepsilon_h - 1} = 5.678 \times 10^{-8} \times \frac{473^4 - 80^4}{1/0.025 + 1/0.5 - 1} = 69.3W/m^2$$

$A=36\times(0.175\times0.25)+12\times[1-(1-0.014)^2]\times3.0=1.551m^2$

69.3×1.551= 108W/port

(d) Summation of heat leak

132+168+108= 408W/port

Total heat leak from the thermal shield of the divertor ports is 20×408=8.2kW.

d. Structural integrity

The stresses that appear in each part of the divertor port's thermal shield will be lower than those in the equatorial port's. Therefore, stress-evaluation for this thermal shield is omitted.

e. Heat transfer and pressure loss

The performance of heat transfer and pressure loss is evaluated. The heat transfer tube made of type 304 stainless steel is 27.2mm in outer diameter and 2.5mm in thickness.

(a) Heat removal of unit tube-path

i. Heat leak

through the MLI blanket		168W
from the support		132W
from non-insulated portion		108W
Summation		408W

ii. External heating

Nuclear heating	$q \bullet V=6\times[(30000\times0.3)\times1\times10^{-3}]=$	54W
Joule heating	100W	
Summation		154W

iii. Total removal heating of unit port 562W

iv. Total removal heating for series cooling

A series cooling path for two divertor ports should be removed $2\times562=1124$W/path. Considering heat leak through the transfer piping between the adjacent ports, a somewhat large margin should be taken into account. Therefore, the total heat removal of the series cooling is set up to 1400W/path.

□□□; Factor of two is multiplied by the analytical result conducted in FY'96 because of volumetric correction for the shield plate.

(b) Necessary flow rate of coolant

i. Mass flow rate of coolant

Mass flow rate $G=Q/\Delta h=1400/52.2=26.9$g/s

Mean velocity in tube

$$u=(G/\rho)/A$$
$$=(26.9\times10^{-3}/9.105)/(0.0222^2\pi/4)=7.64\text{m/s}$$

Reynolds number $Re = ud\rho/\eta$

$$=7.64\times0.0222\times9.105/(9.372\times10^{-6})=1.648\times10^5$$

ii. Pressure loss due to friction in unit tube length, ΔP_1

Friction factor $\lambda=0.3164/Re^{0.25}=0.3164/(1.648\times10^5)^{0.25}=0.0157$

Pressure loss $\Delta P_1=\lambda/d\times(\rho u^2/2)$

$$=0.0157/0.0222\times(9.105\times7.64^2/2)=1.88\times10^{-4}\text{MPa/m}$$

iii. Pressure loss at a 180° bending tube, ΔP_2

Pressure loss $\Delta P_2=K_{180°}\times(\rho u^2/2)$

$$=1.015\times(9.105\times7.64^2/2)=2.70\times10^{-4}\text{MPa}$$

vi. Pressure loss at a 90° bending tube, ΔP_3

Pressure loss $\Delta P_3=K_{90°}\times(\rho u^2/2)$

$$1.301\times(9.105\times7.64^2/2)=3.46\times10^{-4}\text{MPa}$$

v. Evaluation

Total pressure loss $\Delta P=2[L\times\Delta P_1+N_2\times\Delta P_2+N_3\times\Delta P_3]$

$$=2[60\times(1.88\times10^{-4})+6\times(2.70\times10^{-4})+36\times(3.46\times10^{-4})]$$
$$=0.051\text{MPa/path}$$

As shown above, the total pressure loss of the unit heat transfer path to cooled down adjacent two divertor ports is lower than the target, 0.1MPa.

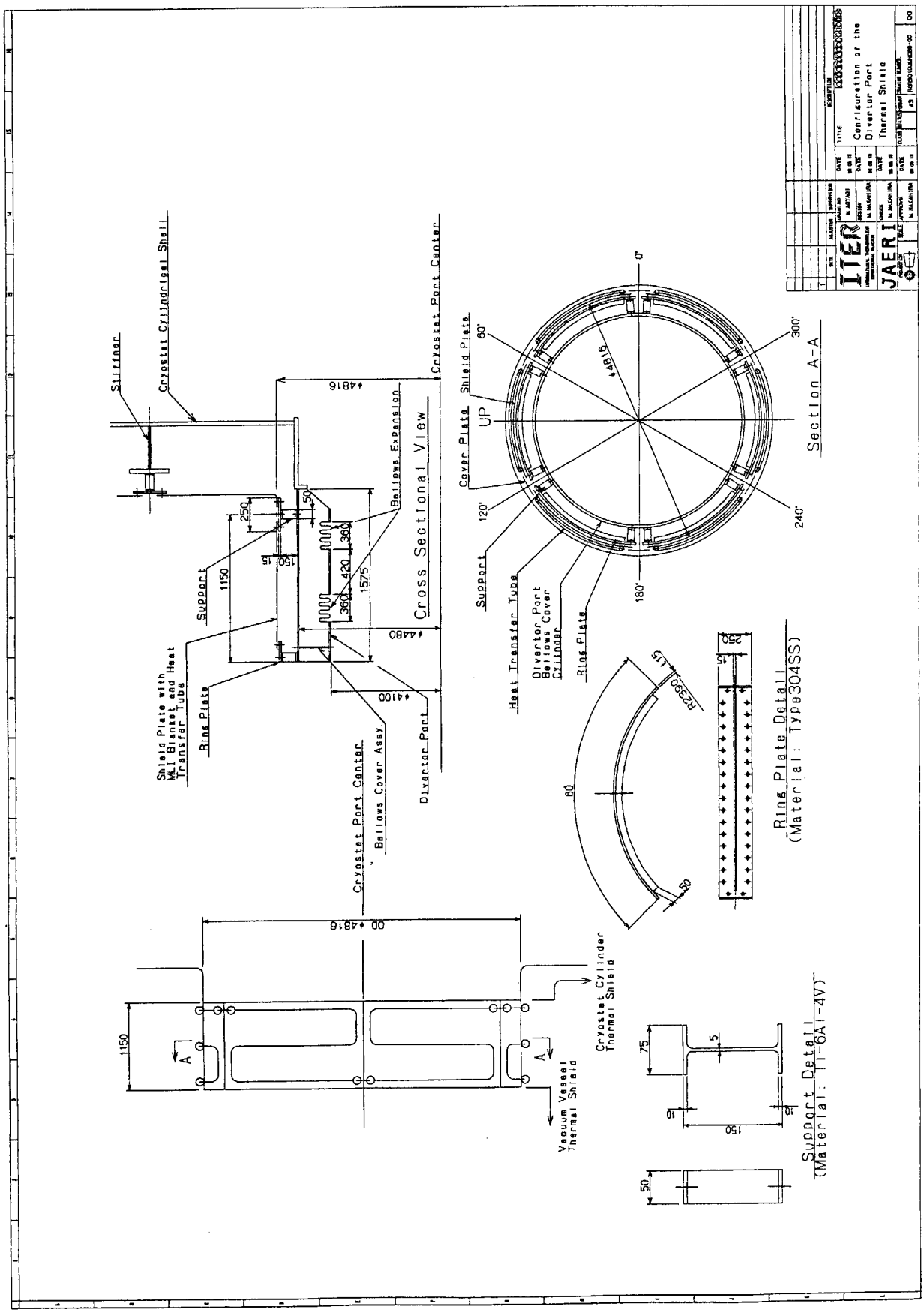

Fig. 3-20(1/2) Configuration of the Divertor Port Thermal Shield

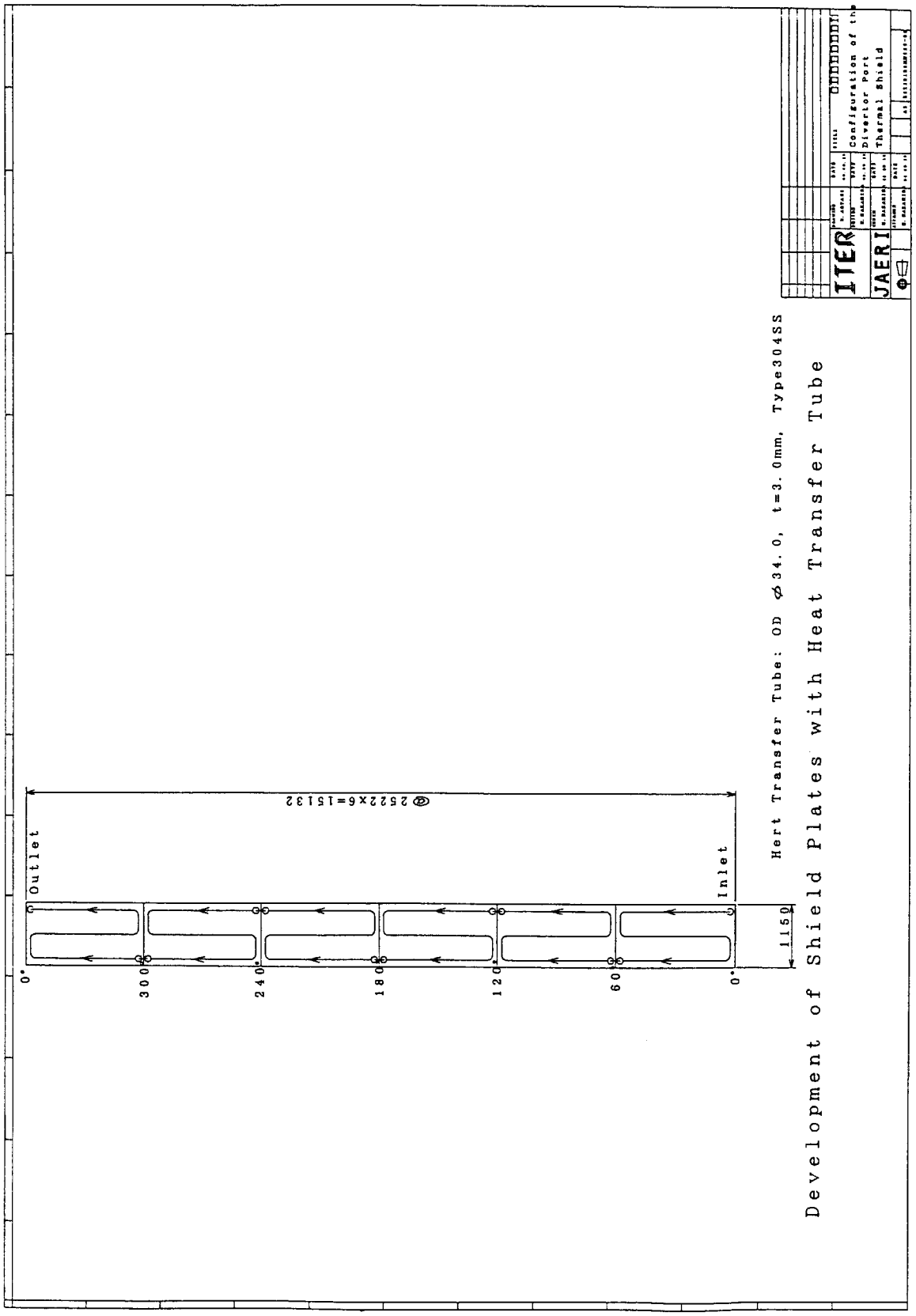

Fig. 3-20(2/2) Configuration of the Divertor Port Thermal Shield

3.5.7 Gravity support thermal shield

a. Design concept

i. Basically, the concept is the same as the cryostat cylinder thermal shield.
ii. The shield plates should be subdivided not to the absorb deflectional behavior of the gravity support itself.
iii. The shield plates should be also covered the ring pedestal.
iv. The heat transfer tube to be applied is 27.2mm in outer diameter and 2.5mm in thickness.
v. As pressure loss per a unit gravity support is relatively small, two supports can be cooled down by a unit tube-path.

b. Configuration

Figure 3-21 shows the configuration of the thermal shield and arrangement of the heat transfer tube.

c. Heat leak

As shown in Figure 3-21, number of the shield plate and the support made of titanium alloy is 16 and 36, respectively . The total surface area of the gravity support is $32m^2$.

(a) Heat leak from the support

$$q = A \cdot \bar{\lambda} \frac{\Delta T}{L} = (0.05 \times 0.005) \times 5.63 \times \frac{300-80}{0.13} = 2.4W$$

2.4×36= 87W

(b) Heat leak through the insulation

$q=1.5w/m^2$

1.5×32= 48W

(c) Heat leak from the non-insulated portion

$$q = \sigma \frac{T_h^4 - T_c^4}{1/\varepsilon_c + 1/\varepsilon_h - 1} = 5.678 \times 10^{-8} \times \frac{300^4 - 80^4}{1/0.025 + 1/0.5 - 1} = 11.6W/m^2$$

$A=36\times(0.175\times0.25)+[1-(1-0.014)^2]\times32=2.465m^2$

11.6×2.465= 29W

(d) Summation of heat leak

87+48+29= 164W

Total heat leak from the thermal shield of the gravity supports is 20×164=3.3kW.

d. Structural integrity

(a) Integrity of the support made of Ti-6Al-4V

Dead weight of typical thermal shield (1.71m×1.98m=$3.4m^2$)

Shield plate ($3.4m^2$×t3mm)	800N
Ring plate (0.25×1.71m×t15mm+stiffner)	600N
MLI blanket ($3.4m^2$×t12μm×50-layer)	30N
Heat transfer tube (OD27.2mm×t2.5mm×10m)	160N
Total	1590N→×1.2→2000N

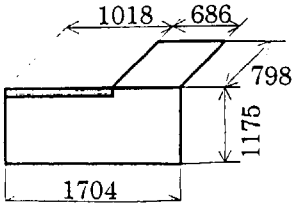

i. Stress due to dead weight

Applied force V=2000/2=1000N

Bending moment M=VL=1000×130=130000Nmm

Modulus of section $Z_V=5\times50^2/6=2083mm^3$

Bending stress $\sigma_b=M/Z=130000/2083=63MPa$

Allowable limit 1.5kSm=1.5×1×298=447MPa

ii. Stress due to seismic force [Horizontal/0.2G, Vertical/-1.2G]

Applied force H=0.2×2000/2=200N [Horizontal]

V=(1+0.2)×2000/2=1200N [Vertical]

Bending moment $M_H=HL=200\times130=26000Nmm$ [Horizontal]

$M_V=VL=1200\times130=156000Nmm$ [Vertical]

Modulus of section $Z_H=50\times5^2/6=208mm^3$ [Horizontal]

$Z_V=5\times50^2/6=2083mm^3$ [Vertical]

Bending stress $\sigma_{b,H}=M_H/Z_H=26000/208=125MPa$ [Horizontal]

$\sigma_{b,V}=M_V/Z_V=156000/2083=75MPa$ [Vertical]

Allowable limit 1.5kSm=1.5×1.2×298=536MPa

iii. Stress due to thermal shrinkage [300K→80K, type304SS]

Thermal shrinkage $\delta_1=(1710/2)\times0.0029=2.5mm$ [long side direction]

Thermal shrinkage $\delta_2=(1175/2)\times0.0029=1.8mm$ [short side direction]

Constraint disp. $\Delta\delta=\delta_1=2.5mm$

Bending stress $\sigma_b=3Eh\Delta\delta/(2L^2)$

$=3\times118000\times5\times2.5/(2\times130^2)=131MPa$

Allowable limit 3Sm=3×298=894MPa

iv. Stress due to combined loading

Load combination thermal shrinkage +(dead weight + seismic force)

Evaluated stress 131+125=256MPa

Allowable stress 3Sm=3×298=894MPa

(b) Natural period of the thermal shield

i. Natural period of in-plane mode

Mass M=F/g=1000/9.8=102kg

Stiffness $K=2\times(3EI/L^3)$

$=2\times[3\times(1.18\times10^{11})\times(0.005^3\times0.05/12)]/0.13^3$

=167843N/m

Natural period $T=2\pi(M/K)^{1/2}=2\pi(102/167843)^{1/2}=0.16s$

ii. Natural period of out-of-plane mode

Corrected density $\rho=7900\times(800+30+160)/800=9777kg/m^3$

Flexural rigidity $D=Eh^3/12(1-\nu^2)$

$=2\times10^{11}\times0.003^3/12/(1-0.3^2)$

=495N/m

Factor k=9.631

Equivalent side length

$$\bar{a}=\sqrt{a\times b}=\sqrt{1.71\times1.98}=1.84m$$

Natural period

$$T=\frac{2\pi}{k}\sqrt{\frac{\rho h\bar{a}^4}{D}}=\frac{2\pi}{9.631}\sqrt{\frac{9.777\times0.003\times1.84^4}{495}}$$

(c) Integrity and deflection of the ring plate

i. Stress and deflection due to dead weight

Bending moment $M=FL/12=1000\times1710/12=142500Nmm$

Modulus of section $Z_V=132005mm^3$

Bending stress $\sigma_b=M/Z_V=142500/132005=1.1MPa$

Allowable limit $1.5kSm=1.5\times1\times138=207MPa$

Deflection $\delta=FL^3/(384EI_V)$

$=1000\times1710^3/[384\times200000\times6445468]=0.1mm$

ii. Stress and deflection due to seismic force

(i) Horizontal direction, 0.2G

Bending stress $\sigma_b=(0.2FL/12)/Z_H$

$=(0.2\times1000\times1710/12)/156362=0.2MPa$

Allowable limit $1.5kSm=1.5\times1.2\times138=248MPa$

Deflection $\delta=0.2FL^3/(384EI_{MIN})$ $I_{MIN}=MIN(I_X, I_Y)$

$=0.2\times1000\times1710^3/(384\times200000\times6415468)=0.1mm$

(ii) Vertical direction, 1.2G

Bending stress $\sigma_b=(1.2FL/12)/Z_V$

$=(1.2\times1000\times1710/12)/132005=1.3MPa$

Allowable limit $1.5kSm=1.5\times1.2\times138=248MPa$

Deflection $\delta=1.2FL^3/(384EI_V)$

$=1.2\times1000\times1710^3/(384\times200000\times6415468)=0.1mm$

e. Heat transfer and pressure loss

Performance of heat transfer and pressure loss are evaluated. The heat transfer tube made of type 304 stainless steel is 27.2mm in outer diameter and 2.5mm in thickness. A tube-path cools down two gravity support's thermal shields in series.

(a) Heat removal of unit tube-path

i. Heat leak

through the MLI blanket		48W
from the support		87W
from non-insulated portion		29W
Summation		164W

ii. External heating

Nuclear heating	$q\bullet V=(320000\times0.3)\times1\times10^{-5}=$	1W
Joule heating	35W	
Summation		36W

iii. Total removal heating of unit port 200W

iv. Total removal heating for series cooling

A series cooling path for two gravity supports will be removed $2\times200=400W$/path. The total heat removal of the series cooling is set up to 500W/path in this design.

(b) Necessary flow rate of coolant

i. Mass flow rate of coolant

Mass flow rate $G=Q/\Delta h=500/52.2=9.6g/s$

Mean velocity in tube

$$u=(G/\rho)/A$$
$$=(9.6\times10^{-3}/9.105)/(0.0222^2\pi/4)=2.73m/s$$

Reynolds number $Re = ud\rho/\eta$

$$=2.73\times0.0222\times9.105/(9.372\times10^{-6})=5.888\times10^4$$

ii. Pressure loss due to friction in unit tube length, ΔP_1

Friction factor $\lambda=0.3164/Re^{0.25}=0.3164/(5.888\times10^4)^{0.25}=0.0203$

Pressure loss $\Delta P_1=\lambda/d\times(\rho u^2/2)$

$$=0.0203/0.0222\times(9.105\times2.73^2/2)=3.11\times10^{-5}MPa/m$$

iii. Pressure loss at a 180° bending tube, ΔP_2

Pressure loss $\Delta P_2=K_{180°}\times(\rho u^2/2)$

$$=1.015\times(9.105\times2.73^2/2)=3.45\times10^{-5}MPa$$

vi. Pressure loss at a 90° bending tube, ΔP_3

Pressure loss $\Delta P_3=K_{90°}\times(\rho u^2/2)$

$$=1.301\times(9.105\times2.73^2/2)=4.42\times10^{-5}MPa$$

v. Evaluation

Total pressure loss $\Delta P=2[L\times\Delta P_1+N_2\times\Delta P_2+N_3\times\Delta P_3]$

$$=2[190\times(3.11\times10^{-5})+32\times(3.45\times10^{-5})+198\times(4.42\times10^{-5})]$$
$$=0.032MPa/path$$

As shown above, the total pressure loss of a unit heat transfer path to cooled down adjacent two gravity supports is lower than the target, 0.1MPa.

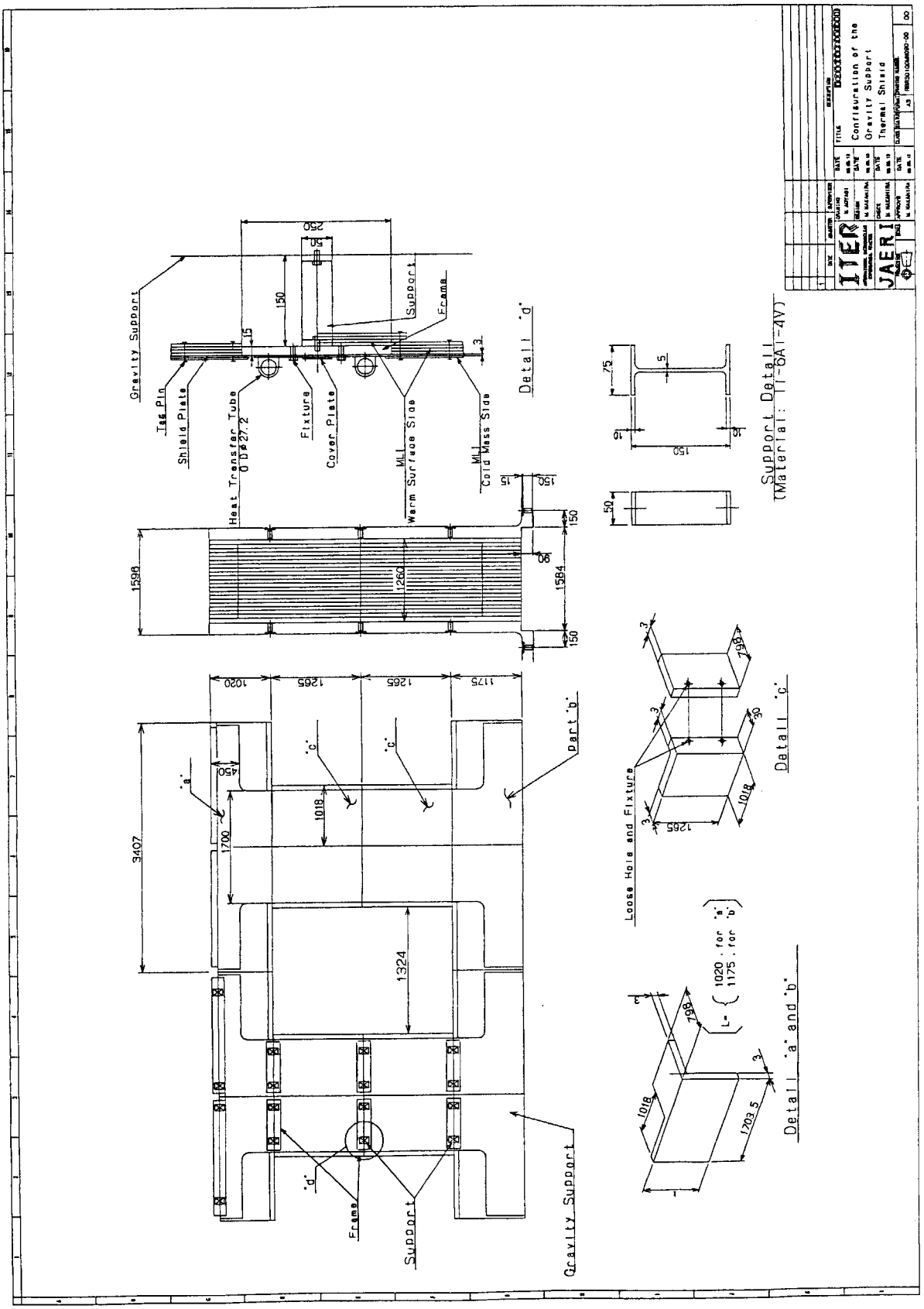

Fig. 3-21(1/2) Configuration of the Gravity Support Thermal Shield

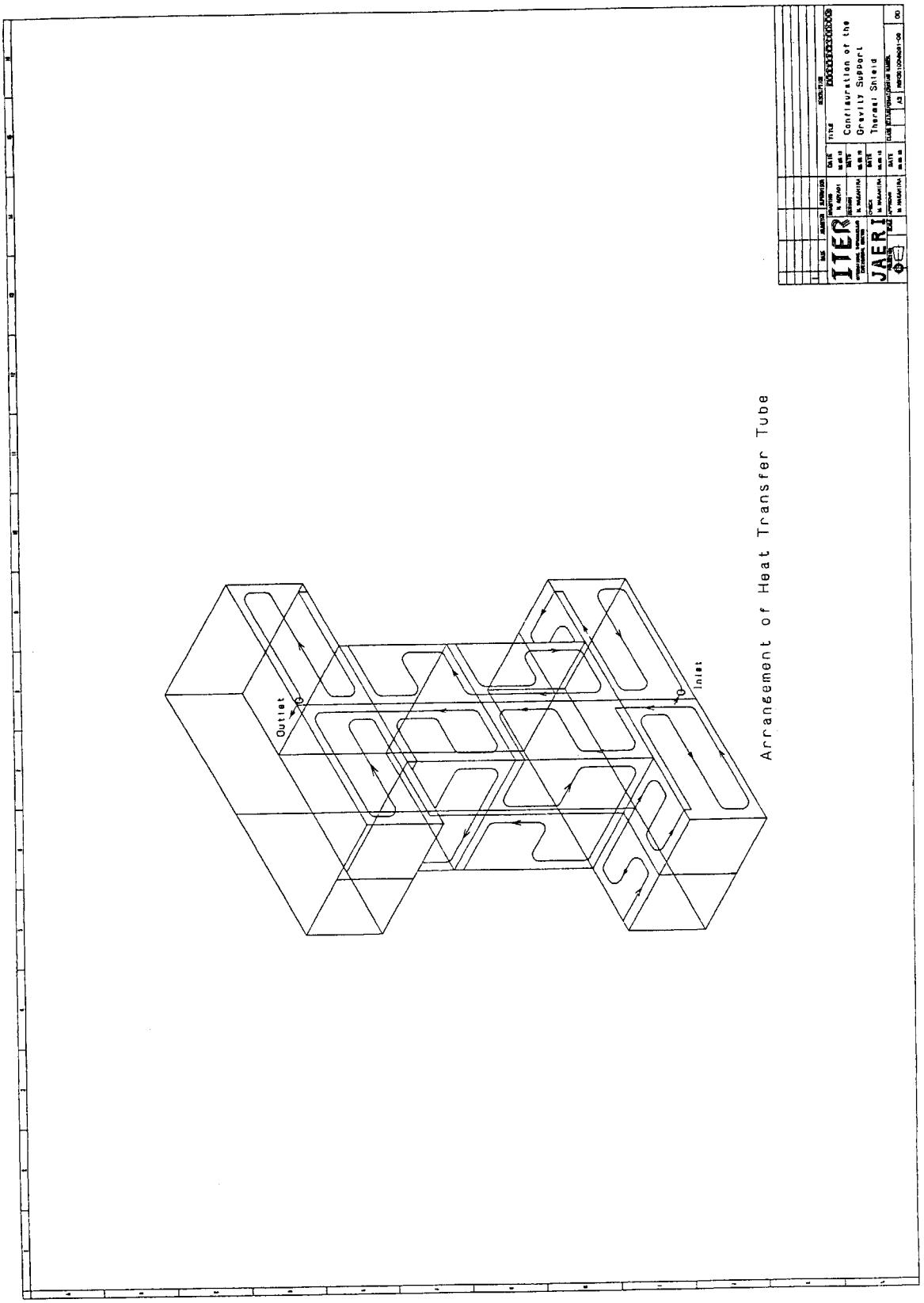

Fig. 3-21(2/2) Configuration of the Gravity Support Thermal Shield

3.6 Summary of detailed design

In this section, design outputs of structural integrity, heat leak and specifications of heat transfer tube for each of the thermal shields are summarized. Also, heat leak radiated to the cold magnet is evaluated.

(1) Structural integrity

Stresses that appear in the support made of titanium alloy is tabulated in Table 3-9. As shown in the table, structural integrity can be confirmed.

Table 3-9 Stress evaluation results for the support

(unit of stress; MPa)

Portion \ loading combination		DW	DW+SL	DW+SL+TS	Judgment
Cryostat	Cylindrical shell	175 (447)	350 (536)	785 (894)	good
	Upper cover	8 (298)	250 (536)	470 (894)	good
	Lower cover	8 (298)	250 (536)	470 (894)	good
Ports	Upper port	66 (447)	132 (536)	394 (894)	good
	Equatorial port	97 (447)	194 (536)	608 (894)	good
	Divertor port	97 (447)	194 (536)	608 (894)	good
Gravity support	---	63 (447)	125 (536)	256 (894)	good

[NOTES]

1. "DW" means dead weight.
2. "SL" means seismic force, e.g. 0.2G.
3. "TS" means thermal shrinkage of the shield plate.
4. Number in the parentheses means the allowable stress limit prescribed in ASME B&PV Code Sec. VIII, Division-2.

(2) Heat leak to the thermal shield

Table 3-10 shows a summary of heat leak transmitted from the warm surface of the cryostat, the ports and the gravity supports to their thermal shields. The results evaluated can be confirmed to be lower than the limitations.

Table 3-10 Heat leak to the thermal shield

Item / Portion		Heat leak (kW)	Limitation (kW)	Judgment
Cryostat	Cylindrical shell	11.6	---	---
	Upper cover	7.7		
	Lower cover	8.6		
Subtotal	A	27.9	45	good
Ports	Upper ports	31.2	---	---
	Equatorial ports	15.4		
	Divertor ports	8.2		
Subtotal	B	54.8	75	good
Gravity supports	C	3.3	---	---
Total	A+B+C	86.0	120	good

(3) Specifications of heat transfer tube

The size of the heat transfer tube, the number of the tube-path and the pressure loss are tabulated in Table 3-11. The pressure loss of the heat transfer tube on the shield plates is approximately 50kPa, that corresponds to half of the target for the overall pressure loss.

Table 3-11 Specifications of heat transfer tube

Portion / Item			Tube size OD×THK (mm)	Number of tube-path (---)	Pressure loss (kPa)
Cryostat	Cylindrical shell		34.0×3.0	20	53
	Upper cover	Outer block	27.2×2.5	10	44
		Inner block	27.2×2.5	2	24
	Lower cover	Outer block	34.0×3.0	4	51
		Inner block□□□	34.0×3.0	4	37
Ports	Upper ports		34.0×3.0	20	56
	Equatorial ports		27.2×2.5	20	36
	Divertor ports		27.2×2.5	10	51
Gravity supports	----		27.2×2.5	10	32

□□□□ The central coil support assembly is also included here.

(4) Heat leak to the cold magnet

Heat leak due to thermal radiation to the cold magnet can be evaluated by using the following equation.

$$Q = \sigma \cdot A_c \frac{T_h^4 - T_c^4}{1/\varepsilon_c + \left(1/\varepsilon_h - 1\right) \cdot \left(A_c/A_h\right)}$$

where,

Q; total heat leak (W)
σ; Stefen - Boltzmann constant $=5.67\times10^{-8}Wm^2/K^4$
T_h; warm surface temperature (K)
T_{ic}; cold surface temperature $=4.5K$
ε_h; emissivity at warm surface $=0.05$ (Al-deposited surface of the MLI)
ε_c; emissivity at cold surface $=1.0$ ("black body" is assumed)
A_{HD}; warm surface area $=10000m^2$
A_c; cold surface area $=8020m^2$

The warm surface temperature, T_h, can be obtained from the temperature distribution analyses. According to the results, the highest temperature on the shield plate is as follows:

i. thermal shield equipped with the MLI blanket; $T_{MLI}=86.7K$
ii. thermal shield equipped with the reflecting plates; $T_{MRP}=96.1K$

Both of the temperature are the results under the condition that the inlet temperature of gaseous helium is 80K. However, some temperature rise of the coolant due to the heat exchange should be considered. In this design, bulk-temperature rise, ΔT, was assumed to be 10K as shown in 3.5.1-e-(b). The equivalent temperature of the warm surface can be estimated by weighting the surface area for each kind of the shield plate. The portion to be applied to the reflecting plates is limited in the vicinity of the NBI ducts on the cylindrical shell. Therefore, the number of the shield plate equipped with the reflecting plates is approximately thirty, e.g. five rows by six columns. The total surface area of the thermal shield equipped with the reflecting plates, A_{MRF}, is estimated as $30\times(5.7\times1.5)\approx260m^2$.

Therefore, the equivalent temperature of the warm surface, T_h, is

$$T_h = [(T_{MRP}+\Delta T)A_{MRP}+(T_{MIL}+\Delta T)(A_h-A_{MRP})]/A_h$$
$$= [(96.1+10)\times260+(86.7+10)\times(A_h-260)]/A_h$$
$$= 97K.$$

Finally, heat leak due to thermal radiation is obtained as

$$Q = 5.67\times10^{-8}\times8020\times\frac{97^4-4.5^4}{1/1.0+\left(1/0.05-1\right)\cdot\left(8020/1000\right)} = 2480W$$

The result above satisfies the target of the heat leak to the cold magnets, 2500W.

4. Cooling system design description

This chapter describes the fundamental design output of the gaseous helium transfer system arranged between three pairs of the valve boxes. In this task, the sizing estimation for each of the control valves and the overall pressure loss assessment are performed. For the pressure loss assessment, the arrangements of the transfer piping are designed considering the location of the valve boxes and structural integrity of the piping itself. Also, an engineering flow sheet of the cooling system are drawn up.

4.1 Sizing of control valve

The 80K-gaseous helium coolant supplied from the cryoplant is distributed and transferred to each of the heat transfer tube set up on the shield plates. According to the JCT's planning, there are three pairs of the valve boxes for the cryostat thermal shields. Each of the valve boxes consist of the inlet valve box and the outlet valve box. The inlet valve box is an adiabatic vacuum vessel contained the control valves and a manifold to split the coolant. The outlet valve boxes is also an adiabatic vacuum vessel with no control valves. The later contains only a manifold to join the heat-exchanged coolant.

The opening of each control valve should be controlled by the feed-back signal from the flow element to keep the required mass flow rate.

(1) Sizing method

The control valve should be selected to fit the following Cv value. The formula is quoted from the selecting data for the products of TOKO VALEX Co., Ltd..

$$Cv = \frac{Q}{3.13}\sqrt{\frac{\rho_n T}{\Delta P(P_1 + P_2)}}$$

where,

Cv; Cv value	(--)
Q; volumetric flow rate of the gas under the normal state[□□□]	(m^3/h)
ρ_n; density of the gas under the normal state[□□□]	(kg/m^3)
T; absolute temperature of the gas	(K)
ΔP; pressure drop ($=P_1 - P_2$)	(kPa)
P_1; inlet pressure	(kPa)
P_2; outlet pressure	(kPa)

; The normal state means 273.15K with 101.325kPa.

(2) Sizing results

a. Characteristic of the gaseous helium

T=80K

ρ_n=0.17625kg/m^3

b. Pressure drop

The overall pressure loss should be lower than the target of the limitation, i.e. 100kPa..The pressure loss at the heat transfer tube on the shield plates is evaluated approximately 50kPa shown in the previous chapter.

Considering the pressure loss at the transfer piping and some contingencies, the pressure drop due to the control valve, ΔP , should be limited within 10kPa. As the inlet pressure is specified as P_1=1800kPa, the outlet pressure is easily obtained as $P_2=P_1-\Delta P$=1800-10=1790kPa.

The volumetric flow rate of the gaseous helium under the standard state can be obtained as $Q=F/\rho_n$. Here, the symbol, F, means the required mass flow rate.

c. Required mass flow rate

The required mass flow rate of the gaseous helium coolant that classified into each of the valve boxes are as follows:

i. Lower cryostat valve box

lower cover,	inner block	24.9(g/s)×4(paths)=	100(g/s)
lower cover,	outer block	24.9(g/s)×4(paths)=	100(g/s)
gravity supports		9.6(g/s)×10(paths)=	96(g/s)
divertor ports		26.9(g/s)×10(paths)=	270(g/s)
equatorial ports		26.9(g/s)×10(paths)=	424(g/s)
subtotal			990(g/s)

ii. Cryostat cylinder valve box

cryostat cylinder		28.7(g/s)×20(paths)=	576(g/s)
subtotal			576(g/s)

iii. Upper cryostat valve box

upper cover,	inner block	15.4(g/s)×10(paths)=	154(g/s)
upper cover,	outer block	13.4(g/s)×2(paths)=	27(g/s)
upper ports		32.6(g/s)×20(paths)=	652(g/s)
subtotal			833(g/s)

The required mass flow rate of the coolant to be supplied from the cryoplant is 2.4kg/s.

d. Calculated Cv value

The calculated Cv values for each of the control valves are tabulated in Table 4-1.

e. Designed Cv value

i. Flow rate characteristic

The so-called equal-percentage characteristics as shown in the figure on the right is considered.

ii. Effective opening range

The effective opening range of the control valve is set up to be 10%~90%. Namely, the rated flow can be achieved at the 90% of the full opening. Considering the equal-percentage characteristic, the flow rate at the 90% opening of the total travel is approximately 60% of the rated flow. Therefore, the designed Cv value should be multiplied the calculated Cv value by 1.7, i.e. 1/0.6. The designed Cv values for each of the control valves are also tabulated in Table 4-1.

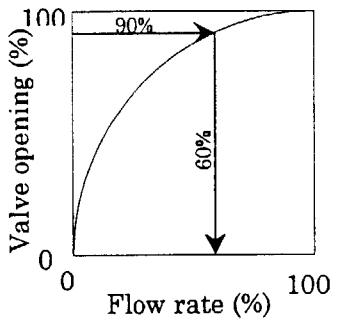

Equal-percentage

f. Sizing of the control valve

According to the following design concepts, the control valves are selected using the designed Cv value.

i. The number of the branch line distributed in the cryostat vessel should be limited approximately five to ensure the flow distribution.

ii. The size of the control valves should be smaller than 3" to prevent large heat leakage to the valve box. In addition, smaller control valves are widely used in

the cryogenic engineering.

Table 4-1 shows the sizing results for each of the control valves.

From the table, twenty-one control valves are required in all. Ten control valve for the lower cryostat valve box, four control valves for the cryostat cylinder valve box and seven control valves for the upper cryostat valve box are selected by the above-mentioned procedure. The outer bore of the control valves are 34.0mm , 48.6mm or 60.5mm.

The heat leakage from the control valves to the valve boxes are also estimated as tabulated in Table 4-2. The heat leakage from each control valve is estimated under the condition that the length of the valve-extension is 500mm or 1000mm and no thermal anchors are attached to the valve body. The reference data of the heat leakage are quoted from the general specification of the "T-8800 cryogenic control valve, TOKO VALEX Co., Ltd.". As the original data, Q_0, are based upon the heat conduction from 300K to 4K, each of the heat leak data, Q_j, tabulated in Table 4-2 are corrected by the following manner:

$$Q_j = Q_0 \times \left[\frac{\overline{\lambda}_{300\to 80} \times (300-80)}{\overline{\lambda}_{300\to 4} \times (300-4)} \right].$$

Where, the symbol, $\overline{\lambda}_{T_h \to T_c}$, is a mean thermal conductivity for the temperature range of $T_c \leq T \leq T_h$. For type 316-L stainless steel, $\overline{\lambda}_{300\to 80}$ and $\overline{\lambda}_{300\to 4}$ are calculated to be 12.3W/m•K and 10.3W/m•K, respectively.

Table 4-1 Control valve's sizing results

Valve box	Thermal shield to be applied	Number of the control valve	Temporally identification	Mass flow rate G(g/s)	Volumetric flow rate Q(m^3/hr)	Calculated *Cv* value	Designed *Cv* value	Outer bore of the valve (mm)
Lower cryostat valve box	Outer block of the lower cover	1	CV1	100	2,044	13.0	30	48.6
	Inner block of the lower cover	1	CV2	100	2,044	13.0	30	48.6
	Gravity supports	2	CV3, CV4	48	981	6.3	20	48.6
	Divertor ports	2	CV5, CV6	135	2,749	17.5	40	60.5
	Equatorial ports	4	CV7~CV10	106	2,157	13.7	30	48.6
	Subtotal	10	---	990	(20,176)	---	---	---
Cryostat cylinder valve box	Cryostat cylinder	4	CV11~CV14	144	2,933	18.6	40	60.5
	Subtotal	4	---	576	(11,732)	---	---	---
Upper cryostat valve box	Upper ports	4	CV15~CV18	163	3,332	21.1	40	60.5
	Outer block of the upper cover	2	CV19, CV20	77	1,574	10.0	20	48.6
	Inner block of the upper cover	1	CV21	27	552	3.5	10	34.0
	Subtotal	7	---	833	(17,028)	---	---	---
Total		21	---	2,399	(48,963)	---	---	---

The volumetric flow rates are calculated under the normal state, that is 273.15K with 101.325kPa.
The designed *Cv* values are multiplied the calculated *Cv* value by 1.7.
Each of the bore are selected by using the general specification of "T-8800 cryogenic control valve, TOKO VALEX Co., Ltd.".
The subtotal of the mass flow rate are the sum of the product of the individual one and the number of the control valve.

Table 4-2 Heat leak estimation for each valve box

Valve box	Thermal shield to be applied	Number of the control valve, N_j	Temporally identification	Outer bore of the valve (mm)	Heat leak from one, Q_j (W)	Subtotal, $N_j \times Q_j$ (W)	Total, $\Sigma(N_i \times Q_i)$ (W)
Lower cryostat valve box	Outer block of the lower cover	1	CV1	48.6	1.8 (L1000)	1.8 (L1000)	19.6 (L1000) 44.4 (L500)
					4.0 (L500)	4.0 (L500)	
	Inner block of the lower cover	1	CV2	48.6	1.8 (L1000)	1.8 (L1000)	
					4.0 (L500)	4.0 (L500)	
	Gravity supports	2	CV3, CV4	48.6	1.8 (L1000)	3.6 (L1000)	
					4.0 (L500)	8.0 (L500)	
	Divertor ports	2	CV5, CV6	60.5	2.6 (L1000)	5.2 (L1000)	
					6.2 (L500)	12.4 (L500)	
	Equatorial ports	4	CV7~CV10	48.6	1.8 (L1000)	7.2 (L1000)	
					4.0 (L500)	16.0 (L500)	
Cryostat cylinder valve box	Cryostat cylinder	4	CV11~CV14	60.5	2.6 (L1000)	10.4 (L1000)	10.4 (L1000) 24.8 (L500)
					6.2 (L500)	24.8 (L500)	
Upper cryostat valve box	Upper ports	4	CV15~CV18	60.5	2.6 (L1000)	10.4 (L1000)	15.2 (L1000) 35.5 (L500)
					6.2 (L500)	24.8 (L500)	
	Outer block of the upper cover	2	CV19, CV20	48.6	1.8 (L1000)	3.6 (L1000)	
					4.0 (L500)	8.0 (L500)	
	Inner block of the upper cover	1	CV21	34.0	1.2 (L1000)	1.2 (L1000)	
					2.7 (L500)	2.7 (L500)	
Total		21	---	---	---	---	45.2 (L1000) 104.7 (L500)

These reference data are quoted from the general specification of "T-8800 cryogenic control valve, TOKO VALEX Co., Ltd.". The symbol "L" means the length of the valve-extension. The length considered and 1,000mm or 500mm. Note that no thermal anchors are considered in the estimation.

4.2 Overall pressure loss

The overall pressure loss of the gaseous helium cooling system are assessed considering the configuration of the transfer piping arranged between both of the valve boxes and the flow conditions.

(1) Design of the transfer piping

The transfer piping should be designed based upon the following concepts:

i. The transfer piping outside of the cryostat should be covered by the outer shell, that is arranged between the cryostat and the valve boxes, to prevent large heat leakage.
ii. The transfer piping inside the cryostat is a single wall piping.
iii. The penetrations for the transfer piping should be set up to the cryostat cylinder. Three penetrations for the inlet transfer piping and three for the outlet transfer piping are required.
iv. The transfer piping should be split into each heat transfer tube of the thermal shield.
v. For good flow distribution, restricting orifices that adjust the pressure loss of each branch equally should be set up.
vi. The flow distribution elements, i.e. tee-joints for the split and the join should be arranged between the cryostat wall and the thermal shield.
vii. The transfer piping between the cryostat and the thermal shields should be equipped with the multi-layer insulation to prevent the radiation heat transmitted from the warm surface.
viii. To make the in-tube flow stable, the join tee-joints should be located at higher level than the corresponding split tee-joints in case of the vertically arranged transfer piping.
ix. The piping should be supported properly to keep integrity and to prevent large deformation.
x. To limit heat leakage transmitted from the support structure to the transfer piping, spacers made of a low conductivity material such as GFRP should be inserted to the gap between the piping and the structure.
xi. The transfer piping and the support structure should be consistent with thermal shrinkage of the piping itself.
xii. Bending pipes should be positively applied to reduce number of the welding joints.

Considering the concepts above and the arrangement of the valve boxes, the configuration of each transfer piping is designed as shown in following figures.

i. Figure 4-1; typical transfer piping arranged between both of the lower cryostat valve boxes
ii. Figure 4-2; typical transfer piping arranged between both of the cryostat cylinder valve boxes
iii. Figure 4-3; typical transfer piping arranged between both of the upper cryostat valve boxes

The bending portions of the transfer piping can mitigate the secondary stress range due to thermal shrinkage. As described in section 3.4 of this report, the thermal stress range can be evaluated simply as $\sigma = C_2 \frac{3ED\delta}{2L^2}$. According to the criterion prescribed in ASME Boiler and Pressure Vessel Code, Section VIII, division 2, the allowable stress limit is 3Sm, that is the so-called shakedown limit.

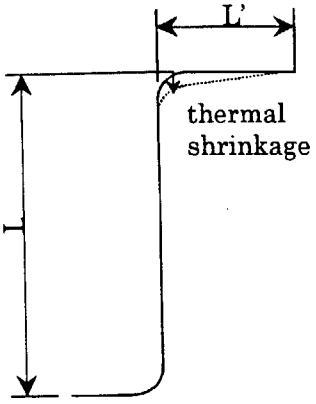

The design stress intensity, Sm, is 138MPa for type 304 stainless steel. Because of a simple evaluation procedure, factor of three or four should be considered as a safety margin. The thermal shrinkage is estimated as $\delta = \varepsilon_\theta L'$ for the length, L'. Here, ε_θ is the thermal strain corresponds to 300K→80K cooling and is 0.0029 for type 304 stainless steel.

For example, the vertical portion of the transfer piping for the cryostat cylinder thermal shields can be assessed as follows:

- Outer diameter of the piping; D=60.5mm
- Stress intensity of bending pipe; C_2=2.30 (t=3.5mm,R=181.5mm)
- Modulus of the longitudinal elasticity; E=200000MPa
- Accommodation length for the shrinkage; L=4000mm
- Length of vertical piping; L'=21000mm
- Thermal stress range; $\sigma = \dfrac{3 \times 200000 \times 60.5 \times (0.0029 \times 21000)}{2 \times 4000^2} = 159\,MPa$

The stress range above seems to be too large to keep the integrity of the transfer piping totally. Therefore, a bending portion is set up to the vertical piping as shown in Figure 4-1.

Figure 4-4 shows the concept of the support structure for the transfer piping. As shown in the figure, GFRP spacers are inserted to the gaps of the piping and the structure. The span of the support structure should be set up considering the primary stress due to the own weight, i.e. gravity force, and the seismic force. According to the following guideline, the span can be set up.

A pipe with length, l, simply supported at both of the end and subjected to equally distributed force, f, is considered as a simple model. The allowable span can be assessed as following manner:

- Maximum bending moment; $M=f \cdot l^2/8$
- Maximum bending stress; $\sigma=B_2 \cdot M/Z$
- Modulus of section; $Z=\pi(D_o^4-D_i^4)/32D_o$
- Equally distributed force; $f=\alpha\rho g\pi(D_o^2-D_i^2)/4$
- Acceleration ; α=1 for gravity force, α=1.2 for gravity plus seismic force
- Allowable stress limit; S≤1.5kSm, k=1 for gravity force, k=1.2 for gravity plus seismic force
- Allowable span; $l_{all} \leq (8ZS/f)^{1/2} \approx (2D_o S/\alpha\rho g)^{1/2}$

Where, B_2 means the stress intensity factor for the primary stress prescribed in the class-1 piping design criterion of ASME Boiler and Pressure Vessel Code, Section III. The span of the transfer piping should be shorter than the allowable span. The detailed piping design including stress evaluation by FEA will be required in future design stage.

(2) Pressure loss estimation for the transfer piping

a. Estimation method

The procedure of the pressure loss estimation for the transfer piping is basically the same as that of the heat transfer tube described in section 3.5 of this report. The pressure loss elements to be considered are the friction loss and the shape loss due to bending pipes, elbows, split tee-joints and join tee-joints. Each of the pressure loss

coefficients are quoted from "JSME Data Book, Hydraulic Losses in Pipes and Ducts".

The procedure to assess the pressure losses of the transfer piping is as follows:

(a) Mean velocity in tube

$$u=(G/\rho)/A$$

(b) Reynolds number

$$Re = u \bullet D_i \bullet \rho/\eta$$

Where, the density of the gaseous helium is $\rho=9.105kg/m^3$ and the viscosity is $\eta=9.372\times10^{-6}kg/ms$ under the condition of 90K with 1.75MPa. Each symbol, "G", "A" and "D_i", means the mass flow rate, the sectional area ($=\pi D_i^2/4$) and the inside diameter, respectively.

(c) Pressure loss estimation for each of the elements

i. Pressure loss due to friction in unit pipe, ΔP_1

Friction factor; $\lambda=0.3164/Re^{0.25}$

Pressure loss; $\Delta P_1=\lambda/d\times(\rho u^2/2)$

ii. Pressure loss at a 90° bending pipe, ΔP_2

Loss factor; $K_{90°}=0.95+17.2(R/a)^{-1.96}$, $R=3D_o$, $a=D_i/2$

Pressure loss; $\Delta P_2=K_{90°}\times(\rho u^2/2)$

iii. Pressure loss at a 90° long elbow, ΔP_3

Loss factor; $K_{LE}=0.95+17.2(R/a)^{-1.96}$, $R=1.5D_o$, $a=D_i/2$

Pressure loss; $\Delta P_3=K_{LE}\times(\rho u^2/2)$

iv. Pressure loss at a split tee-joint, ΔP_4

Loss factor, K_{split}; refer to the function described in the reference above

Pressure loss; $\Delta P_4=K_{split}\times(\rho u^2/2)$

"u" means the upstream velocity.

v. Pressure loss at a join tee-joint, ΔP_5

Loss factor K_{join}; refer to the function described in the reference above

Pressure loss; $\Delta P_5=K_{join}\times(\rho u^2/2)$

"u" means the downstream velocity.

(d) Overall pressure loss estimation

i. Total pressure loss at the transfer piping

Summing up each of the loss elements, the total pressure loss at the transfer piping, ΔP_{TP}, can be obtained as,

$$\Delta P_{TP}=\sum(\Delta P_j)=\sum(\Delta P_j)_{run\ pipe}+\sum(\Delta P_j)_{branch\ pipe}.$$

Here, "run pipe" means the main line connect to the valve boxes and "branch pipe" means the split line connect to each heat transfer tube on the shield plates, respectively.

ii. Total pressure loss at the heat transfer tube

The total pressure losses at each heat transfer tube, ΔP_{HTT}, are summarized in Table 3-11.

iii. Total pressure drop at the control valve

The pressure drop due to the control valve, ΔP_{CV}, is assumed 10kPa as described in section 4.1.

iv. Overall pressure loss of the cooling system

Finally, the overall pressure loss of the gaseous helium cooling system can be obtained as,

$$\Delta P_{overall}=\Delta P_{TP}+\Delta P_{HTT}+\Delta P_{CV}.$$

b. Results of the estimation

Table 4-3 shows the results of the overall pressure loss estimation for each transfer piping. The estimation is based upon the piping configuration shown in Figure 4-1, 4-2, 4-3 and the flow rate condition shown in Table 4-1.

As shown in the Table 4-3, the overall pressure losses can be confirmed to be lower than 80kPa. The results satisfy the target of the limitation, that is 100kPa, with proper margin.

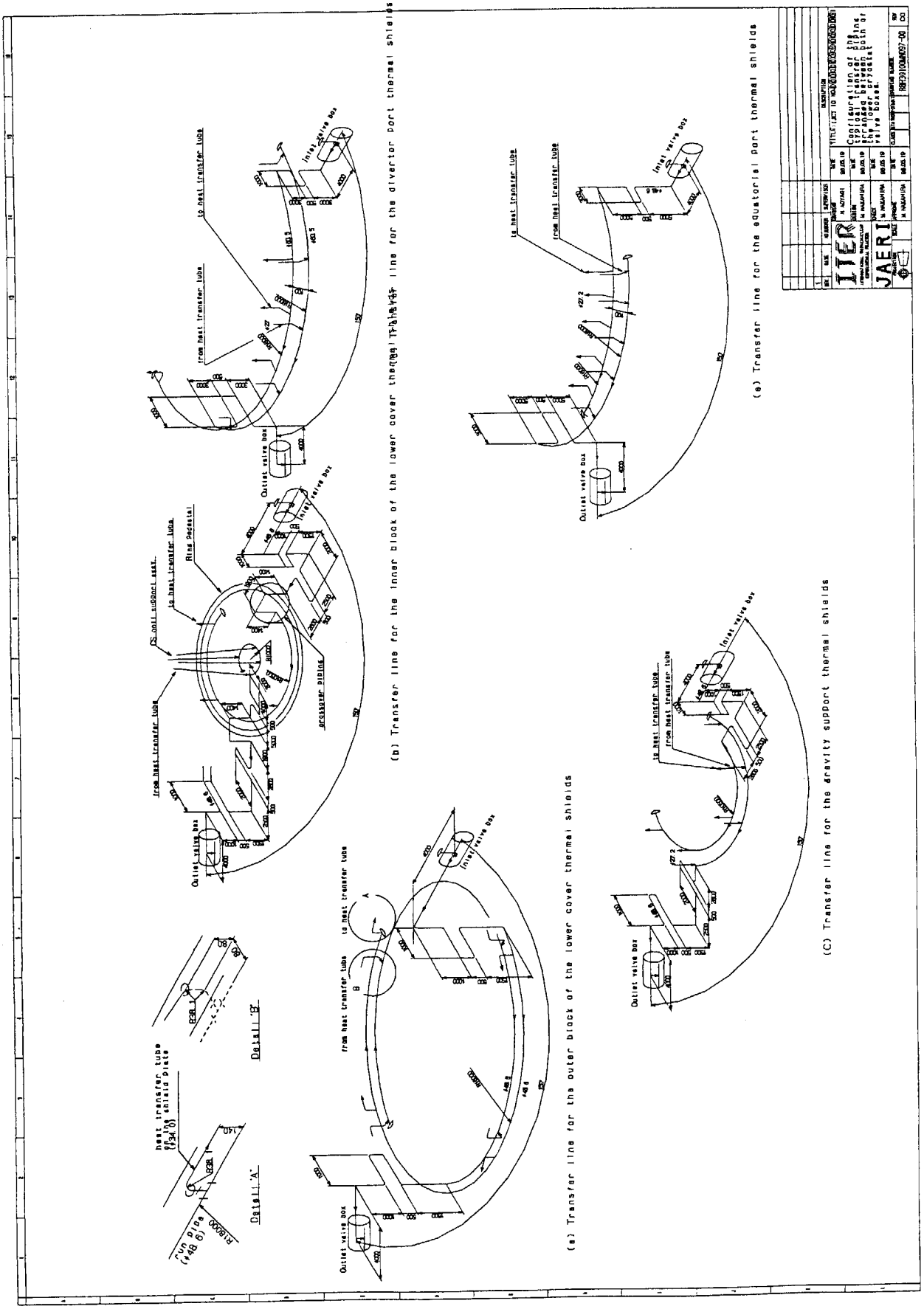

Fig. 4-1 Configuration of the Typical Transfer Piping Arrangement between the Lower Cryostat Valve Boxes

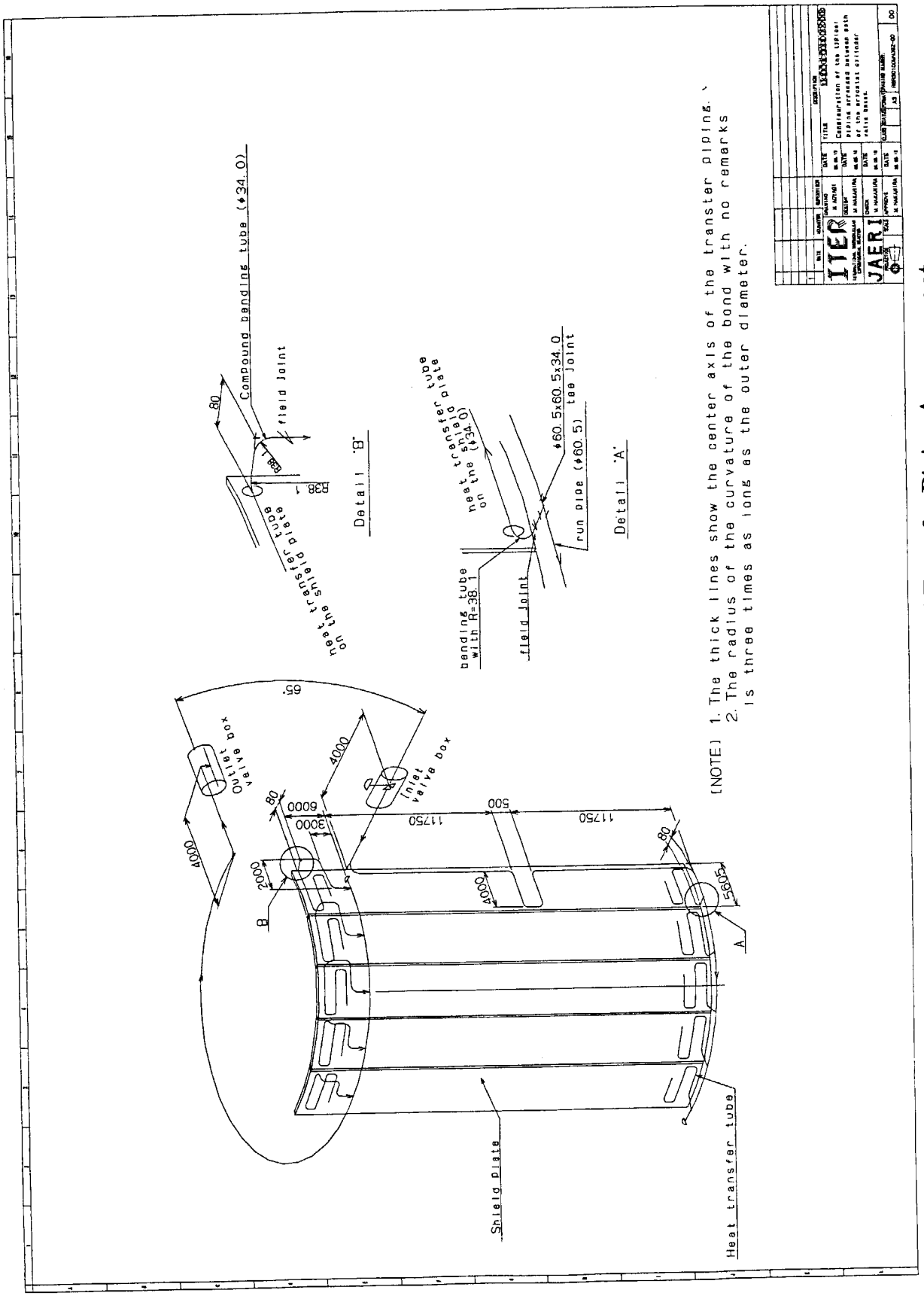

Fig. 4-2 Configuration of the Typical Transfer Piping Arrangement between the Cryostat Cylinder Valve Boxes

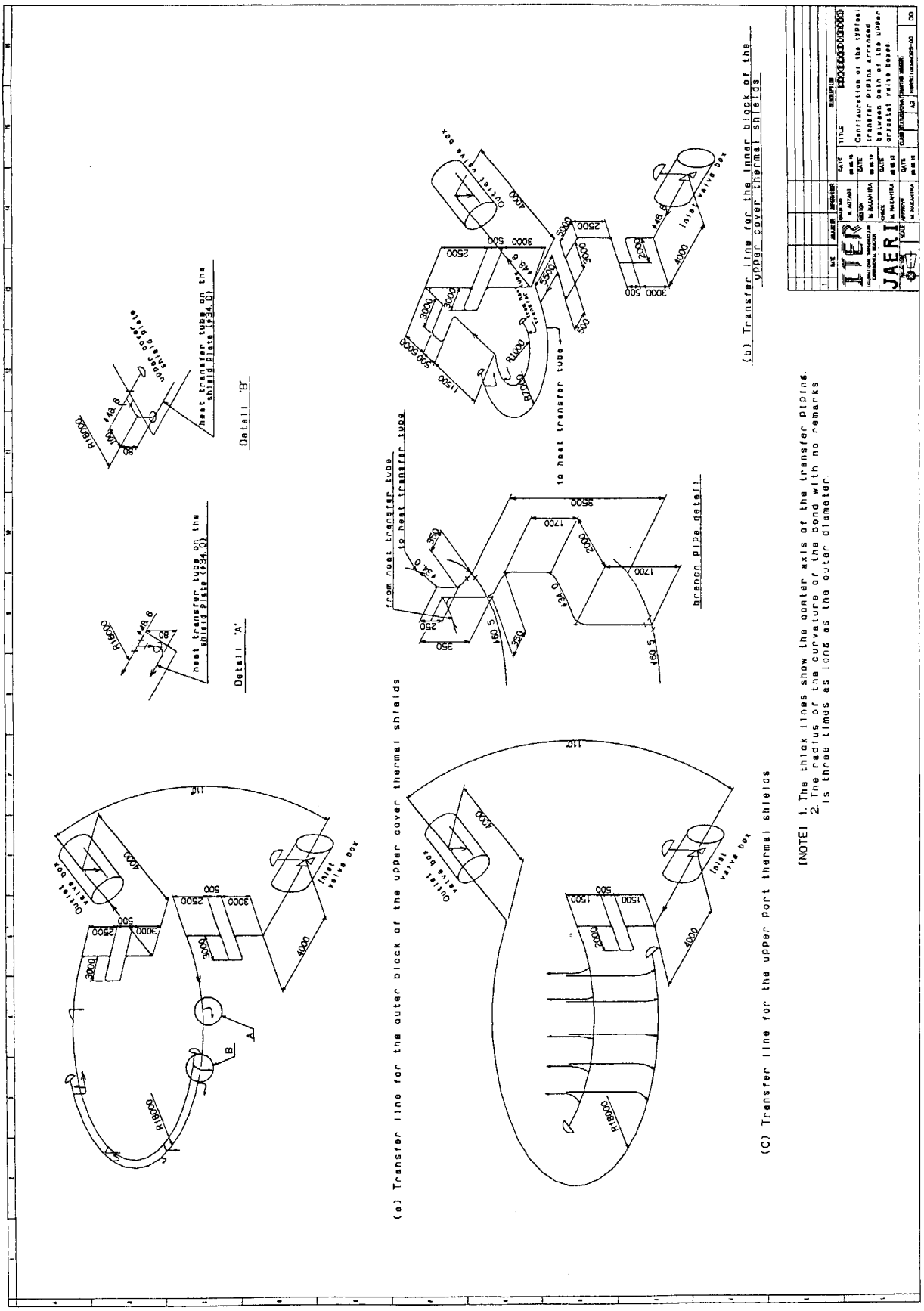

Fig. 4-3 Configuration of the Typical Transfer Piping Arrangement between the Upper Cryostat Valve Boxes

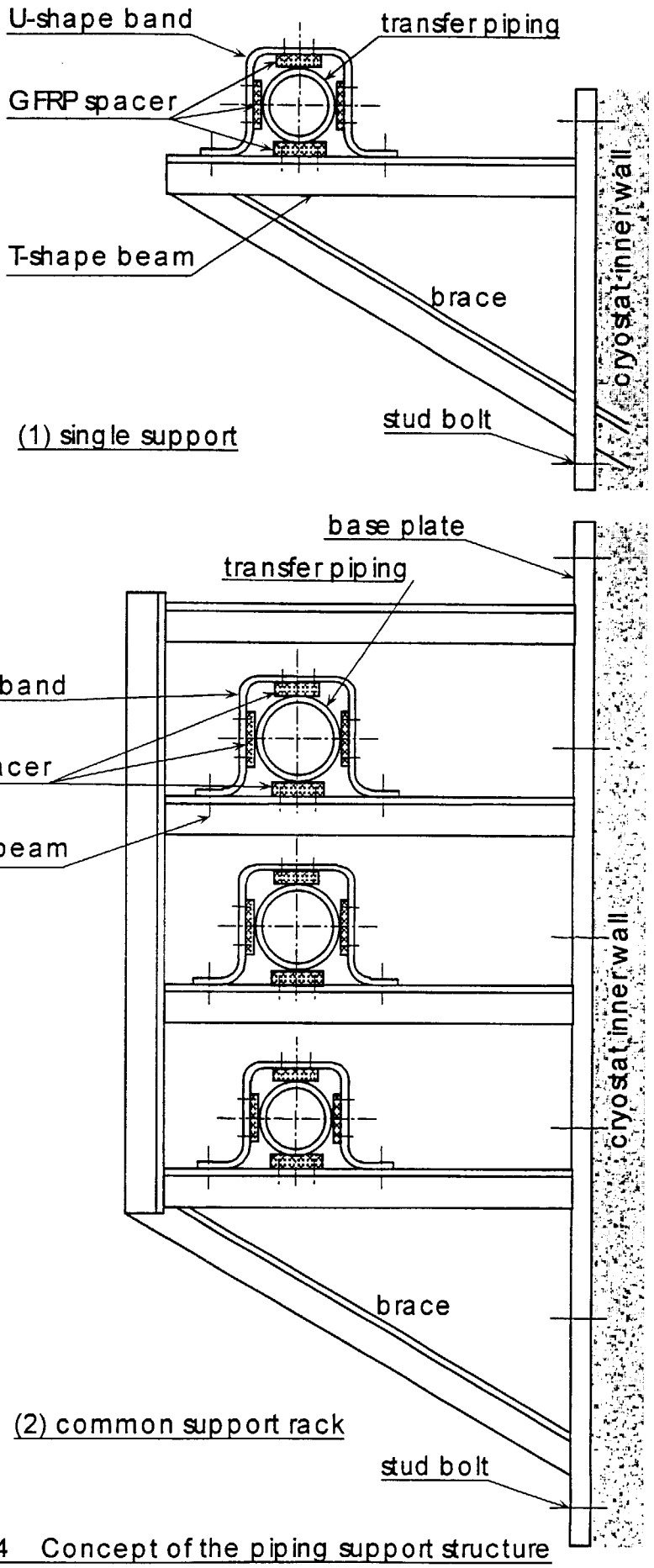

Fig. 4-4 Concept of the piping support structure

Table 4-3 Overall Pressure Loss Estimation of the Cooling System

	valve box	lower cryostat valve box					cryostat cylinder	upper cryostat valve box		
category	portion	outer block of the lower cover	inner block of the lower cover	gravity supports	divertor ports	equatorial ports	cryostat cylinder	upper ports	outer block of the upper cover	inner block of the upper cover
control valve temporary identification		CV1	CV2	CV3, CV4	CV5, CV6	CV7~CV10	CV11~CV14	CV15~CV18	CV19, CV20	CV21
tansfer line/ run pipe	tube OD (mm)	48.6	48.6	48.6	60.5	48.6	60.5	60.5	48.6	34
	tube thickness (mm)	3	3	3	3.5	3	3.5	3.5	3	3
	tube ID(mm)	42.6	42.6	42.6	53.5	42.6	53.5	53.5	42.6	28
	sectional area (m^2)	0.00143	0.00143	0.00143	0.00225	0.00143	0.00225	0.00225	0.00143	0.00062
	mass flow (g/s)	100	100	48	135	106	144	163	77	27
	density (kg/m^3) 90K, 1.75MPa	9.105	9.105	9.105	9.105	9.105	9.105	9.105	9.105	9.105
	velocity (m/s)	7.706	7.706	3.699	6.596	8.168	7.035	7.964	5.933	4.816
	Reynolds number	3.189E+05	3.189E+05	1.531E+05	3.428E+05	3.380E+05	3.657E+05	4.139E+05	2.456E+05	1.310E+05
	friction factor	0.0133	0.0133	0.0160	0.0131	0.0131	0.0129	0.0125	0.0142	0.0166
	press loss (kPa/m)	0.0845	0.0845	0.0234	0.0484	0.0936	0.0542	0.0673	0.0535	0.0627
	pipe length (m)	220	130	200	250	220	210	200	240	130
	DP_{tube} (kPa)	18.587	10.983	4.677	12.101	20.582	11.380	13.463	12.834	8.153
	N_{bend}	14	32	22	12	12	7	7	12	22
	pressuer loss coefficient	1.346	1.346	1.346	1.353	1.346	1.353	1.353	1.346	1.301
	DP_{bend} (kPa)	5.096	11.647	1.845	3.216	4.907	2.135	2.735	2.590	3.022
	N_{elbow}	0	0	0	0	0	0	0	0	0
	pressuer loss coefficient	2.492	2.492	2.492	2.519	2.492	2.519	2.519	2.492	2.315
	DP_{elbow} (kPa)	0	0	0	0	0	0	0	0	0
	N_{split}	1	1	1	1	1	1	1	1	1
	pressuer loss coefficient	0.06	0.06	0.08	0.16	0.08	0.08	0.08	0.08	0.05
	DP_{split} (kPa)	0.0162	0.0162	0.0050	0.0317	0.0243	0.0180	0.0231	0.0128	0.0053
	N_{join}	4	4	5	5	5	5	5	5	5
	pressuer loss coefficient	1.42	1.42	1.42	2.84	1.42	1.42	1.42	1.42	1.42
	Q(%)	0.25	0.25	0.2	0.2	0.2	0.2	0.2	0.2	0.5
	DP_{join} (kPa) #1	0.0240	0.0240	0.0035	0.0225	0.0173	0.0128	0.0164	0.0091	0.0375
	pressuer loss coefficient	0.24	0.24	0.24	0.48	0.24	0.24	0.24	0.24	0.24
	Q(%)	0.5	0.5	0.4	0.4	0.4	0.4	0.4	0.4	1
	DP_{join} (kPa) #2	0.0162	0.0162	0.0024	0.0152	0.0117	0.0087	0.0111	0.0062	0.0253
	pressuer loss coefficient	0.2	0.2	0.2	0.4	0.2	0.2	0.2	0.2	0
	Q(%)	0.75	0.75	0.6	0.6	0.6	0.6	0.6	0.6	0
	DP_{join} (kPa) #3	0.0304	0.0304	0.0045	0.0285	0.0219	0.0162	0.0208	0.0115	0.0000
	pressuer loss coefficient	0.18	0.18	0.18	0.36	0.18	0.18	0.18	0.18	0
	Q(%)	1	1	0.8	0.8	0.8	0.8	0.8	0.8	0
	DP_{join} (kPa) #4	0.0487	0.0487	0.0072	0.0456	0.0350	0.0260	0.0333	0.0185	0.0000
	pressuer loss coefficient	0	0	0.16	0.32	0.16	0.16	0.16	0.16	0
	Q(%)	0	0	1	1	1	1	1	1	0
	DP_{join} (kPa) #5	0.0000	0.0000	0.0100	0.0634	0.0486	0.0361	0.0462	0.0256	0.0000
	DP_{join} (kPa) sub-subtotal	0.119	0.119	0.028	0.175	0.134	0.100	0.128	0.071	0.063
	subtotal, run pipe (kPa)	23.818	22.766	6.555	15.524	25.648	13.633	16.349	15.507	11.243
transfer line branch pipe	tube OD (mm)	34	34	27.2	27.2	27.2	34	34	27.2	27.2
	tube thickness (mm)	3	3	2.5	2.5	2.5	3	3	2.5	2.5
	tube ID(mm)	28	28	22.2	22.2	22.2	28	28	22.2	22.2
	sectional area (m^2)	0.000616	0.000616	0.000387	0.000387	0.000387	0.000616	0.000616	0.000387	0.000387
	mass flow (g/s)	25	25	9.6	27	21.2	28.8	32.6	15.4	13.5
	velocity (m/s)	4.459	4.459	2.724	7.661	6.015	5.137	5.815	4.370	3.831
	Reynolds number	1.213E+05	1.213E+05	5.875E+04	1.652E+05	1.297E+05	1.397E+05	1.582E+05	9.424E+04	8.261E+04
	friction factor	0.0170	0.0170	0.0203	0.0157	0.0167	0.0164	0.0159	0.0181	0.0187
	press loss (kPa/m)	0.0548	0.0548	0.0309	0.1889	0.1237	0.0702	0.0872	0.0707	0.0562
	pipe length (m)	2	8	18	10	2	10	8	2	2
	DP_{tube} (kPa)	0.110	0.438	0.557	1.889	0.247	0.702	0.698	0.141	0.112
	N_{bend}	0	5	10	10	4	2	7	0	0
	pressuer loss coefficient	1.301	1.301	1.295	1.295	1.295	1.301	1.301	1.295	1.295
	DP_{bend} (kPa)	0.000	0.589	0.437	3.459	0.853	0.313	1.402	0.000	0.000
	N_{elbow}	2	2	8	0	0	3	0	2	2
	pressuer loss coefficient	2.315	2.315	2.291	2.291	2.291	2.315	2.315	2.291	2.291
	DP_{elbow} (kPa)	0.419	0.419	0.619	0.000	0.000	0.834	0.000	0.398	0.306
	N_{split}	1	1	1	1	1	1	1	1	1
	pressuer loss coefficient	0.85	0.85	0.85	1.7	0.85	0.85	0.85	0.85	1.35
	DP_{split} (kPa)	0.230	0.230	0.053	0.337	0.258	0.192	0.245	0.136	0.143
	N_{join}	1	1	1	1	1	1	1	1	1
	pressuer loss coefficient	16.25	16.25	16.25	32.5	16.25	16.25	16.25	16.25	16.25
	Q(%)	0.2	0.2	0.2	0.2	0.2	0.2	0.2	0.2	0.2
	DP_{join} (kPa)	0.176	0.176	0.040	0.257	0.197	0.146	0.188	0.104	0.069
	subtotal, branch pipe (kPa)	0.934	1.852	1.706	5.942	1.556	2.187	2.532	0.780	0.630
transfer line total	total pressure loss (kPa)	25	25	9	22	28	16	19	17	12
HTT on shield plate	total pressure loss (kPa)	51	37	32	51	36	53	56	44	24
control valve	pressure drop (kPa)	10	10	10	10	10	10	10	10	10
the whole system	overall pressure loss (kPa)	77	64	43	79	66	72	78	62	37
	limit of the pressure loss (kPa)	100	100	100	100	100	100	100	100	100

4.3 Gaseous helium transfer system

Figure 4-5 shows the engineering flow sheet for the gaseous helium transfer system. The system includes three pairs of the valve boxes, twenty-one transfer lines with control valves and one-hundred heat transfer tube paths with the restricting orifices. To achieve good flow distribution to each path of the heat transfer tube, pressure loss adjustments by the restricting orifices should be required using actual helium circulation as a post-construction work.

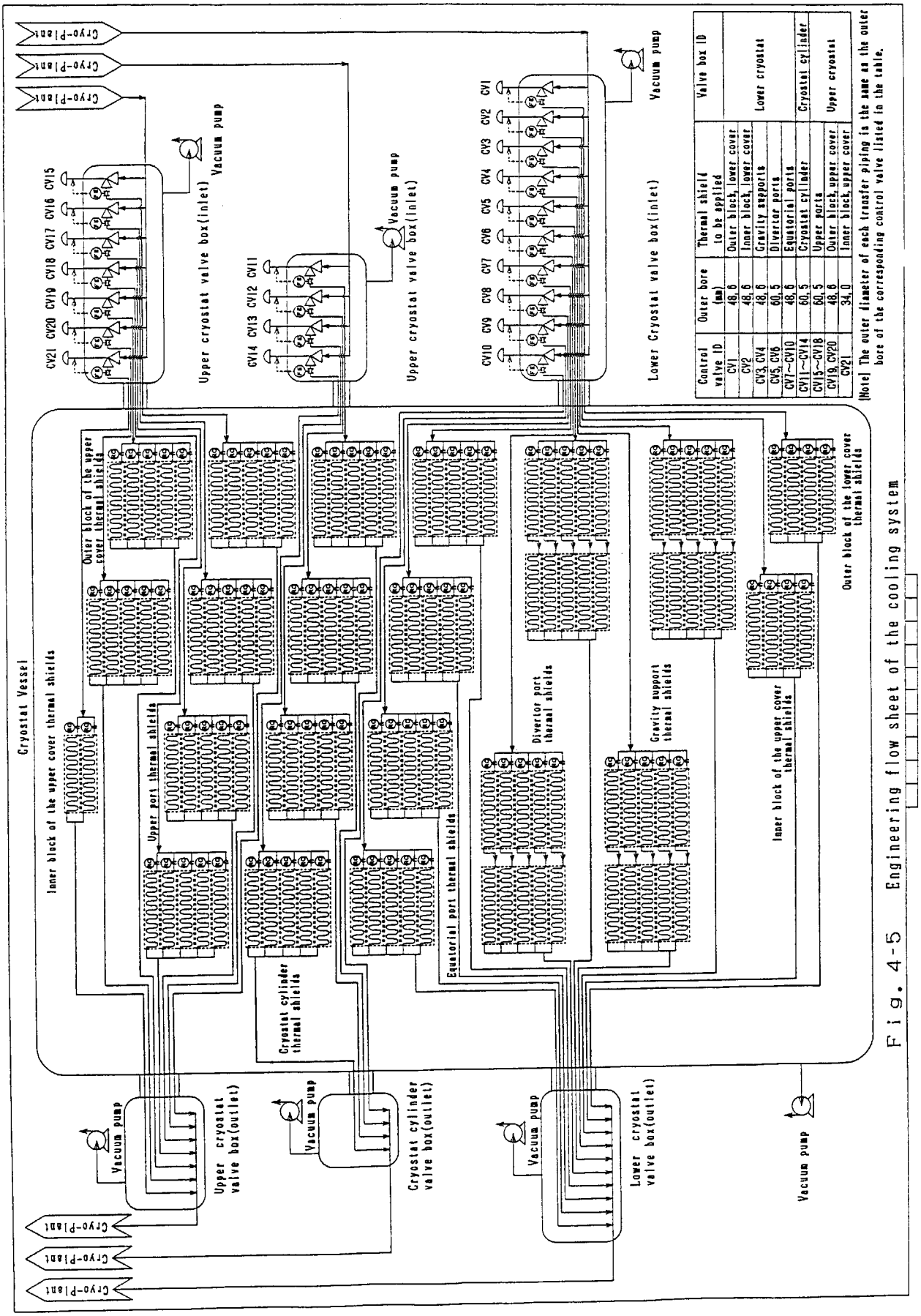

Control valve ID	Outer bore (mm)	Thermal shield to be applied	Valve box ID
CV1	48.6	Outer block, lower cover	Lower cryostat
CV2	48.6	Inner block, lower cover	
CV3, CV4	48.6	Gravity supports	
CV5, CV6	60.5	Divertor ports	
CV7~CV10	48.6	Equatorial ports	
CV11~CV14	60.5	Cryostat cylinder	Cryostat cylinder
CV15~CV18	60.5	Upper ports	Upper cryostat
CV19, CV20	48.6	Outer block, upper cover	
CV21	34.0	Inner block, upper cover	

[Note] The outer diameter of each transfer piping is the same as the outer bore of the corresponding control valve listed in the table.

Fig. 4-5 Engineering flow sheet of the cooling system

5. Fabrication and installation sequence

5.1 Shop fabrication

Each of the parts consisting of the thermal shields will be manufactured and sub-assembled in the vendor's factory. The productivity of the major parts are studied.

(1) Fabrication of the major parts

a. Shield plate

i. Cut out the shield plate from a plate made of type 304 stainless steel.
ii. Make holes to be furnished the ring plate, cover plate and insulation blanket for the shield plate.
iii. Form the shield plate using bending machines or press machines.

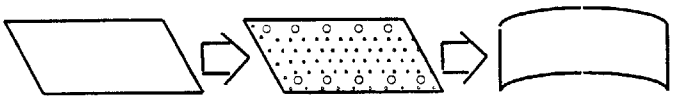

b. Ring plate

i. Cut out two plates made of type 304 stainless steel.
ii. Weld the plates to make a T-shaped ring plate.
iii. Make hales to be connected to the support.
iv. Form the ring plate using bending machines or press machines.
v. Weld stud bolts on the ring plate to set up the shield plate.

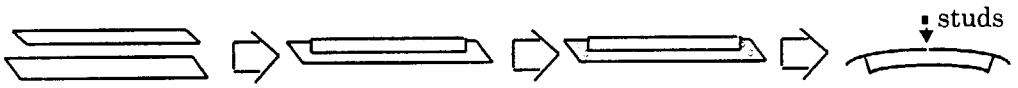

c. Cover plate

i. Cut out from a plate made of type 304 stainless steel.
ii. Form the cover plate using bending machines or press machines.
iii. Make hales to be furnished for the shield plate.

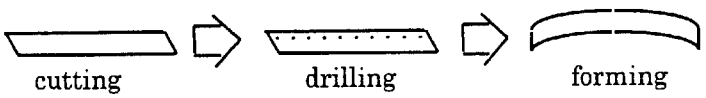

d. Support

i. Form the support roughly.
ii. Finish the support by machining.
iii. Make hales to be furnished for the warm surface and to fit up the ring plate.

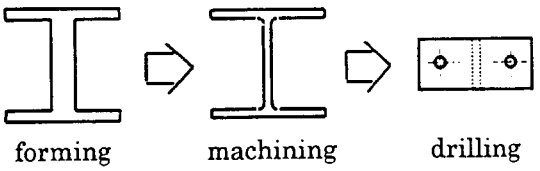

As hardness of the titanium alloy is high enough, the machining is generally hard. Therefore, the material of the machining tools should be a good affinity with the alloy.

e. MLI blanket

i. Produce rolls of the polymer film made of polyester or polyimide.
ii. Deposit aluminum to the both sides of the film.
iii. Make the film to be crinkled or embossed.

The polymer film to be applied to the high temperature ports should be crinkled or should be embossed at approximately 180°C to prevent the surface from flattening due to relaxation.

The width of the film should be limited within 2m because of the productivity. Therefore, some overlaps will be set up in the case of a wider blanket than the unit width of the film.

f. Parts for the MLI blanket

Thread to bundle the blanket and tag-pins to furnish the blanket for the shield plate should be radioactive-resistant. For lower dose portion of up to 0.1MGy, polyester is applicable for their material. However, polyimide should be required at higher dose portion. The thread made of polyimide is already in use and the tag-pins made of polyimide can be produced by the injection forming method.

g. Parts for the reflecting plates

(a) Reflecting plate

i. Cut out the plates from plate made of type 304 stainless steel.
ii. Make holes.
iii. Deposit silver to both sides of the plate in a vacuum furnace.

(b) Bolts, nuts and spacers

i. Machine the bolts, nuts and spacers from laminated plate made of GFRP.

The glass fiber consisting of the GFRP should be a Boron-free type, that is sufficient radioactive-resistant.

h. Heat transfer tube

The number of the welding joint in the tube assembly is preferred as fewer as possible to prevent leakage of the coolant. Therefore, the application of a bending tube with a straight pipe is desirable. The crossover tube to be fitted up to the interface between adjacent two shield plates should be also a bending tube and is pre-machined its edge penetrations in the factory. Each welding joint of the heat transfer tube assembled in the factory is the required liquid penetrant testing (PT).

The followings are the reason why PT is applicable to welding joints of the tube. The heat transfer tube will be classified into the class-3 piping of the nuclear facilities. In the governmental notice on welding of the electricity structure, e.g. MITI ordinance number 81, the magnetic particle testing (MT) or PT is required for butt welding joints of smaller pipe than 61mm in outer diameter. As the tube is made of type 304 stainless steel, MT cannot be applicable. Therefore, the method of non-destructive examination to be applied to the welding joints is PT. To the field welding joints, PT will be also applied.

(2)Assembly

The followings are the sequence of the thermal shield subassembly equipped with the thermal insulation and the heat transfer tube.

a. Assembly of the MLI blanket

i. Cut out the insulation film.
ii. Stack the films and make a blanket
iii. Saw the blanket by thread.
iv. Put the blanket between two thick films (t=100μm) made of KAPTON™.
v. Bundle the blanket and thick films with the tag-pins.

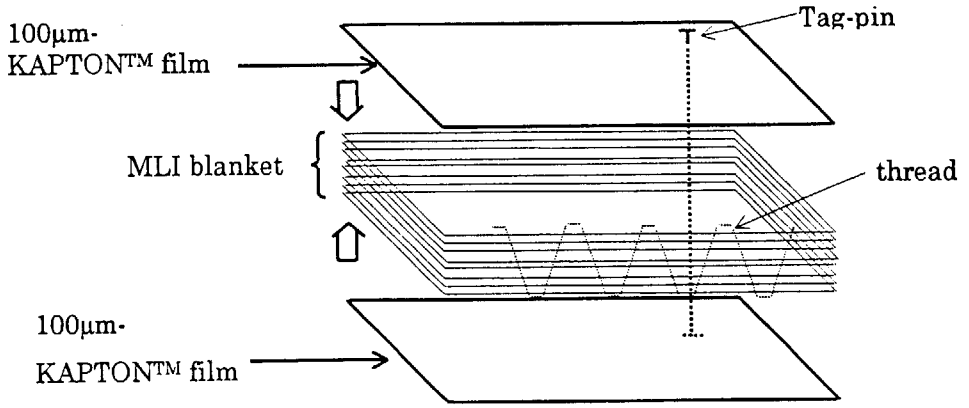

b. Assembly of the reflecting plate
i. Put the shield plate on a working table.
ii. Pass the GFRP-bolts through the plate.
iii. Put the GFRP-spacers on the plate.
iv. Put the reflecting plates on the spacer.
v. Tighten the GFRP-nuts after the stacking of the reflecting plates is completed.

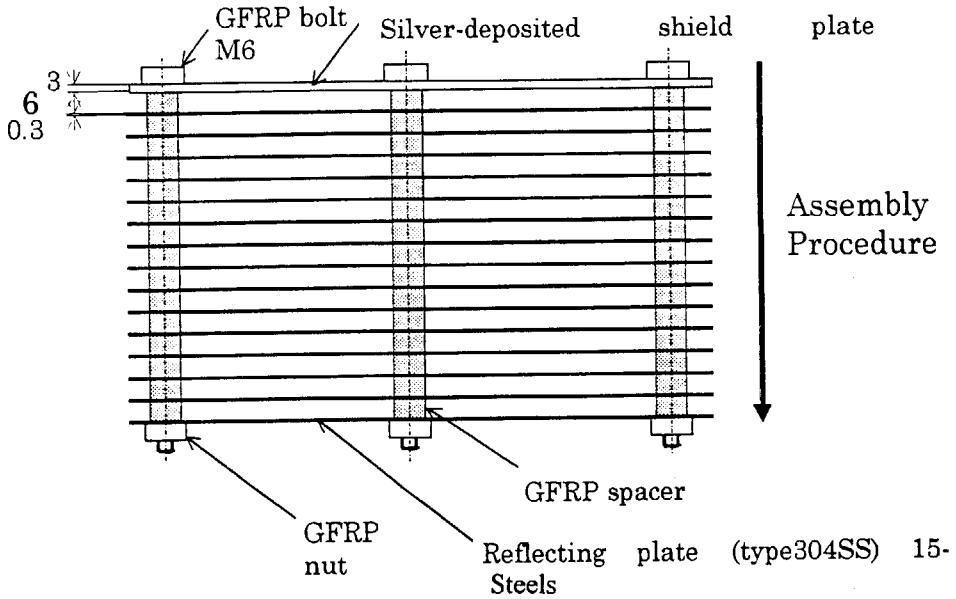

c. Assembly of the shield unit
   i. Weld the heat transfer tube on the shield plate.
   ii. Set the cover plate on the shield plate by bolting.
   iii. Plate the shield plate with the tube and cover plate.
   iv. Furnish the MLI blanket for the shield plate by tag-pins. In the case of the reflecting plates, the plates are furnished for the shield plate according to the procedure described in (2)-b of this chapter.

Figure 5-1(1/2) and Figure 5-1(2/2) show the fabrication sequence of the thermal shield assembly equipped with the MLI blanket and that equipped with the reflecting plates, respectively.

As a previous step of the silver plating, some treatments on the shield plate are required to stabilize the coated surface. Also, the inner surface of the heat transfer tube and the edge penetrations should be masked.

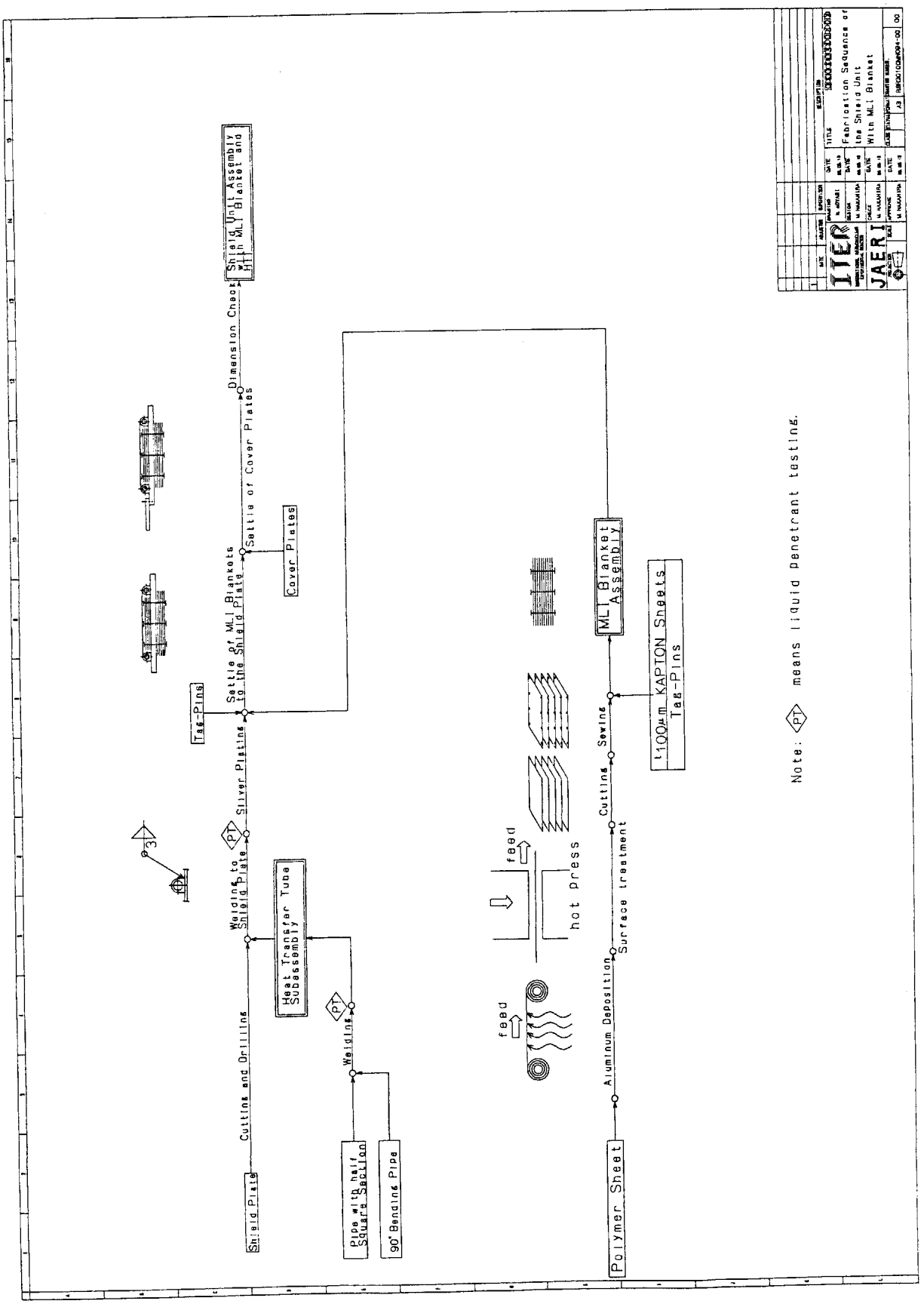

Fig. 5-1(1/2) Fabrication Sequence of the Shield Unit with MLI Blanket

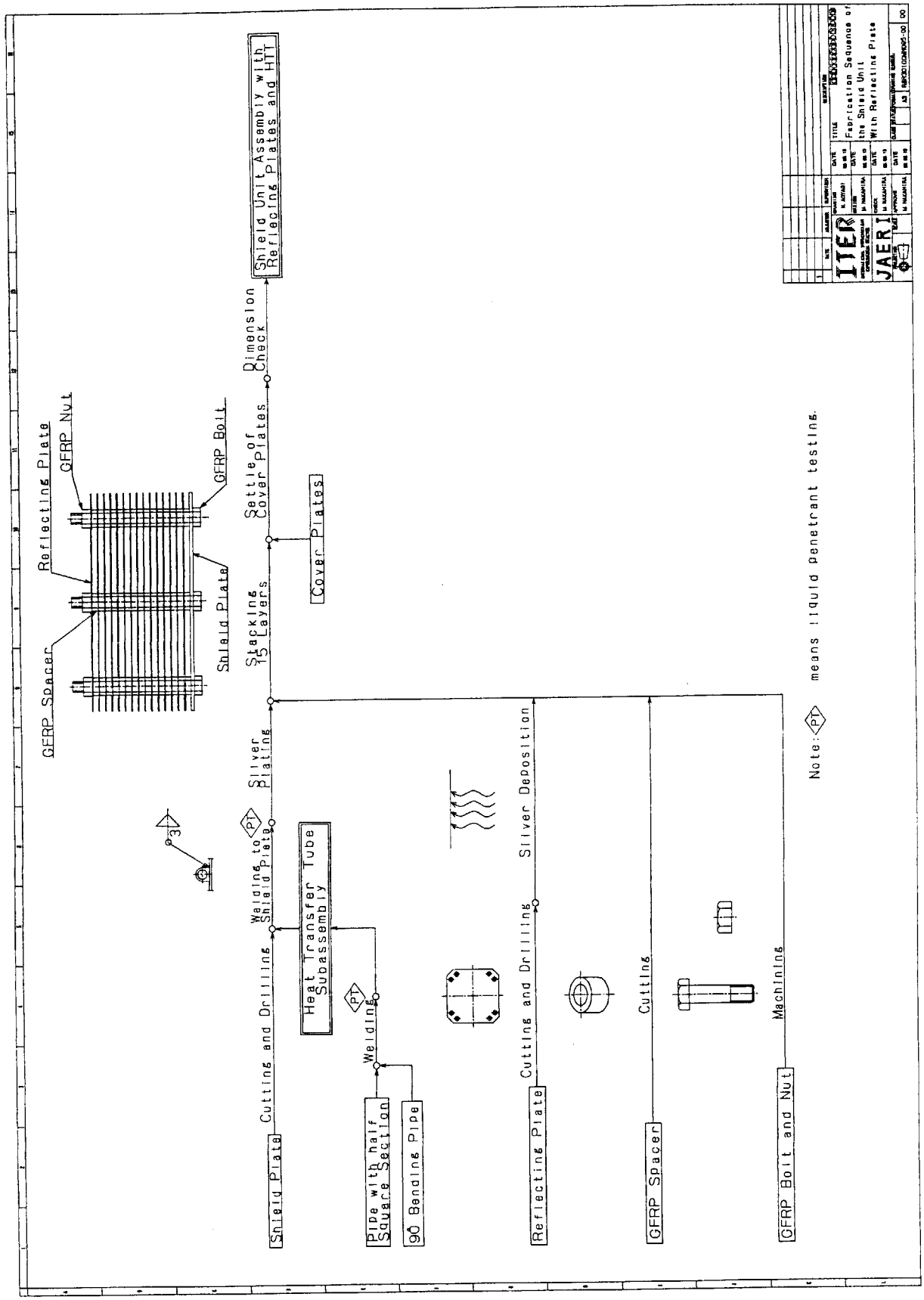

Fig. 5-1(2/2) Fabrication Sequence of the Shield Unit with MLI Blanket

5.2 Installation and testing procedure

The thermal shield assembly will be packed in closed containers and transported to the ITER construction site. After the receipt inspection at the site, each thermal shield will be installed. The opening of the package, the receipt inspection and the assembly work should be carried out in the assembly hall to prevent the MLI blanket and coated plates from the adherence of humidity and salt.

The crossover tube will be connected to the heat transfer tube by the butt welding process. The integrity of the field welding joints should be confirmed by liquid penetrant testing and helium leak testing. The socket welding process may be also feasible to make the field welding easy. However, taking into account of the maintenance work with remote handling tools, the butt welding process is more advantageous than the socket welding process. For the butt welding joints, the penetrant testing will be regally required as shown in 5.1.

The installation sequence to be considered is as follows:

a. Cryostat cylinder thermal shield

After the completion of the cryostat cylinder, its thermal shields will be furnished for the stiffening rings. The butt welding of tube and liquid penetrant testing will be carried out in series. The piping to transfer gaseous helium to the thermal shield from the valve boxes are also connected to the tube.

b. Port thermal shield

After the installation of the ports, its thermal shields will be furnished for the port-surface. The butt welding of the tube and liquid penetrant testing will be carried out in series. The upper port thermal shields are firstly installed and next to the equatorial port thermal shields and finally the divertor port thermal shields are installed to make the installation easy. The interfaces of the port thermal shield and the cylindrical shell thermal shield will be also connected in this stage.

c. Upper cover thermal shield

After the installation of the upper cover block, the thermal shields will be furnished for the surface. The butt welding of the tube and liquid penetrant testing will be carried out in series. The interfaces of the upper cover thermal shield and the cylindrical shell thermal shield will be also connected in this stage.

d. Gravity support and lower cover thermal shield

After the installation of the tokamak structure, the lower cover thermal shields and the gravity support thermal shields will be furnished for the warm surface including the center solenoid support assembly. The butt welding of the tube and liquid penetrant testing will be carried out in series. The interfaces of the lower cover thermal shield and the cylindrical shell thermal shield will be connected in this stage. The lower cover thermal shield and the gravity support thermal shield are also connected each other at the ring pedestal of the lower cover.

The installation procedure of each thermal shield are as follows:

i. Furnish the titanium supports for the warm surface of the cryostat, the ports and the gravity supports.
ii. Furnish the ring plate for the support.
iii. Furnish the shield plate equipped with insulation and the heat transfer tube for the ring plate.
iv. Adjust the location of the cover plate.
v. Weld the crossover tube to the heat transfer tube and carry out penetrant testing to the field joints.

vi. Measure the leak rate from the field joints using helium gas.
vii. Equalize the pressure loss of each tube-path adjusting their restricting orifices. In this procedure, circulation of the actual gaseous helium flow is required.

Figure 5-2 shows the installation procedure of the thermal shield.

The supports and the ring plates are permanent components and are basically out of the scope of the maintenance activity. Therefore, some relaxation-resistant fixtures such as lock nuts are required as the mechanical interfaces of these parts, because the connection of titanium alloy with stainless steel by welding is generally difficult.

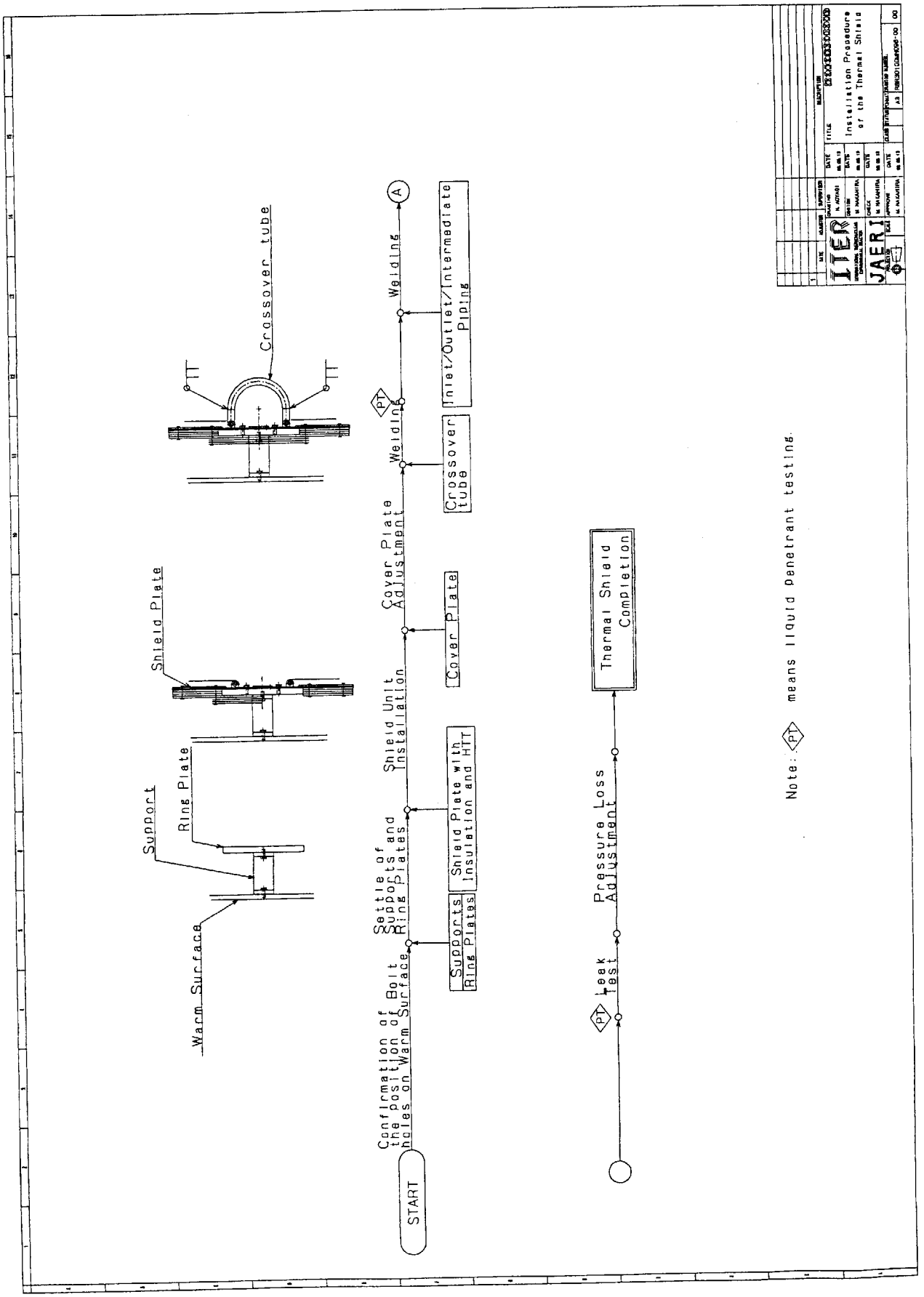

Fig. 5-2 Installation Procedure of the Thermal Shield

5.3 Work schedule

Table 5-1 shows the work schedule of the shop fabrication including packing and shipping. Table 5-2 shows the work schedule of installation at the site including testing.

Table 5-1 Work Schedule of the Thermal Shield (Shop Fabrication with Packing and Shipping)

	Month from starting of fabrication																								Remarks
	1	2	3	4	5	6	7	8	9	10	11	12	13	14	15	16	17	18	19	20	21	22	23	24	
1. Fabrication																									
(1) Shield plate																									
(2) Cover plate																									
(3) Ring plate																									
(4) Support																									titanium alloy
(5) Polyester film																									polyester, polyimide
(6) Reflecting plate																									including silver deposition
(7) Fixtures for insulation																									tag-pins, thread, GFRP parts, etc.
(8) Heat transfer tube																									including the crossover tube
(9) Other parts																									bolst, nuts, etc.
2. Assembly and Welding																									
(1) MLI blanket assy.																									
(2) Reflecting plates assy.																									
(3) Shield unit assy.																									including silver plating
3. Inspection and testing																									VT, DT, PT, HT, LT
4. Packing									▽		▽		▽		▽		▽		▽		▽				
5. Shipping									▽		▽		▽		▽		▽		▽		▽				

Note;

1. This schedule shows shop fabrication, packing and shipping of the thermal shield after completion of the detail design.
2. For the transportation to the construction site, six batches are assumed.

Table 5-2 Work Schedule of the Thermal Shield (Site installation and testing)

	Month from starting of installation																								Remarks
	1	2	3	4	5	6	7	8	9	10	11	12	13	14	15	16	17	18	19	20	21	22	23	24	
1. Installation																									
(1) Cryostat cylinder TS																									
a. Setting of supports	—																								
b. Setting of ring plated		—																							
c. Setting on shield plate																									including welding of crossover tube
(a)Lower block TS			—	—																					
(b)Middle block TS					—	—																			
(c)Higher block TS							—	—																	
(2) Upper cover TS									—	—															
(3) Port TS																									
a. Setting of supports											—														
b. Setting of ring plated												—													
c. Setting on shield plate																									
(a) Upper port TS													—	—											
(b) Equatorial port TS															—										
(c) Divertor port TS																—									
(4) Gravity support TS																	—	—							
(5) Lower cover TS																			—	—					
(6) Piping and welding																					—	—			including welding
2. Testing																									
(a) Penetrant testing					—		—		—		—				—	—	—		—		—	—			for field welding joint of HTT
(b) He leak testing																							—		for all HTT passes
(c) Pressure loss testing																								—	including adjusting

Note;

1. This schedule shows installation and testing of the thermal shield after receipt at the site.
2. The supports and the ring plates of the thermal shield at the upper cover, the lower cover and the gravity supports shall be furnished for the structure in the assembly hall.

6. Future works and R&D activities

This chapter shows items to be studied and developed relevant to the thermal shield design.

(1) Performance of the thermal insulation

The ports will be heated up at 473K in the baking operation of the vacuum vessel. The insulation of the ports should be heat-resisted of up to the temperature. A combination of the embossed polyimide films as the inner blanket and the crinkled or dimpled polyimide films as the outer blanket was taken into account as the insulation. However, there are no experiences of this kind of insulation in past. Therefore, testing on performance and durability for the combined blanket is required to confirm their applicability.

(2) Emissivity of the coated surface

The shield plates should be coated by aluminum or silver with a plating process. Both sides of the reflecting plates should be deposited by silver. Both sides of the polymer films consisting of the MLI blanket should be also deposited by aluminum. To confirm the performance and temperature-resistance of these coated surface, measurements on their emissivity under the actual conditions should be carried out.

(3) Development of the remote handling tools

Because the inside of the cryostat is close enough, the remote handling tools should be compact and should be multi-joints powered manipulators. Study on maintenance work of the heat transfer tube with these tools is required. The mechanism-analyses and the mock-up testing should be included in the study. The holding jigs applied to the maintenance work should be also developed.

(4) Coupled design with warm structure

In the present task, the warm surface of the cryostat is assumed to be kept at 300K. However, nuclear heating in the operation and joule heating due to the coil-quench-incident will heat up the warm structure at higher temperature. Performance of the thermal shield subjected these heat loading should be also taken into account. For these advanced design, temperature distribution analyses with joule heating estimation should be carried out by FEA.

7. Conclusions

The thermal shield design was performed. The conclusions are summarized below.

i. For high dose portion of up to 10-MGy in the vicinity of the NBI ducts, the multistoried reflecting plates made of type 304 stainless steel can be applied as the thermal insulation in place of the MLI blanket. By the heat flux calculations, heat leakage through fifteen plates supported by GFRP spacers, bolts and nuts were confirmed to be almost the same as that of the MLI blanket.

ii. The arrangements of the heat transfer tube on the shield plate were studied using FEA. From the analytical results, two-turn arrangement for the shield plate equipped with the MLI blanket and four-turn arrangement for that with the reflecting plates can be confirmed to be applicable to keep the hot-spot temperature lower than 100K.

iii. The structural integrity of the crossover tube without bellows expansions was studied by FEA approach. The stresses that appear in the tube were confirmed to be lower than the allowable stress limit prescribed in ASME B&PV Code.

iv. Detailed design of the thermal shields were performed. The structural integrity, the heat leakage, the heat removal and the pressure loss of each thermal shield were assessed. The heat leakage to the 80K thermal shield and that to the 4.5K cold magnets were confirmed to be lower then their limitations. The pressure loss at each tube-path can be limited within approximately half of the target. As the design outputs, the overall configuration with the tube arrangement was drawn for each thermal shield.

v. The cooling system including the control valves and the transfer piping were studied to limit the overall pressure loss lower than the target, 0.1MPa. The control valves in the valve boxes were designed with suitable *Cv* characteristics. Finally, the flow diagram of the cooling system was developed.

vi. The productivity of the major parts and the fabrication sequence in vendor's workshop were clarified. Also, the installation and testing procedure at the ITER construction site were outlined.

vii. The items to be studied and developed relevant to the advanced design of the thermal shields were listed up.

viii. The overall construction cost including material procurements, shop fabrication, shipping, installation, inspections and testing were estimated based upon the current design output.

Acknowledgement

The authors would like to express their sincere appreciation to Drs. M. Ohta, T. Nagashima, S. Matsuda and Y. Seki for their continuous guidance and encouragement. They also would like to acknowledge all of members who supported this work.

This is a blank page.

国際単位系 (SI) と換算表

表1　SI基本単位および補助単位

量	名称	記号
長さ	メートル	m
質量	キログラム	kg
時間	秒	s
電流	アンペア	A
熱力学温度	ケルビン	K
物質量	モル	mol
光度	カンデラ	cd
平面角	ラジアン	rad
立体角	ステラジアン	sr

表2　SIと併用される単位

名称	記号
分，時，日	min，h，d
度，分，秒	°，′，″
リットル	l，L
トン	t
電子ボルト	eV
原子質量単位	u

1 eV = 1.60218 × 10^{-19} J

1 u = 1.66054 × 10^{-27} kg

表3　固有の名称をもつSI組立単位

量	名称	記号	他のSI単位による表現
周波数	ヘルツ	Hz	s^{-1}
力	ニュートン	N	m·kg/s^2
圧力，応力	パスカル	Pa	N/m^2
エネルギー，仕事，熱量	ジュール	J	N·m
工率，放射束	ワット	W	J/s
電気量，電荷	クーロン	C	A·s
電位，電圧，起電力	ボルト	V	W/A
静電容量	ファラド	F	C/V
電気抵抗	オーム	Ω	V/A
コンダクタンス	ジーメンス	S	A/V
磁束	ウェーバ	Wb	V·s
磁束密度	テスラ	T	Wb/m^2
インダクタンス	ヘンリー	H	Wb/A
セルシウス温度	セルシウス度	℃	
光束	ルーメン	lm	cd·sr
照度	ルクス	lx	lm/m^2
放射能	ベクレル	Bq	s^{-1}
吸収線量	グレイ	Gy	J/kg
線量当量	シーベルト	Sv	J/kg

表4　SIと共に暫定的に維持される単位

名称	記号
オングストローム	Å
バーン	b
バール	bar
ガル	Gal
キュリー	Ci
レントゲン	R
ラド	rad
レム	rem

1 Å = 0.1 nm = 10^{-10} m

1 b = 100 fm^2 = 10^{-28} m^2

1 bar = 0.1 MPa = 10^5 Pa

1 Gal = 1 cm/s^2 = 10^{-2} m/s^2

1 Ci = 3.7 × 10^{10} Bq

1 R = 2.58 × 10^{-4} C/kg

1 rad = 1 cGy = 10^{-2} Gy

1 rem = 1 cSv = 10^{-2} Sv

表5　SI接頭語

倍数	接頭語	記号
10^{18}	エクサ	E
10^{15}	ペタ	P
10^{12}	テラ	T
10^{9}	ギガ	G
10^{6}	メガ	M
10^{3}	キロ	k
10^{2}	ヘクト	h
10^{1}	デカ	da
10^{-1}	デシ	d
10^{-2}	センチ	c
10^{-3}	ミリ	m
10^{-6}	マイクロ	μ
10^{-9}	ナノ	n
10^{-12}	ピコ	p
10^{-15}	フェムト	f
10^{-18}	アト	a

（注）

1. 表1－5は「国際単位系」第5版，国際度量衡局 1985年刊行による。ただし，1 eVおよび1 uの値はCODATAの1986年推奨値によった。
2. 表4には海里，ノット，アール，ヘクタールも含まれているが日常の単位なのでここでは省略した。
3. barは，JISでは流体の圧力を表わす場合に限り表2のカテゴリーに分類されている。
4. EC閣僚理事会指令ではbar，barnおよび「血圧の単位」mmHgを表2のカテゴリーに入れている。

換　算　表

力	N(=10^5dyn)	kgf	lbf
	1	0.101972	0.224809
	9.80665	1	2.20462
	4.44822	0.453592	1

粘度　1 Pa·s(N·s/m^2) = 10 P(ポアズ)(g/(cm·s))

動粘度　1 m^2/s = 10^4 St(ストークス)(cm^2/s)

圧力	MPa(=10 bar)	kgf/cm^2	atm	mmHg(Torr)	lbf/in^2(psi)
	1	10.1972	9.86923	7.50062 × 10^3	145.038
	0.0980665	1	0.967841	735.559	14.2233
	0.101325	1.03323	1	760	14.6959
	1.33322 × 10^{-4}	1.35951 × 10^{-3}	1.31579 × 10^{-3}	1	1.93368 × 10^{-2}
	6.89476 × 10^{-3}	7.03070 × 10^{-2}	6.80460 × 10^{-2}	51.7149	1

エネルギー・仕事・熱量	J(=10^7 erg)	kgf·m	kW·h	cal(計量法)	Btu	ft·lbf	eV
	1	0.101972	2.77778 × 10^{-7}	0.238889	9.47813 × 10^{-4}	0.737562	6.24150 × 10^{18}
	9.80665	1	2.72407 × 10^{-6}	2.34270	9.29487 × 10^{-3}	7.23301	6.12082 × 10^{19}
	3.6 × 10^6	3.67098 × 10^5	1	8.59999 × 10^5	3412.13	2.65522 × 10^6	2.24694 × 10^{25}
	4.18605	0.426858	1.16279 × 10^{-6}	1	3.96759 × 10^{-3}	3.08747	2.61272 × 10^{19}
	1055.06	107.586	2.93072 × 10^{-4}	252.042	1	778.172	6.58515 × 10^{21}
	1.35582	0.138255	3.76616 × 10^{-7}	0.323890	1.28506 × 10^{-3}	1	8.46233 × 10^{18}
	1.60218 × 10^{-19}	1.63377 × 10^{-20}	4.45050 × 10^{-26}	3.82743 × 10^{-20}	1.51857 × 10^{-22}	1.18171 × 10^{-19}	1

1 cal = 4.18605 J(計量法)

= 4.184 J　(熱化学)

= 4.1855 J　(15 °C)

= 4.1868 J(国際蒸気表)

仕事率　1 PS(仏馬力)

= 75 kgf·m/s

= 735.499 W

放射能	Bq	Ci
	1	2.70270 × 10^{-11}
	3.7 × 10^{10}	1

吸収線量	Gy	rad
	1	100
	0.01	1

照射線量	C/kg	R
	1	3876
	2.58 × 10^{-4}	1

線量当量	Sv	rem
	1	100
	0.01	1

(86年12月26日現在)

ITER CRYOSTAT THERMAL SHIELD DETAILED DESIGN